

# **Role of the Perisynaptic Extracellular Matrix in Synaptic Plasticity**

**Dissertation**

zur Erlangung des akademischen Grades

**doctor rerum naturalium**

**(Dr. rer. nat.)**

genehmigt durch die Fakultät für Naturwissenschaften

der Otto-von-Guericke-Universität Magdeburg

von: Integrated MSc (Microbiology) Jeet Bahadur Singh

geb. am 31<sup>st</sup> December 1989 at Lucknow, UP, India

Gutachterin: apl. Prof. Dr. Constanze Seidenbecher

Gutachter: Prof. Dr. Guus Smit

eingereicht am: 13 June 2017

verteidigt am: 07 December 2017

*Dedicated to my late grandfather and  
my parents*

# Acknowledgements

---

***Success doesn't happen overnight. It takes patience, time and a little guidance...***

*It is a moment of great pleasure for me and at the same time a bit arduous too, to acknowledge and express my sincere gratitude to all near and dear ones who in one way or the other have rendered their precious help and assistance towards the successful completion of this endeavor.*

*I extend infinite gratitude to my guide DR. RENATO FRISCHKNECHT, for all the guidance and constant supervision which have helped me in completion of my thesis. He was always there may be its late in night he was there to help me. His office door was open all the time for discussions and it's those discussions which helped me shape my PhD thesis. I am indebted to, constant encouragement and invaluable suggestions and the faith bestowed on me to handle this excellent research problem. I would like to express my sincere thanks and deep sense of honor for his worthy guidance and suggestions extended to me during the entire stretch of stay in Magdeburg.*

*I avail this opportunity to express my profound thanks and deep respect to Prof. Dr. Constanze Seidenbecher for her valuable suggestions during the group meetings and being my PhD supervisor.*

*I would like to mention my gratitude to our ECM family and Molecular physiology group for their help, discussions and inputs during our seminars and the daily work. I would like to mention Dr. Martin Hine and Dr. Arthur for their many useful suggestions during group meetings. I would also like to thank all the technicians of the department for their very important and continuous help. Special thanks to Kathrin Hartung for all the help.*

*I am thankful and indebted for the friendly help, cheerful atmosphere and long hours of discussions in the institute, around Elbe and conferences to Barbara, Jose, Stefan and all the other friends from our floor at the institute. Now it's important to mention my office colleagues especially Carolina for all the sugar over the years and Franzi and Jessica for all the German translation which saved me many time.*

*Thanks to all my friends and all others who made my stay at LIN a memorable one which included Sujoy, Paramesh, Anil, Sampath and Rajeev over the time and stay here. List of my friends is very long it's tough to include all here but you know.....*

*I am indebted to my parents for their selfless love and faith in me. I would also like to thank my elder brothers Dr. RAJESH, BRAJESH and SANDEEP for encouraging at every step. They supported me when I had no ends.*

*Along with my PhD I also found the partner of my life TANVI an important part of my life which was also achieved during my PhD.*

*I could not have words to thanks all, as this was not a day's goal.....*

## Summary

---

The adult brain of rodents is characterized by a specific form of extracellular matrix (ECM) which forms after the first postnatal weeks. ECM has been implicated in structural and functional synapse stabilization, which is necessary to guarantee life-long reliable brain function. It is made of proteoglycans and glycoproteins that form a meshwork filling the extracellular space. It has been suggested that specific substructures of the ECM have restrictive effects on outgrowth, synaptogenesis and structural plasticity. This effect is largely mediated by chondroitin sulfates bound to proteoglycans of the lectican family, which are important constituents of brain ECM in rodents and human. Indeed, experimental removal of chondroitin sulfates by glycosidases leads to reestablishment of juvenile-like structural and functional plasticity. Learning-induced structural plasticity occurs also in the adult brain. Therefore I hypothesized that a well-regulated mechanism must exist that allows for local and restricted structural plasticity also in adulthood. Interestingly, proteoglycans of the lectican family are subjected to proteolytic cleavage by enzymes of the ADAMTS family. However, physiological context and role of this cleavage and the neuronal plasticity-induced ECM dynamics are not well understood.

Therefore I investigated the proteolytic cleavage of lecticans and its regulation during synaptic plasticity. I analysed the shortest lectican family member, brevican, as prototypic proteoglycan since it is highly abundant in brain regions displaying significant usage-dependent plasticity. I induced chemical LTP (cLTP) in acute hippocampal slices and measured brevican secretion and quantified cleavage using Western blotting. Furthermore, I employed the same experimental system to perform an unbiased approach to investigate overall ECM remodelling using mass spectrometry. I observed a marked increase in brevican cleavage compared to control slices 15-60 min after cLTP induction, which I further confirmed by immunohistochemistry. Treatment with a specific ADAMTS protease inhibitor interfered with the cLTP-induced brevican cleavage and unmasked an increase in brevican secretion upon cLTP induction.

The findings obtained in the thesis suggest a critical contribution of glia cells and NMDA-dependent signalling in the cLTP-induced ECM remodelling. Glia has been known to provide D-serine which is a co-agonist for NMDAR site, and glia blockade reduced brevican cleavage and secretion, suggesting a key role of glia. I also illustrate protease involvement in the expression of structural plasticity and found a reduction in size and number of dendritic

protrusions in presence of protease inhibitor after stimulation. Taken together, my work suggests a sequence of events taking place after cLTP induction that on the one hand leads to partial ECM degradation but on the other hand to secretion of new ECM molecules to stabilize new synaptic connections. Thus, proteases could serve as a potential target that may be exploited to modulate neuronal plasticity especially after injury to the CNS, in neurological diseases or disorders affecting learning and memory processes that require structural plasticity.

## Zusammenfassung

---

Die extrazelluläre Matrix (ECM) des adulten Gehirns bildet sich in Nagetieren in den ersten Wochen nach der Geburt aus. Die ECM spielt nicht nur eine besondere Rolle in der strukturellen sondern auch in der funktionellen Stabilisierung von Synapsen, welche vor allem notwendig ist, um eine lebenslange, verlässliche Gehirnfunktion zu garantieren. Zum einen ist die ECM aus Proteoglykanen, zum anderen aus Glykoproteinen aufgebaut, welche in den extrazellulären Raum ausfüllendes Netz bilden. Es wird vermutet, dass bestimmte ECM-Komponenten einen restriktiven Effekt auf strukturelle Plastizität und Synaptogenese ausüben. Dieser wird durch an Proteoglykane der Lectican-Familie gebundene Chondroitinsulfate vermittelt, welche einen wichtigen Bestandteil der adulten Hirn-ECM darstellen. Tatsächlich führt der experimentelle Abbau von Chondroitinsulfaten durch Glykosidasen zu einer juvenil-ähnlichen strukturellen und funktionellen Plastizität. Lern-induzierte strukturelle Plastizität tritt jedoch auch im adulten Gehirn auf. Daraus schlussfolgerte ich, dass ein wohlgeordneter Mechanismus existieren muss, der auch im Erwachsenenalter lokale und begrenzte strukturelle Plastizität erlaubt. Interessanterweise unterliegen die Proteoglykane der Lectican-Familie einer proteolytischen Spaltung durch Enzyme der ADAMTS-Familie. Der physiologische Zusammenhang und die Rolle dieser Spaltung und die Plastizitäts-induzierten Dynamiken der ECM an Neuronen sind jedoch bis jetzt noch nicht gut verstanden.

Hierfür untersuchte ich die proteolytische Spaltung von Lecticanen und deren Regulation während synaptischer Plastizität. Brevican, das kleinste Lectican, wurde als ein Vertreter der Proteoglykane analysiert, da es in den Hirnregionen, welche eine deutliche nutzungs-abhängige Plastizität aufweisen, stark exprimiert wird. Ich habe chemisch ausgelöste LTP (cLTP) in akuten hippocampalen Schnitten induziert und anschließend mittels quantitativem Western-Blot sowohl die Sekretion von Brevican als auch dessen Spaltung analysiert. Ein umfassendes Bild von der Umstrukturierung der ECM ermittelte ich mittels Massenspektrometrie. Ich konnte einen merklichen Anstieg in der Spaltung von Brevican verglichen mit Kontrollschnitten etwa 15-60 min nach cLTP Induktion beobachten, welchen ich ebenfalls mit Immunhistochemie bestätigen konnte. Die Behandlung mit einem spezifischen Inhibitor für ADAMTS-Proteasen wirkte sich hemmend auf die cLTP-induzierte Brevicanspaltung aus, brachte aber eine vermehrte Brevican-Sekretion zum Vorschein.

Die in meiner Arbeit erhaltenen Ergebnisse legen eine entscheidende Beteiligung von Gliazellen und NMDA-abhängigen Signalwegen an der cLTP-induzierten Umstrukturierung

der ECM nahe. Astrogliazellen sekretieren D-Serin, welches an NMDA-Rezeptoren als Co-Agonist fungiert. Die Inhibierung von Gliazellen führte zu reduzierter Brevicanspaltung und -sekretion, was auf eine Schlüsselrolle der Glia in dem zugrundeliegenden Mechanismus hindeutet. Ebenfalls konnte ich die Beteiligung von Proteasen an der strukturellen Plastizität deutlich durch Reduktion der Zahl und Größe dendritischer Protrusionen in Anwesenheit eines Proteaseinhibitors während der Stimulation zeigen. Zusammengefasst deuten die Ergebnisse meiner Arbeit darauf hin, dass eine Abfolge von Ereignissen nach cLTP Induktion dazuführt, dass einerseits eine partielle Degradation der ECM stattfindet, andererseits aber auch neue ECM-Moleküle sekretiert werden, um neue synaptische Verbindungen zu stabilisieren. Somit könnten Proteasen als potentielles Target dienen, um neuronale Plastizität zu regulieren, besonders nach Hirnverletzungen, bei neurologischen Krankheiten oder Störungen, die Lern- und Erinnerungsprozesse betreffen, welche strukturelle Plastizität erfordern.

# Table of Contents

---

<b>1.</b>	<b>Introduction</b>	<b>1</b>
1.1	ECM and synaptic function	1
1.1.1	ECM: Long-term Plasticity (LTP) and structural plasticity	2
1.1.2	NMDA receptor activation and LTP	3
1.1.3	Biochemical hallmarks of LTP-Calcium/calmodulin-dependent kinase II (CaMKII)	5
1.2	The perisynaptic extracellular matrix of the brain and its role in synaptic plasticity	6
1.2.1	The lectican family and brevican as prototypic member	8
1.2.2	Proteolysis of brain ECM components	9
1.2.2.1	Proprotein convertases (PCs)	11
1.2.3	Integrins as ECM receptors	13
1.2.4	Role of D-serine in synaptic plasticity and communication with glia	14
1.3	Neuron-glia interactions in synaptic plasticity	15
1.3.1	The Ng2 proteoglycan on oligodendrocyte precursor cells	16
1.4	Aims of the study	17
<b>2.</b>	<b>Materials and Methods</b>	<b>19</b>
2.1	Materials	19
2.1.1	Chemicals	19
2.1.2	Animals	19
2.1.3	Antibodies used for WB, IF, and IHC	19
2.2	Biochemical methods	24
2.2.1	Protein concentration determination using Amido black assay	24
2.2.2	SDS-Page using Laemmli system	24
2.2.3	Western blotting	25
2.2.4	Immunoblot detection	25
2.2.5	Quantification of Western blot	25
2.2.5.1	Normalization methods	26
2.2.5.1.1	Coomassie staining normalization	26
2.2.5.1.2	2,2,2-Trichloroethanol (TCE) normalisation	26
2.2.6	Acute hippocampal slice preparation	27



2.2.7	Enzymatic extraction of ECM with Chondroitinase ABC and induction of activity-dependent modulation	27
2.2.8	Immunostaining in hippocampal slices	28
2.2.9	Pharmacological treatments in acute hippocampal slices	28
2.3	Microscopy and image analysis	29
2.3.1	Confocal microscopy	29
2.3.2	STED microscopy	29
2.3.3	Processing of Slick V-cre slices for spine head protrusions (SHP) analysis	30
2.4	LC-MS/MS Analysis	30
2.4.1	Fractionation of proteins by SDS-PAGE	30
2.4.2	Gel cutting	30
2.4.3	Destaining	31
2.4.4	Drying	31
2.4.5	In-gel tryptic digestion	31
2.4.6	Peptide extraction and storage	32
2.4.7	Peptides dissolve for HPLC	32
2.5	Statistical analysis	32
<b>3.</b>	<b>Results</b>	33
3.1	Validation of enzymatic extraction of ECM with Chondroitinase ABC and induction of activity-dependent modulation	33
3.2	Activity induced proteolytic cleavage of brevican and ultrastructure representation of perisynaptic brevican	35
3.3	Dissection of endogenous proteases involved in degradation of brevican	40
3.4	Role of proprotein convertases in cleavage of brevican	42
3.5	Cleavage of brevican requires network activity and NMDAR	45
3.6	Activity-dependent cleavage and secretion of brevican via an NMDAR-CaMKII signalling pathway	47
3.7	Role of $\beta$ 1 class integrins in the activity-dependent modulation of ECM	49
3.8	Screening for modulation of ECM using an unbiased LC-MS approach	50
3.9	Increased level of extracellular brevican does not results from protein synthesis	52
3.10	Role of glia in secretion and cleavage of brevican	52
3.11	Influence of specific protease inhibitor of ADAMTS4 on induction of	56

chemical LTP	
3.12 Activity-dependent modulation and role of proteases in modulation of dendritic protrusions	57
3.13 Activity-dependent proteolytic cleavage of NG2 results in increased levels of ectodomain associated with the ECM	58
<b>4. Discussion</b>	<b>61</b>
4.1 Brevican as marker of ECM and its modulation upon activity	61
4.2 Perisynaptic localization of brevican	62
4.3 Activity-dependent modulation of ECM	62
4.3.1 Role of proprotein convertases in cleavage of brevican	62
4.3.2 Endogenous proteases involved in degradation of brevican	63
4.4 Key players involved in modulation of ECM	63
4.4.1 Cleavage of brevican requires NMDAR and network activity	63
4.5 Role of glia in secretion and cleavage of brevican	65
4.6 Functional impact of ECM modulation	66
4.6.1 Influence of specific protease inhibitor of ADAMTS4 on induction of chemical LTP	66
4.6.2 $\beta$ 1-integrin signaling affects the activity-dependent modulation of ECM	67
4.6.3 Activity-dependent modulation and role of proteases in structural plasticity	68
4.7 The role of sheddases ADAM10 in NG2 cleavage in primary OPC	68
4.8 Conclusion	69
<b>5. Bibliography</b>	<b>72</b>
<b>6. Abbreviations</b>	<b>79</b>
<b>7. Figures</b>	<b>81</b>
<b>8. Scientific publications</b>	<b>83</b>
<b>9. Curriculum Vitae</b>	<b>84</b>
<b>10 Erklärung</b>	<b>85</b>



# 1. Introduction

---

The main question driving my thesis was to investigate the role of the regulation of the extracellular matrix (ECM) expression and degradation and its influence on synaptic plasticity. This is important to know since our current view of the synapse includes pre- and postsynaptic elements as well as astroglia (tripartite synapse) and the perisynaptic ECM (synaptic quadriga) (Dityatev et al., 2010). These four components interact with each other and modulate neuronal communication. To study the influence of the ECM I developed a method to investigate endogenous mechanisms that lead to modulation of the ECM during neuronal activity. Specifically I determined the role of sheddases and proteases in degradation and cleavage of ECM. I have further outlined the signaling molecules and the role of N-Methyl-D-aspartic acid receptor (NMDAR) in the regulation of cleavage and secretion of the ECM protein brevican and shed some light on the mechanisms of protease activation. Finally, the role of proteases in structural plasticity is highlighted by measuring the activity-dependent formation of dendritic protrusions in acute hippocampal slices.

## 1.1 ECM and synaptic function

The ECM of the brain exerts an ambiguous function in the brain. ECM has been found to play an important role in synaptic stabilization and plasticity, ion homeostasis and neuroprotection as they are enwrapping neurons and their synaptic contacts. It has been shown that brevican localizes to close vicinity of synaptic cleft perisynaptically and biochemical fractionation has confirmed an enrichment of membrane-bound brevican in a synaptic fraction (Seidenbecher et al., 1997; Seidenbecher et al., 2002). Synapses have been divided into two groups based on the information transfer unit in the nervous system - chemical and electrical synapses. The chemical synapses consist of pre- and a post-synaptic elements that communicate via chemical mediators, which is the hotspot for highly specialized molecular machinery for synaptic functions. As mentioned before ECM and glial end-feet together with both synaptic compartments make up the tetrapartite synapse. The electrical synapses help in communication via gap junctions primarily found in glia cells by allowing charged ions and small molecules.

Brevican knockout is viable and fertile and have no morphological differences in their phenotype whereas appearance of their PNN are slightly less prominent compared to wild type (Brakebusch et al., 2002). However, from the functional point of view LTP induction

was normal but its maintenance was strongly impaired, suggesting a role of brevican in synaptic plasticity.

It has been suggested that lateral diffusion of AMPA-receptors within the postsynaptic membrane was a modulator of short-term plasticity (Heine et al., 2008). Therefore, mechanisms leading to a higher or lower lateral diffusion and consequently altering exchange of synaptic receptor are very likely to modulate short-term plasticity. Indeed it has been shown that *in vitro* degradation of ECM using hyaluronidase (Hyase) an enzyme which degrades hyaluronic acid increases lateral diffusion of AMPA-receptors and interferes with short-term plasticity in dissociated hippocampal neurons (Frischknecht et al., 2009). Therefore, local changes in the structure or density of the ECM represent an attractive mechanism how cells may alter AMPA-receptor diffusion and modulate short-term plasticity. In addition, lack of components of the ECM or its degradation by enzymatic means leads to altered LTP thus the ECM is indispensable for normal adult synaptic plasticity.

The ECM of the brain also plays a role in acting as a barrier against the formation of new synaptic contacts. It restricts structural plasticity and its appearance marks the end of the experience-dependent plasticity like the so-called critical periods (Pizzorusso et al., 2002, Pizzorusso et al., 2006). It was shown that in young animals monocular deprivation leads to an ocular dominance shift. Removal of ECM by the chondroitinase ABC (ChABC) from the mature rat's visual cortex restores ocular dominance plasticity which implies that maturation of PNNs inhibits neuronal plasticity in visual cortex. In addition Gogolla et al., 2009 showed that ChABC degradation facilitates erasure of fear memories from adult mice. Recently it has reported that ECM degradation in the auditory cortex helps in enhancement of cognitive flexibility that can build on learned behavior and it does not affect general sensory learning (Happel et al., 2014). Thus, the perisynaptic ECM inhibits structural plasticity and rearrangements of the neuronal networks and appearance of the PNNs that leads to the functional switch from developmental to adult modes of synaptic plasticity.

### **1.1.1 ECM: Long-term Plasticity (LTP) and structural plasticity**

Recent studies suggest that ECM plays a role in synaptic plasticity and homeostatic processes such as scaling of synaptic responses, metaplasticity and stabilization of synaptic connectivity (Dityatev et al., 2010). Brevican knock-out mice have slightly less prominent PNNs as compared to wild type. LTP induction is normal in these mice, however, their maintenance is impaired (Brakebusch et al., 2002). Similar LTP phenotype was observed in mice lacking

neurocan (Zhou et al., 2001). Experiments with tenascin-R (TNR) knock-out mice showed reduced LTP while long-term depression (LTD) was normal. Further, it was found that after enzymatic digestion of chondroitin sulfates LTD was impaired in the CA1 region of the hippocampus (Bukalo et al., 2001). In contrast it has been shown that ECM removal improves LTP in the visual cortex *in vivo* (de Vivo et al., 2013). In continuation of this work, it was revealed that a deficiency of TNR leads to disinhibition of the CA1 region of the hippocampus and to a metaplastic shift in the threshold for induction of LTP (Bukalo et al., 2007). Application of Chondroitinase ABC (Ch ABC) on organotypic hippocampal slices with mature CSPGs lead to the enhancement of motility in the dendritic spines and it leads to the appearance of spine head protrusions through the restriction of  $\beta$ 1-integrin activation and signaling at synaptic sites (Orlando et al., 2012); suggesting the role played by perisynaptic CSPGs in restricting the remodeling of neuronal circuits at the synaptic level. There was another recent study in the auditory cortex where ECM digestion via Hyase provided reversal learning by affecting short-term as well long-term plasticity without interfering with previously formed memories paving way for a short time window for activity-dependent changes (Happel et al., 2014). These results indicate that remodeling of the ECM is critical for both functional and structural long-term synaptic plasticity.

### **1.1.2 NMDA receptor activation and LTP**

Induction of LTP in the hippocampus requires activation of NMDAR, a specific type of ionotropic glutamate receptor. NMDAR are tetramers comprising two GluN1 subunits and two GluN2 subunits which subdivided in four subclasses GluN2A-D and GluN3 A-B subunits (Law et al., 2003). It has become evident that there NMDARs do not only exists as di-heteromeric e.g. GluN1/GluN2B but also as tri-heteromeric receptors (GluN1/GluN2A/GluN2B) (Sheng et al., 1994). Depending on their composition NMDAR differ in their opening kinetics and conductance. GluN2B-containing NMDAR are known to have higher  $\text{Ca}^{2+}$  permeability and activate slower compared to GluN2A-containing receptors (Erreger et al., 2005; Sobczyk et al., 2005). NMDAR subunit composition goes through a developmental shift where GluN2B subunit predominates with its presence from embryonic to early postnatal periods in the brain. GluN2A subunit expression increases after the first three postnatal weeks and there is a decline in GluN2B subunit at this point of development of the brain (Monyer et al., 1994; Kirson and Yaari, 1996). NMDA receptors are found at synaptic sites of the adult forebrain in form of di-heteromeric GluN1/GluN2A- and tri-heteromeric GluN1/GluN2A/GluN2B-NMDA receptors (Rauner and Kohr, 2011). Di-

heteromeric receptors consisting of GluN1/GluN2B are suggested to be prominent at extrasynaptic sites (Dalby and Mody, 2003; Townsend et al., 2003).

Activation of NMDA receptors requires several steps which include glutamate and glycine (or D-serine) binding (Johnson and Ascher, 1987). It's found embedded in the postsynaptic density (PSD) (Sheng and Kim, 2002) a microscopic structure consisting of an intracellular meshwork of proteins, important for the organization of postsynaptic receptors (Kennedy, 2000). NMDA receptors among the ionotropic glutamate receptors have high permeability for  $\text{Ca}^{2+}$  ions, which allows them to activate intracellular signalling cascades (Mayer et al., 1987). Extracellular  $\text{Mg}^{2+}$  block their pore during resting membrane potential and channel opening is only possible by depolarization which leads to the removal of  $\text{Mg}^{2+}$  block and allows the glutamate to open the channel (reviewed in (Bliss and Collingridge, 1993)). This dependence of NMDA receptor on glutamate and magnesium unblocking of the channel makes NMDA receptors a 'coincidence detector' which is a requirement for NMDA dependent LTP. NMDARs also need D-serine and glycine as coagonist to activate it. Thus NMDAR plays key role in LTP.

NMDARs are associated to the cytoplasmic C-terminus with intracellular signaling molecules such as  $\text{Ca}^{2+}$ /Calmodulin-dependent protein kinase II (CaMKII), which is the most prominent signaling molecule linked to NMDAR. GluN2B subunits have a higher affinity for CaMKII than GluN2A (Strack and Colbran, 1998). GluN2B subunit has been suggested to be a key player in hippocampal LTP and GluN2B subunits of NMDA receptors are responsible for autophosphorylation of CaMKII (Barria and Malinow, 2005). CaMKII is known to be highly abundant at synapses (Erondu and Kennedy, 1985) and thus important for induction of LTP (Otmakhov et al., 1997). NMDAR and CaMKII interplay will be discussed in detail in section 1.7. NMDAR subunit composition and expression plays important role in developmental plasticity. It has been illustrated that GluN2B subunits of NMDAR presence at synaptic sites point towards permissive factor regulating ocular dominance plasticity of developing cortex (Erisir and Harris, 2003). Visual deprivation of adult rodents brings back the juvenile form of NMDAR in the visual cortex by activating juvenile plasticity (He et al., 2006). This suggests it might be possible that activity-dependent modulation of ECM could provide such short time window of opportunities for NMDARs subunit to a juvenile state (effect the GluN2A/GluN2B ratio) and thus activating important intracellular signaling cascades. It has been also been indicated that cell surface molecules such as integrin family members also get effected upon the modulation of ECM. The link between NMDAR and

integrins have been focussed in the next section and how ECM interplays important and intermediate role in the plasticity of the brain. Lets first understand the role of D-serine the co-agonist of NMDAR.

### **1.1.3 Biochemical hallmarks of LTP-Calcium/calmodulin-dependent kinase II (CaMKII)**

CaMKII is one of the most abundant proteins in the hippocampus forming one to two percent of the total proteins in the hippocampus (Lynch, 2004). It is present in both the pre- and post-synapse however, its expression is higher in PSD. The PSD includes embedded channels, receptors and signaling molecules on the postsynaptic locus, necessary for communication between pre- and post-synapse. CamKII varies in molecular weight from 50 to 60 kDa consisting of four homologous isoforms  $\alpha$ ,  $\beta$ ,  $\gamma$ , and  $\delta$ .  $\alpha$  and  $\beta$  are the most abundant of the four isoforms found in the brain (Kennedy et al., 1983). Calmodulin (CaM) is 17 kDa calcium sensing protein and CaMK family kinases are one of the many downstream targets of CaM. Intracellular  $\text{Ca}^{2+}$  elevation leads to the activation of CaMKII and CaM binding. CamKII $\alpha$  can be autophosphorylated at Thr<sup>286</sup> in a  $\text{Ca}^{2+}$ /CaM-independent or autonomous activity by a neighboring activated CaMKII subunit (Miller and Kennedy, 1986). Thr<sup>286</sup> autophosphorylation in CaMKII has been implicated in certain forms of synaptic plasticity and learning and memory (Giese et al., 1998). They also elucidated that Thr<sup>286</sup> mutant mice had no NMDAR dependent LTP in the hippocampal CA1 area and it also displayed no spatial learning in the behavioural Moris water maze test test. CaMKII  $\beta$  has a higher affinity for  $\text{Ca}^{2+}$ /Calmodulin (CaM) compared to CaMKII $\alpha$  (Brocke et al., 1999). It's known to respond to the levels of calcium concentration and downstream cellular communication thus playing important role in molecular mechanisms of LTP. It is activated after NMDAR stimulation and plays a key role in NMDAR-dependent LTP (Lisman et al., 2002) by binding to the cytoplasmic domain of the GluN2B subunits of NMDA receptors and are known to be most widely binding partner of CAMKII. This subunit of NMDARs is playing a crucial role in synaptic plasticity by recruiting CaMKII to the synapses, which is a key component of underlying signaling cascades (Bayer et al., 2001; Barria and Malinow, 2005). On the other hand published work suggest that using antagonist for the CaMKII or by genetic deletion of CaMKII $\alpha$  (Silva et al., 1992) leads to the abolishment or significant reduction of LTP. These findings point towards the key role of CaMKII/NMDAR complex during LTP induction, behavioural memory and experience dependent memory (reviewed in(Sanhueza and Lisman, 2013)).



CaMKII has been known to play an important role in structural plasticity, as a scaffolding protein at the post-synaptic site and activity-dependent mediator of neuronal maturation (Wu and Cline, 1998). Synaptic stimulation leads to translocation of CaMKII to dendritic spine and activation of CaMKII can lead to morphological changes of dendritic spines. It has been shown (Shen and Meyer, 1999) that calmodulin binding and autophosphorylation are not only responsible for CaMKII enzymatic activity but also for translocation and localization of CaMKII at synaptic target sites: 1- dissociation of CaMKII from F-actin 2- binding of CaM to  $\alpha$ - and  $\beta$ -CaMKII leads to the PSD translocation of CaMKII. It has been illustrated that density of CaMKII in the PSD increases after LTP and there is also increase in spine size (Otmakhov et al., 2004b). Cell depolarization leads to the CaMKII activation in dendritic spines and dendritic shafts from various  $\text{Ca}^{2+}$  sources: L-type voltage-sensitive calcium channels (VSCCs) activates the CaMKII in dendritic spines, however in the shafts mostly by non-L-type channels in addition to the small contribution from VSCCs (Lee et al., 2009). Thus CaMKII activation in spines plays important role in structural changes at the synapse.

## **1.2 The perisynaptic extracellular matrix of the brain and its role in synaptic plasticity**

ECM is a three-dimensional net-like structure surrounding cells; filling the extracellular void around them. It is not just an inert filling material but rather a dynamic, physiologically active component surrounding all living tissues. In fact it plays an important role in determining the shape and functions of the surrounding tissues (Soleman et al., 2013). ECM forms the major component of cartilage and bone, however although less prominent, it is also present in the brain and spinal cord. ECM composition, physical and topological appearance is heterogeneous in nature (Frantz et al., 2010). In the brain, the ECM undergoes several changes during development and which include restrictive changes for structural plasticity that alter functional neuronal plasticity. The focus of my work lies in the ECM from vertebrates however, the ECM is present ubiquitously from simpler to most complex living beings.

Brain ECM is a net like three-dimensional structure, which envelops cell soma, proximal neurites, and synaptic contacts. The presence of ECM in the brain was reported in the early 70s of the last century (Zimmermann and Dours-Zimmermann, 2008). The most elaborated form of ECM are the perineuronal nets (PNNs) which have been discovered more than 100 years ago by Ramon y Cajal and Camillo Golgi. These PNNs start forming at the second week after birth in rodents and reach their mature distribution after the third month of their

life. PNNs leave out holes for synaptic contact sites which give the lattice-like appearance to these structures (Celio and Blumcke, 1994).

The ECM comprises a complex network of macromolecules including glycoproteins, polysaccharides, and proteoglycans. Glycosaminoglycan (GAG) chains are attached covalently to the core protein and contribute to the net negative charge to the glycans (with the exception of hyaluronic acid) (reviewed in Elena Vecino and Jessica C. F. Kwok 2016). Five forms of GAGs have been described which include hyaluronan, chondroitin sulfate (CS), dermatan sulfate, heparan sulfate and keratan sulfate. Among this hyaluronic acid (HA) a major organizing polysaccharide of the brain's ECM forms the backbone of a meshwork consisting of proteoglycans belonging mainly to the lectican family of CS proteoglycans (Yamaguchi, 2000). Chondroitin sulfate proteoglycan (CSPGs) are one of the most abundant proteoglycans majorly constituting brain ECM (Carulli et al., 2005). The main lectican family members are aggrecan and versican which are ubiquitously expressed whereas neurocan and brevican are nervous system specific family members. Versican and neurocan can be considered as genuine components of juvenile ECM. Aggrecan, a lectican that is primarily contributed by glial cells, is most prominent in the mature nervous system. Similarly brevican is upregulated during adolescence and secreted by neurons and glial cells (Yamada et al., 1994; Seidenbecher et al., 1998; John et al., 2006) and subsequently incorporated into the ECM around neurons (Carulli et al., 2006) or directly bound to the cell surface (Hedstrom et al., 2007; Frischknecht et al., 2009). Lecticans can be considered as connectors between neural surfaces. They bind to the cell surface components via the C-terminal globular domains and to HA of ECM via the N-terminal globular domains. In this way the lecticans along with link proteins HA, and glycoproteins like tenascins, form huge carbohydrate-protein aggregates, binding them on the cell surfaces. This aggregation might lead to the compartmentalization of the neuronal surfaces (Max F.K. Happel and Renato Frischknecht, 2016). ECM structure also incorporate various other components as it is shown in Figure 1 including small signalling molecules such as semaphorin 3a or orthodenticle homebox2 (Oxt2). Other ECM components embedded includes reelin, laminins, thrombospondins, heparinsulfate proteoglycans, receptors such as integrins, and even transcription factors are incorporated to form the complex structure. The more specific ECM rigid in nature is called perineuronal nets (PNNs), and known to be rich in CS and aggrecan. This type of ECM is mainly found around parvalbumin containing GABAergic interneuron (Figure 1C). The other type of ECM of which Brevican a proteoglycan mentioned above could be an example as it is

found to be loosely enwrapping cell bodies and synaptic contacts making it a specialized form of ECM shown in Figure 1C.

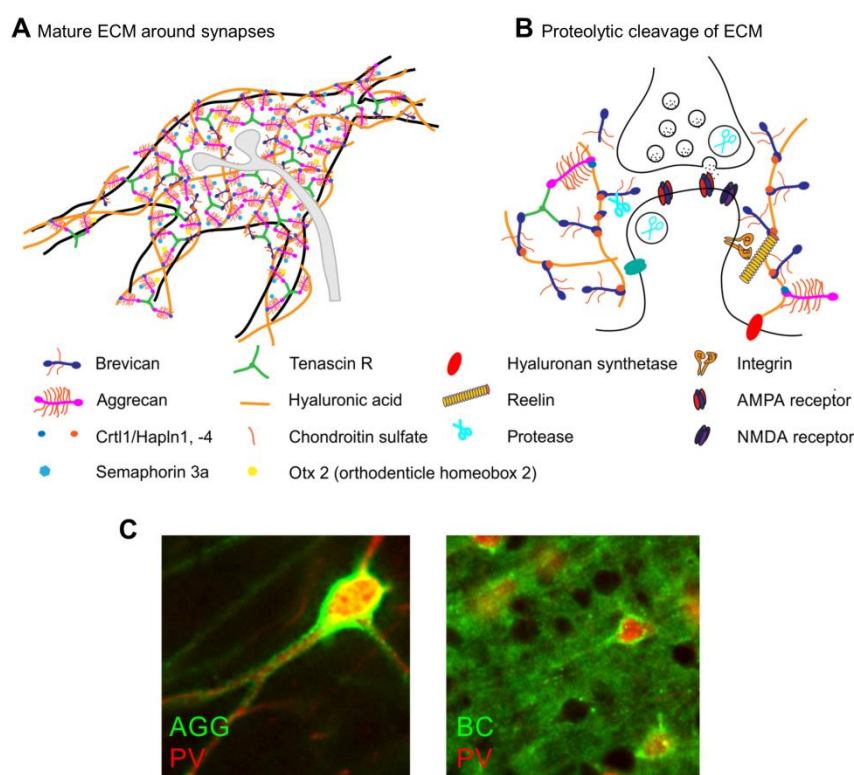


**Figure 1. ECM and its components in detail; mature and degraded ECM.**

- (A) Mature ECM tightly enwraps synapses, consisting of hyaluronic acid (orange), left side depicting mature PNNs and the cartoon in (right) showing loose ECM perisynaptically. It consists of CSPGs, lecticans and small signalling molecules such as semaphorin3a or Otx2 bound to CS. Loose ECM consists mainly of brevican as aggrecan is less rich in CS. Several cellular processes are regulated by ECM proteins (e.g. reelin) by signal through their receptors (e.g. integrins) shown here.
- (B) Mature ECM can be degraded or loosened to allow for structural plasticity and functional plasticity with the help of glycosidases shown as for example hyaluronidases (scissors in the cartoon).
- (C) Parvalbumin positive interneuron (PV, red) surrounded by aggrecan stained (AGG, green) a typical PNN marker, *left*. Dendritic spine and synapses of excitatory neurons are also surrounded by brevican (BC, green in the *middle*) (Modified from Happel and Frischknecht, 2016).

### 1.2.1 The lectican family and brevican as prototypic member

Brevican is the most abundant and smallest member of the lectican family in the brain and is found in PNN-like structures on most excitatory as well as inhibitory cells and it is also a marker for loose ECM. It binds to hyaluronic acid at N-terminal and with C-terminal to extracellular glycoprotein tenascin-R (TNR). Brevican is also a substrate for a number of matrix metalloproteases. It exists in full-length form and can be cleaved by ADAMTS4 (Nakamura et al., 2000) at a specific cleavage site in the central non-globular region. This cleavage site is conserved among the other lectican family members (Zimmermann and Dours-Zimmermann, 2008) (Figure 2). Brevican expression increases gradually with

development (Seidenbecher et al., 1998) and its maturation marks the end of critical period plasticity in the visual cortex of rodents (Pizzorusso et al., 2002). Brevican is known to be secreted by both neuron and glia (Hamel et al., 2005; John et al., 2006) and the mechanisms leading to brevican secretion and formation of mature ECM is in part affected via activity-driven process which is still elusive (Dityatev et al., 2007). Brevican is functionally known to play role in injury, lesion-induced plasticity, tumorigenesis and in Alzheimer's disease (Frischknecht and Seidenbecher, 2012). Taken together, brevican is ubiquitously expressed in the mature brain and has been used as marker of ECM in my thesis.

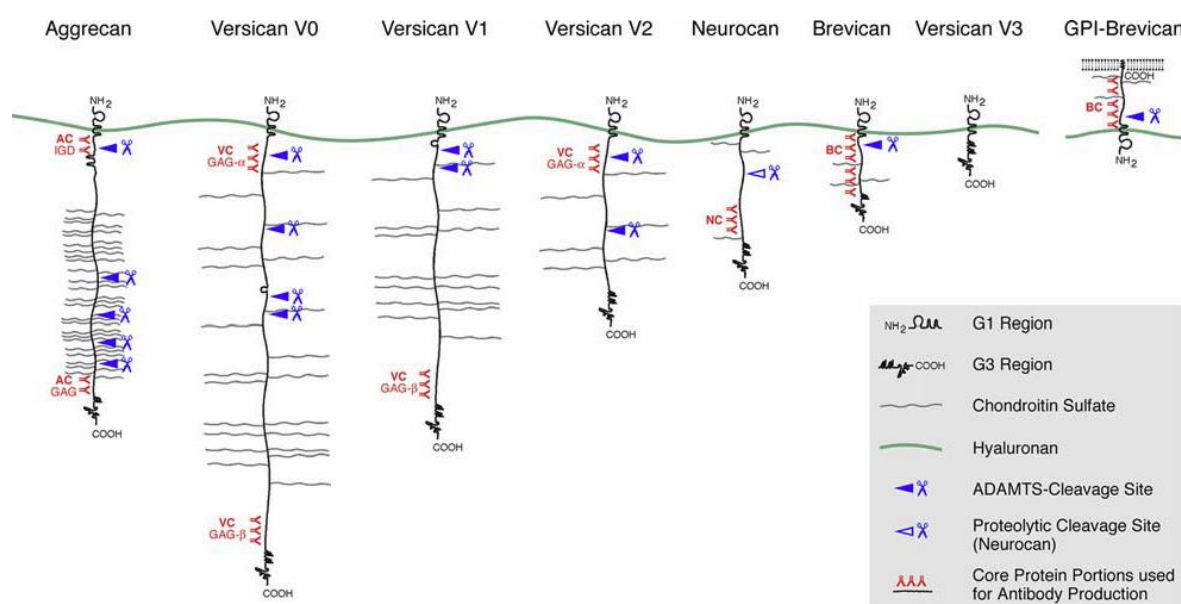


**Figure 2. Conserved proteolytic cleavage sites found over the different members of the lectican family.**

CSPG Lecticans have highly conserved homologous G1 and G3 domain. Glycosaminoglycan side chains bind to their central part, immunoglobulin (Ig)-like loop is included in all lectican at N-terminal G1 regions where hyaluronic acid binds and C-terminal globular domain termed G3. There is presence of lectin like domain, which lead to their name as ‘lectican’. Blue triangle with scissors shows the conserved proteolytic cleavage site in the lectican family. Adapted from (Zimmermann and Dours-Zimmermann, 2008)

### 1.2.2 Proteolysis of brain ECM components

There is plethora of ECM digesting enzymes expressed in the brain. These enzymes regulate synaptic function by altering ECM at both stages of juvenile and adult form of ECM (Huntley, 2012; Shinoe and Goda, 2015). Important groups of such enzymes are Matrix metalloproteases (MMPs), a disintegrin and metalloproteinases (ADAMs) and a disintegrin and metalloproteinase with thrombospondin motifs (ADAMTS) and serine proteases. Their structure has been reviewed in (Paulissen et al., 2009) and is shown in Figure 3. Probably the best-studied member of the MMP family in the nervous system is MMP9. Elevated neuronal

activity enhances expression of MMP9 that leads to increased proteolysis of  $\beta$ -dystroglycan (Szklaarczyk et al., 2002; Michaluk et al., 2007). Depletion of MMP9 results in an impairment of LTP at hippocampal synapses. It has been shown that slices from MMP-9-deficient mice have impaired magnitude and duration of hippocampal LTP, but not LTD, whereas addition of recombinant active MMP-9 to slices from MMP-9 mutants restores the magnitude and duration of LTP to wild-type level (Nagy et al., 2006).

Another ECM component agrin plays a pivotal role in the development and maintenance of the neuromuscular junction. MMP3 is known to process it at the neuromuscular junction in an activity-dependent manner (VanSaun et al., 2003). Also, the serine protease neurotrypsin has been reported to process agrin (Reif et al., 2008) and neurotrypsin has been identified as essential for cognitive functions in the human brain. Deletion mutation in the coding region resulting in a truncated protein without protease domain leads to severe mental retardation (Molinari et al., 2002). Furthermore, neurotrypsin is recruited and released at synapses in an activity-dependent manner (Frischknecht et al., 2008). It is expected that neurotrypsin-derived agrin fragments induce the formation of filopodia on neuronal dendrites which may form new synapses in response to strong neuronal activity (Matsumoto-Miyai et al., 2009). Also, Brevican is a substrate for a number of proteases (Nakamura et al., 2000). ADAMTS4/5 is the best-described protease to process brevican and aggrecan. Cleavage of brevican yields an N-terminal fragment of approximately 50 kDa and C-terminal fragments of about 80 kDa. Both fragment sizes are prominent in brain lysates indicating that cleavage occurs to a large extent in vivo (Yamada et al., 1994; Seidenbecher et al., 1995; Matthews et al., 2000). The 50 kDa proteolytic fragment of brevican leads to an increased invasiveness glioma when overexpressed and ADAMTS4 was identified to be the responsible protease for brevican-derived invasiveness of glioma cells (Zhang et al., 1998; Matthews et al., 2000). Recent study from our group suggests further its role in homeostatic plasticity where it was found that there was increase in proteolytic cleavage of brevican followed by prolonged network inactivation (Valenzuela et al., 2014). Homeostatic plasticity resulted in modulation of ECM, which could allow them for higher degree of structural plasticity. However, the role of brevican cleavage in brain function remains elusive.

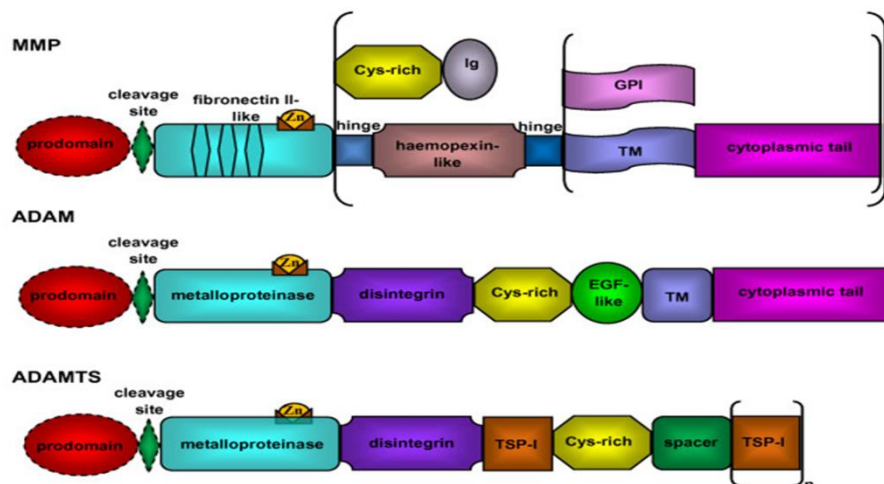


**Figure 3. Structure of MMP, ADAM and ADAMTS.**

**MMP** structure consist of prodomain followed by cleavage site where pro-protein convertase (PCs) cleavage site, a catalytic metalloproteinase domain with fibronectin type II repeats and linker domain, a linker peptide, transmembrane domain (TM) or glycosylphosphatidylinositol (GPI) anchor and a cytoplasmic tail.

**ADAM** have a prodomain preceded by PCs cleavage site metalloproteinase domain, a disintegrin domain, cysteine rich region (Cys-rich) an epidermal- an epidermal-growth factor repeat (EGF-like), a TM and a cytoplasmic tail.

**ADAMTS** is different from ADAM by not having TM and cytoplasmic tail but rather have thrombospondin type I motifs (TSP-1) at their C-terminal. Adapted from (Paulissen et al., 2009)

Taken together, extracellular proteolysis has been suggested to be an important event during different kinds of synaptic plasticity. The potential of proteases to shape the ECM and alter receptor mobility makes them very interesting candidates to regulate synaptic functions. The notion that proteases can be released locally upon a specific trigger such as strong synaptic activity indicates their potential as key enzymes in a suite of events that lead to changes in synaptic plasticity. These examples suggest that the ECM contains a variety of functions that can be unmasked by specific proteolytic enzymes.

### 1.2.2.1 Proprotein convertases(PCs)

PCs are related to bacterial subtilisin-like enzymes. They are known to process various precursor proteins, which results in the release of more active products, or vice versa they become inactive. The family of PCs consist of nine members of which furin, PC1/3, PC2, PACE4, PC4, PC5/6, cleaves its substrate after single or paired basic residues. PC7, SKI-1/S1P cleaves at non-basic residues and NARC-1/PCSK9 cleaves only one substrate and also function as auto-catalyst i.e. for its own activation. As depicted in Figure 4 cleavage site of an ADAMTS (protease) and PCs responsible for making the protease catalytically active. Their presence and overexpression has been known to have important implication in pathological situations such as tumorigenesis and can lead to enhanced pathology in metastatic cancer

cases respectively. Proteases have inhibitory prodomain which has to be cleaved, to make them enzymatically active as it has been shown in (Tortorella et al., 2005) for the ADAMTS-4 (aggrecanase-1).

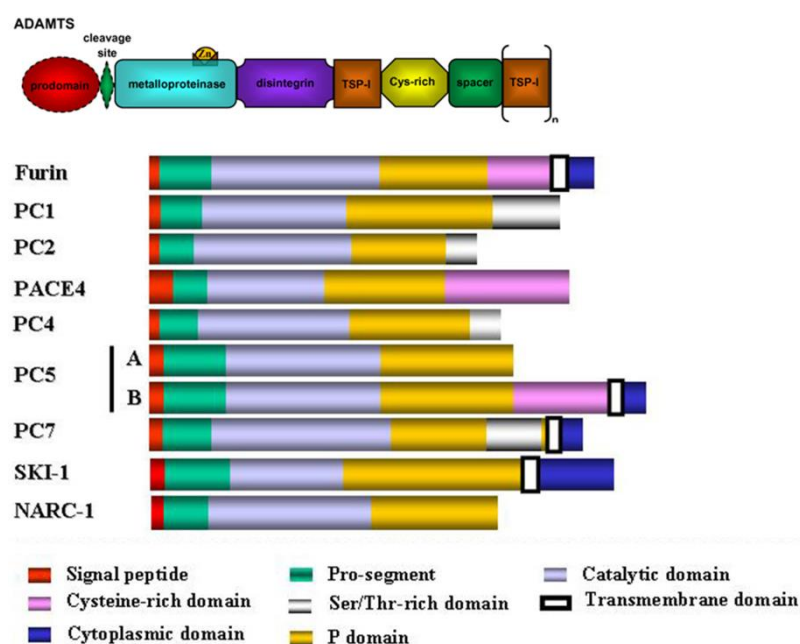


**Figure 4. Schematic representation of proprotein convertases.**

ADAMTS protease has cleavage site at which the PCs act to make it enzymatically active. Adopted from (Paulissen et al., 2009). All the PCs have some conserved domain like signal peptide, pro-segment, catalytic domain but few have transmembrane, cytoplasmic, Ser/Thr-rich domain in variation from other PCs as depicted in the cartoon. Adopted from (Creemers and Khatib, 2008)

Out of many of these PCs, furin is the most studied member and it's known in the field as the major workhorse as it can cleave a large number of proproteins. It's known from the literature (Leduc et al., 1992) that furin occurs as 104 kDa pro-furin precursor and upon autocatalytic processing turns to be ~98 kDa. Furin plays crucial role during embryonic development and is being considered as a potential therapeutic in targeting for tumor growth and metastasis (Bassi et al., 2005). Furin in the CNS is responsible for the processing of neurotrophins pro-nerve growth factor, neural cell adhesion and cueing protein such as L1 CAM and semaphorins. It has also been implicated in neurotrophic viruses, such as influenza virus – H1N1 and H5N1 reviewed in (Seidah, 2011). The other PCs such as PACE4, another member from the family can regulate themselves by autocleavage of propeptide to an active form (Taniguchi et al., 2002). PACE4 lacks transmembrane anchor unlike furin but it has a cysteine-rich domain which is essential for cell surface tethering and binds TIMP-2 (Nour et al., 2005) and anchors heparin at the ECM (Tsuji et al., 2003). It is known that in osteoarthritis PACE4 is overexpressed and its inactivation helps in pain symptoms.

ADAMTS4/5 (aggrecanase) protease is known to be activated by PACE4 and thus degrading aggrecan a major cartilage macromolecule. A key pathological event in the osteoarthritis as this leads to cartilage destruction during the disease (Malfait et al., 2008). These studies from past suggest PCs play a very important role in ailments, thus it would be important to dissect out their role in brain ECM and which could be the most relevant PC

### **1.2.3 Integrin's as ECM receptors**

Integrins are known to play an important role in cell-cell interactions by helping to maintain physical contact and signalling with an extracellular niche and are best known cellular ECM-receptors. Integrins link the ECM to the actin cytoskeleton and thus play an important role in transducing extracellular signals to morphological changes (Hynes, 1987). Arg-Gly-Asp (RGD) is the best understood binding motif of integrins and this motif was firstly identified in fibronectin (Pierschbacher and Ruoslahti, 1984), but also found in tenascins and other ECM proteins. Integrins are known to exist as a heterodimeric molecule consisting of two distinct subunits  $\alpha$  and  $\beta$ . Around 24 different types of integrin are found in humans and consisting of combinations of 8  $\beta$  and 18  $\alpha$  subunits,  $\alpha$  and  $\beta$  also account for ligand specificity (Hynes, 2002). In the nervous system integrins have been found to be involved in the development and maintenance of synaptic contacts.

It has been suggested that integrins play an important role in interaction with the molecules present in the ECM, plays both the roles as adhesion and signalling molecules (Hynes, 2002; Lemons and Condic, 2008). RGD-motif is used as a functional blocking peptide for integrin, this inhibition tends to significantly impair LTP in hippocampal slices (Staubli et al., 1990).  $\beta$ 3 Integrin peptide blocker applications also lead to the suggestion that integrin receptors are implicated in the control of glutamate release, NMDA receptor function and synapse maturation (Orlando et al., 2012). It has been known that immature synaptic boutons had a high probability of glutamate release and this is the time I know that there is a high amount of expression of the NMDA receptor GluN2B subunit at postsynaptic sites. Synapse maturation leads to shifting in the NMDAR subunit composition to predominant GluN2A subunits (Cull-Candy et al., 2001). Several studies have shown that the blockage of integrins leads to impairments of LTP (Staubli et al., 1990). Studies for dissecting a probable method for improving axon regeneration after injury could be achieved by activation of integrins, as inhibition of CSPGs act via inactivation of integrins (Tan et al., 2011). This mechanism acts via a decrease in phosphorylation of focal adhesion kinase and Src levels, thus this result in further activation of signaling cascades. Protease-dependent modulation of ECM has also



been known to affect integrin signaling. In past, it has been suggested that MMP cleaving substrate also includes integrin ligands such as laminin, N-cadherin, dystroglycans and proteoglycans (Lander et al., 1997). New target pathway for MMP-9 action has been suggested which is mediated via  $\beta 1$  integrin, which affects MMP-9 action on NMDAR surface trafficking (Michaluk et al., 2009).  $\beta 1$  integrin activation has been known to play role in increased spine dynamic and appearance of spine head protrusions, once the CSPGs have been digested by application of ChABC (Orlando et al., 2012).

We can hypothesize based on these findings that ECM may regulate NMDA receptors in an integrin-dependent manner. This mechanism could be a way to study the modification of ECM upon activity-dependent modulation.

#### **1.2.4 Role of D-serine in synaptic plasticity and communication with glia**

NMDAR activation requires glutamate from presynaptic site and a coagonist. D-serine is an endogenous amino acid which activates the synaptic NMDARs by binding at its co-agonist site preferentially over glycine (Papouin et al., 2012). D-serine is secreted by astrocytes and therefore there is communication between neuron and glia and glia takes an active part in modulating synaptic plasticity (reviewed in (Volterra and Meldolesi, 2005))(Mothet et al., 2000). Study shows that D-serine is synthesized primarily in glia cells, including Müller cells and astrocytes (Stevens et al., 2003) and its released via a calcium- and SNARE-dependent exocytotic pathway (Mothet et al., 2005). D-serine has also been implicated in different age-related pathophysiology affecting various cognitive deficits associated with aging as its level decline in aged animals (Panizzutti et al., 2014). The classical form of LTP depends on NMDARs as it plays key role in excitatory transmission and synaptic plasticity. It has been implicated that astrocytes can regulate their activation via  $Ca^{2+}$  dependent release of D-serine which is NMDAR co-agonist (Pاناتier et al., 2006). Another study carried upon these key findings pointed out that release of D-serine from astrocytes is a must for NMDAR-dependent plasticity in the nearby excitatory synapses (Henneberger et al., 2010). They also found that blockage of exocytosis or reduction / depletion of D-serine in individual astrocytes blocks local LTP. So it would be important for our study to investigate the role of D-serine in this NMDA-dependent plasticity at the synapse to dissect out how modulation of ECM affects this communication with glia. I have used pharmacological approaches to dissect out how it would affect this neuron-glia interdependence, as they both are embedded in the matrix and part of matrix source is glia as well.

### 1.3 Neuron-glia interactions in synaptic plasticity

In the middle of 19<sup>th</sup> century it was recognized that there are other cell types other than neurons which constitute the CNS. Rudolf Virchow and others brought in the light that these other cells are supporting the nerve cells and coined the term ‘glia’ for them. Glial cells have been further subdivided into three cell types (Allen and Barres, 2009) as follows:

**Microglia** is referred to as macrophages of the CNS since they are activated after damage to the CNS and perform similar tasks as the scavenging cells of the blood. The functions of the dormant microglia in the undamaged CNS are still largely unexplained. One of the most important functions recently described for this population is during synaptic pruning. They are involved in encapsulation and elimination of no longer required synapses during development or generally during plastic changes of the CNS (Kettenmann et al., 2013; Schafer et al., 2013)

**Astrocytes** form the connecting link between blood vessels and the CNS. They are interconnected by gap junctions ( GJ) and thus enable the basic exchange of material between these two systems. GJ : a cluster of intracellular membrane channels, which allow exchange of ions and small molecules (<1kDa) for direct cytoplasmic continuity between adjacent cells (Simon and Goodenough, 1998). GJ consists of hemichannels known as connexions, which are made up of connexions (Sohl and Willecke, 2004). Neurons express seven different connexions and that of astrocytes have three (Cx43, Cx30, Cx26) (De Bock et al., 2013). Cx43 is found to be highly expressed in the brain, as it is involved there in GJ coupling between astrocytes. It has been implicated that GJ communication is important for proliferation and differentiation of neural stem cells (Worsdorfer et al., 2008). In addition, astrocytes provide a variety of substances for the other cell types in the CNS. Thus, their continuities surround neural synapses, which are summarized under the structure of a tripartite synapse. In this structure, among other things, certain neurotransmitters are absorbed by the astrocytes as well as metabolites are transported from the astrocytes to the axonal endings.

**Oligodendrocytes** are the myelin-forming glial cells of the central nervous system (CNS). Oligodendrocytes can differentiate at any age from oligodendrocyte precursor cells (OPC). In addition, the OPC itself forms a stable cell population. Some specific functions of the OPC are described in the following section since this is one of the major focuses of this work. OPCs in the mammalian CNS characteristically express the chondroitin sulfate proteoglycan

NG2, a type-1 transmembrane protein (Nishiyama et al., 2009; Trotter et al., 2010). Recent research revealed numerous trophic support for neurons by oligodendrocytes in form of glial cell line-derived neurotrophic factor, brain-derived neurotrophic factor or insulin-like growth factor-1 (reviewed in (Bradl and Lassmann, 2010)). Disorders such as multiple sclerosis and leukodystrophies lead to a decrease in myelination (demyelination) and ultimately to the death of the oligodendrocytes and associated neurons. The link between neuron to oligodendrocytes was found in the CA1 region of the hippocampus between CA3 to OPCs (Bergles et al., 2000) and later confirmed by (Jabs et al., 2005). These interactions might be important for the development, maintenance, and plasticity of neural circuits. It was reported that these neuron-glia synapses undergo activity-dependent alterations; an indication for neuronal plasticity (Ge et al., 2006).

### **1.3.1 The Ng2 proteoglycan on oligodendrocyte precursor cells**

OPC cells expressing the proteoglycan NG2 represent around 5-10% of all glia cells in the developing and adult CNS and are ubiquitously spread throughout the gray and white matter. They are unique among glia cells in forming glutamatergic and GABAergic synapses with neurons (reviewed in (Trotter et al., 2010)). Studies in the past have shown that neuron-OPC synapses are present in major brain areas. Differentiation of OPC into oligodendrocytes is correlated with downregulation of NG2 expression (De Biase et al., 2010). NG2<sup>+</sup> cells are positioned within the oligodendrocytes in a manner that they can monitor the firing patterns of surrounding neurons. Recent studies show that neuronal activity controls OPC differentiation, migration and myelination as for the myelination of the CNS requires OPCs to generate functionally matured oligodendrocytes (Gibson et al., 2014). It has been suggested that NG2 protein may work in similar fashion at synapses as neuroligins which contain as well LNS domain (Gokce and Sudhof, 2013). It has been suggested that aqueous buffer can be used to extract the NG2 cleavage since it occurs *in vivo* in the CNS (Nishiyama et al., 1995; Deepa et al., 2006). Studies about neuronal adhesion molecules N-cadherin and neuroligin1 reported about activity-dependent cleavage by the  $\alpha$ -secretase ADAM10 which alters both synaptic function and structure (Reiss et al., 2005; Suzuki et al., 2012). Cleavage by  $\alpha$ - and  $\gamma$ -secretase and signaling properties of the generated fragments has been best characterized for the Notch protein, where a membrane-bound C-terminal fragment (CTF) and an intracellular domain (ICD) are generated. It would be interesting to dissect out whether OPC send signals to neuron upon synaptic activity and to elucidate a potential functional role of NG2 cleavage and the OPC-derived NG2 ecto-domain role in neuronal network modulation.

## 1.4 Aims of the study

During my PhD I was interested in regulated extracellular proteolysis and its role in synaptic plasticity. Thus, I developed a method to extract and measure ECM molecules from acute hippocampal slices. I present mainly two projects using this method. The main part of the thesis focuses on activity-dependent proteolysis of ECM proteins, which may allow for synaptic rearrangement in adults in a restrictive area and time. Furthermore, I present data on activity-dependent action of sheddases during synaptic plasticity, which was part of a collaboration of our lab and the lab of Prof. Jacky Trotter in Mainz (published in Sakry et al., 2014).

Recent studies suggest that proteases could be responsible for allowing plasticity even in mature ECM when it's restrictive in nature for plasticity. However exact mechanism of protease activation and contribution of glia to neuron remains relatively uninvestigated. The specific molecules responsible for cascade of signaling mechanism which allows for such window of short opportunity for newer synaptic contact has to be still elucidated. Neuron OPC interdependence has been well studied, still the mechanisms by which they communicate remains to be investigated upon neuronal activity.

The main questions, which I addressed in this study, were:

- 1) **How does neuronal activity induce proteolysis of brevican and thus remodeling of ECM?**
  - I. Induction of chemical LTP (cLTP) to analyze its effects on processing of brevican in acute slices from wild type rats focusing on endogenous metalloproteinases.
    - a) Immunoblot analysis of ECM processing.
    - b) Unbiased proteomic approach to search for ECM modulation
    - c) Functional and structural impact of specific proteases on extracellular proteolysis of ECM as a global and local approach.
    - d) Dissecting the exact mechanisms involved in activation of proteases.
    - e) Involvement / communication between neuron-glia for modulation of ECM.
  - II. Visualization of activity-dependent structural changes of the ECM.
    - a) STED microscopy to study subcellular details of ECM in different neuronal sub compartments.
- 2) **What is the impact of ECM modulation on synaptic function?**

Investigation of molecular hallmarks of synaptic plasticity and structural changes after pharmacologically inhibiting or enhancing ECM modulation.

- a) Quantification of ECM-dependent alterations of the molecular hallmarks of synaptic plasticity pharmacologically by inhibiting or enhancing ECM modulation.
- b) Measuring morphological changes using mice expressing YFP in sparse neurons before and after interference with protease activity.

**3) What is the impact of sheddases on the bidirectional signaling between neurons and oligodendrocyte precursor cells (OPC)?**

## 2. Materials and methods

---

### 2.1 Materials

#### 2.1.1 Chemicals

Chemicals used in all experiments were purchased from the following companies: Invitrogen, Tocris, Sigma-Aldrich, Merck, Roth, Abcam, and Roche. Buffers for protein biochemistry experiments were prepared by using deionized-double distilled water (Seralpur ProCN®, Seral) and for the molecular biology experiments were prepared in ultra-pure water (Milli-Q® System Millipore). Chemicals used for this thesis work are listed below and some of the chemicals and buffers are described in the method section.

#### 2.1.2 Animals

In this work Wistar rats from the animal facilities of the Leibniz Institute for Neurobiology (Magdeburg, Germany) were used. All animal housing and experimental procedures were authorized and approved by the Institutional State and Federal Government regulations (Land Sachsen-Anhalt, Germany).

#### 2.1.3 Antibodies used for WB, IF, and IHC

The primary and secondary antibodies used for Western blotting (WB), immunofluorescence (IF) and immunohistochemistry (IHC) are listed in the table below.

**Table 1. List of the primary antibodies and the dilutions used**

Antibody	Dilution	Species	Company
Aggrecan	1:250	rabbit	Millipore
Aggrecan	1:500	mouse	abcam
Brevican	1:1500	mouse	BD Biosciences
Brevican	1:2000	guinea pig	Prof. Seidenbecher/ Dr. Frischknecht
$\beta$ -actin	WB 1:3000	mouse monoclonal	Sigma
$\beta$ -tubulin-III	WB 1:3000	mouse monoclonal	Sigma
$\beta$ 1-integrin	1:25	rat	BD Pharmingen

(CD29)			
Homer	1:500	mouse and guinea pig	Synaptic system
CaMKII	1:200	mouse	Santa Cruz
p- CaMKII	1:200	mouse	Santa Cruz
MAP2	IF 1:500	rabbit polyclonal	Millipore
p-ERK	WB 1:3000	mouse monoclonal	Sigma
pan-ERK	WB 1:3000	rabbit	Stressgene
Pan-ERK	WB 1:3000	rabbit	Cell signaling
PSD-95	WB 1:1000	mouse	BD Transduction
GM130	IF 1:500	rabbit	Abcam

**Table 2. List of secondary antibodies and dilutions used**

<b>Antibodies</b>	<b>Species</b>	<b>WB dilution</b>	<b>IHC dilution</b>	<b>Company</b>
anti-mouse, rabbit or guinea pig IgG, Alexa Fluor™ 488 - conjugated	goat or donkey		1:1000	Invitrogen
anti-mouse, rabbit or guinea pig IgG Cy3™- conjugated	goat or donkey		1:1000	Jackson Immuno Research
anti-mouse, rabbit or guinea pig IgG Cy5™- conjugated	goat or donkey		1:1000	Jackson Immuno Research
anti-mouse or -rabbit IgG, IRDye™-800CW	goat or donkey	1:15,000		Invitrogen
anti-mouse or -rabbit IgG, IRDye™-800CW	goat or donkey	1:15,000		Rockland
Abberior STAR 580			1:100	Abberior GmbH
Atto 647N			1:500	Atto-Tec GmbH

**Table 3. Pharmacological treatments on acute hippocampal slices**

<b>Name</b>	<b>Working concentration</b>	<b>Function</b>	<b>Company</b>
Autocamtide-2	20 $\mu$ M	calmodulin-dependent protein kinase II (CaM kinase II) inhibitor	Sigma-Aldrich
GI254023X	5 $\mu$ M	ADAM10 inhibitor	Gift from Prof A. Ludwig
Anisomycin	20 $\mu$ M	Protein and DNA synthesis inhibitor	Sigma-Aldrich
Bicuculline methiodide	50 $\mu$ M	Antagonist of GABA <sub>A</sub> receptors	Tocris Bioscience
Carbenoxolone disodium salt	100 $\mu$ M	Broad spectrum blocker of gap junction	Sigma-Aldrich
CD29	200 $\mu$ l/5ml	Beta-integrin blocker	R&D biosystem
Chondroitinase (ChABC)	0.1 u / 500 $\mu$ l	Removal of Chondroitin Sulfate and Dermatan Sulfate side chains of proteoglycans	Sigma-Aldrich
D-(-)-2-Amino-5-phosphonopentanoic acid (D-AP5)	50 $\mu$ M	Antagonist of NMDARs	Tocris Bioscience
D-serine	10 $\mu$ M	Glycine agonist at the NMDA receptor	Tocris Bioscience
Furin Inhibitor I	30 $\mu$ M	Blocks furin activity	Merck Millipore
Endothelin-1	1 $\mu$ M	Blocks coupling between astrocytes	Sigma-Aldrich
GM6001	25 $\mu$ M	Broad spectrum MMPs inhibitor	Tocris Bioscience
Hexa-D-Arginine	0.58 $\mu$ M	PACE4 inhibitor	Tocris Bioscience
Ifenprodil Hemi tartrate	3 $\mu$ M	NMDA receptor antagonist	Tocris Bioscience
4-Aminopyridine (4-AP)	2.5 mM	Potassium channel	Sigma-Aldrich



		blocker	
Picrotoxin	50 $\mu$ M	GABAA receptor antagonist	Sigma-Aldrich
Nifedipine	50 $\mu$ M	L-type VDCC blocker	Tocris Bioscience
6-Cyano-7-nitroquinoxaline-2,3-dione disodium (CNQX)	10 $\mu$ M	AMPA receptors blocker	Tocris Bioscience
Forskolin	50 $\mu$ M	Adenylyl cyclase activator	Tocris Bioscience
Rolipram	0.1 $\mu$ M	Selective cAMP-specific phosphodiesterase (PDE4) inhibitor	Tocris Bioscience
Ro 25-6981	1 $\mu$ M	Selective blocker of NMDA receptors containing the NR2B subunit	Tocris Bioscience
NMDA	50 $\mu$ M	NMDA receptor agonist	Tocris Bioscience
Tetrodotoxin (TTX)	1 $\mu$ M	Sodium channel blocker	Sigma-Aldrich
Timp-3	15 nM for slices	ADAMTS-4 inhibitor	R&D system

**Table 4. Sodium dodecyl sulfate polyacrylamide gel electrophoresis (SDS-PAGE)**

<b>Buffer</b>	<b>Composition</b>
4 x SDS sample buffer	250 mM Tris, pH 6.8, 1 % (w/v) SDS, 40% (v/v), glycerol, 4 % $\beta$ -mercaptoethanol, 0.02 % bromophenol blue
Tissue lysis buffer	50 mM Tris-Cl pH 7.5, 150 mM NaCl, 1 mM EDTA, 1 mM EGTA, 2% sodium dodecyl sulfate, Complete Protease Inhibitor Cocktail (Roche) 1 Tbl. per 10 ml, PhosSTOP Phosphatase Inhibitor Cocktail (Roche) 1 Tbl. Per 10 ml and benzonase 1 $\mu$ l per 1 ml.
Stacking buffer	0.5 M Tris pH 6.8
Rotiphorese 30	30 % Acrylamid, 0.8 % Bisacrylamide (Carl Roth)
Separation gel (20 %)	8.25 ml separation buffer, 7.5 ml 87 % Glycerol, 16.5 ml 40 % Acrylamide, 330 $\mu$ l EDTA (0.2 M), 22 $\mu$ l TEMED, 120 $\mu$ l 0.5 % Bromophenol blue and 75 $\mu$ l 10 % APS

Separation gel (5 %)	8.25 ml separation buffer, 17.94 ml dH <sub>2</sub> O, 1.89 ml 87 % Glycerol, 4.12 ml 40 % Acrylamide, 330 µl EDTA (0.2 M), 22 µl TEMED and 118 µl APS
Stacking gel (5%)	6 ml stacking buffer, 7.95 ml dH <sub>2</sub> O, 5.52 ml 87% Glycerol, 3.90 ml 30 % Acrylamide, 240 µl EDTA (0.2 M), 240 µl 10% SDS, 17.2 µl TEMED, 30 µl, Phenol red and 137 µl - 10% APS
Electrophoresis buffer	192 mM glycine, 0.1 % (w/v) SDS, 25 mM Tris, pH 8.3
Molecular weight marker	Page rules, prestained marker (Fermantas)
Coomassie brilliant blue staining solution	1 mg/1000 ml Coomassie brilliant blue R-250, 60 % (v/v) methanol, 10 % (v/v) acetic acid
Destaining solution	7 % (v/v) acetic acid, 5 % (v/v) methanol
Drying solution	50% (v/v) methanol, 5% (v/v) glycerol

**Table 5. Immunoblotting**

Buffer	Composition
Blotting buffer	192 mM Glycine, 0,2 % (w/v) SDS, 18 % (v/v) methanol, 25 mM Tris pH 8,3
1 x TBS	50 mM Tris, 150 mM NaCl, pH 7.5
1 x TBS-T	50 mM Tris, 150 mM NaCl, 1 % Tween-20 pH 7.5
PVDF membrane	Roti®-Fluro PVDF (Roth)
10x PBS	1.4 M NaCl, 83 mM Na <sub>2</sub> HPO <sub>4</sub> , 17mM NaH <sub>2</sub> PO <sub>4</sub> , pH 7.4
Blocking solution	5% (w/v) non-fatty milk powder / 5% (w/v) BSA in 1x TBS-T

**Table 6. Buffers for immunohistochemistry**

Buffer	Composition
4 % PFA (w / v)	4 % PFA in PBS pH 7.4
Blocking Solution	10 % FCS in PBS, 0,1 % Glycin, 0.3 % Triton X-100
1 x PBS	2,7 mM KCl, 1,5 mM KH <sub>2</sub> PO <sub>4</sub> , 137 mM NaCl, 8 mM Na <sub>2</sub> HPO <sub>4</sub> , pH 7,4
Mowiol (96 ml)	9.6 g Mowiol, 24 ml H <sub>2</sub> O, 24 g Glycerol → 2 h stirring, 48 ml 0.2 M Tris pH 8.5 → 10 min 50 °C, 2.5 g DABCO
Vectashield® (with	Mounting medium (Vector Laboratories Inc.)

DAPI)	
Fluoromount-G™, with DAPI (eBioscience)	Used as mounting medium

**Table 7. Components of Amido black assay**

Buffer	Composition
Amido black solution	14.4 g of amido black in 1l of methanol- acetic acid
Methanol-acetic acid	Methanol: acetic acid= 9 : 1
BSA stock solution	0.5g/ml

**Table 8. Components of Enzymatic extraction of ECM**

Buffer	Composition
aCSF	125 mM NaCl, 2.5 mM KCl, 1.25 mM NaH <sub>2</sub> PO <sub>4</sub> , 25 mM NaHCO <sub>3</sub> , 2 mM CaCl <sub>2</sub> , 1 mM MgCl <sub>2</sub> , 25 mM glucose
Tyrod's buffer	145 mM NaCl, 5 mM KCl, 10 mM glucose, 10 mM HEPES, 2 mM CaCl <sub>2</sub> , 2 mM MgCl <sub>2</sub>
ECM digestion buffer	0.1 M Tris-HCL, pH 8.0, 0.03 M sodium acetate

## 2.2 Biochemical methods:

### 2.2.1 Protein concentration determination using Amido black assay

Protein concentration was determined by the colorimetric amido black assay. 0 to 20 µg of BSA was used to prepare the standard curve. In order to measure the unknown concentration, 2 - 5 µl of samples were used and the final volume was made up to 100 µl with double distilled water. 200 µl of amido black solution was added to both the standard and sample solutions. All samples were incubated for 20 minutes at room temperature and centrifuged at 13,000 g for 5 minutes. The pellet was washed with methanol-acetic acid (9:1) twice and finally resuspended in 500 µl of NaOH (0.1 N). The absorption was measured at 620 nm against NaOH using a microplate reader.

### 2.2.2 SDS-Page using Laemmli system

Proteins were separated using one-dimensional sodium dodecyl sulfate polyacrylamide gel electrophoresis (SDS-PAGE) under fully denaturing and reducing conditions (Laemmli 1970). Gradient gels were prepared in which the separating gel had an acrylamide

concentration of 5 % on top to 20 % at the bottom, with the components mentioned in table 4. Protein samples were diluted with 4 x SDS sample buffer and boiled at 95 °C for 5 min, centrifuged at 14000 g for 10 min and supernatant were loaded on the gel. Gels were placed in an electrophoresis chamber (Mighty Small II MINI Vertical Electrophoresis Unit, Hoefer) and filled with electrophoresis buffer. The gel run was performed with constant 8 mA within the stacking gel and 12 mA during the separation phase. After the SDS-page gels were either used for Western Blotting or they were stained with Coomassie stain solution till proper staining. Coomassie stained gels were kept in destaining solution till the protein bands get visible. For quantification, the gels were scanned by Odyssey Infrared Imaging System (LI-COR Bioscience).

### **2.2.3 Western blotting**

Proteins were electrotransferred from polyacrylamide gels to Roti-Fluoro PVDF transfer membranes (polyvinylidene fluoride membrane; PVDF). The membrane was activated in methanol for 30 sec. The transfer was performed in a Western Blot chamber (Hoefer) filled with blotting buffer at 4 °C for 1 hr 45 min with 200 mA. After the transfer, the membrane was rinsed again with methanol and air dried.

### **2.2.4 Immunoblot detection**

PVDF membrane was blocked in TBS-T containing 5 % BSA for 30 min at room temperature. Primary antibodies were diluted in TBS-T containing 2 % BSA and probed for 2 hrs at room temperature or overnight at 4 °C. After three times washing with TBS-T secondary antibodies diluted in TBS-T were incubated for 45 min at room temperature. After two washes with TBS-T, final washing needs to be done with TBS since Tween-20 interferes with the upcoming scanning procedure. Immunodetection was performed with an Odyssey Infrared Imaging Scanner (LI-COR Bioscience).

### **2.2.5 Quantification of Western blot**

Quantitative immunoblots were detected using Odyssey Infrared Scanner (LI-COR). Integrated density of signals (ID) was measured using Image J software by setting rectangular ROIs around the bands, which had identical dimensions within each experimental group analyzed on the same membrane. Values were normalized to respective loading controls (GAPDH or  $\beta$ -actin) and to the average value of the control group for each individual

membrane. In figures molecular weight of markers are given in kDa, antibodies used for immunodetection on Western blots (WB) are indicated.

### 2.2.5.1 Normalization methods

#### 2.2.5.1.1 Coomassie staining normalization

After Western blotting SDS-PAGE gels are processed for Coomassie staining (Figure 5) and images were taken by LI-COR once the gels are ready after destaining. It was quantified using Image J software by setting rectangular ROIs around the whole vertical lane which had identical dimensions around each lane. I measured intensities of each probe and it was used to normalize their respective probes and I performed analysis for Western blots as mentioned in the previous section.

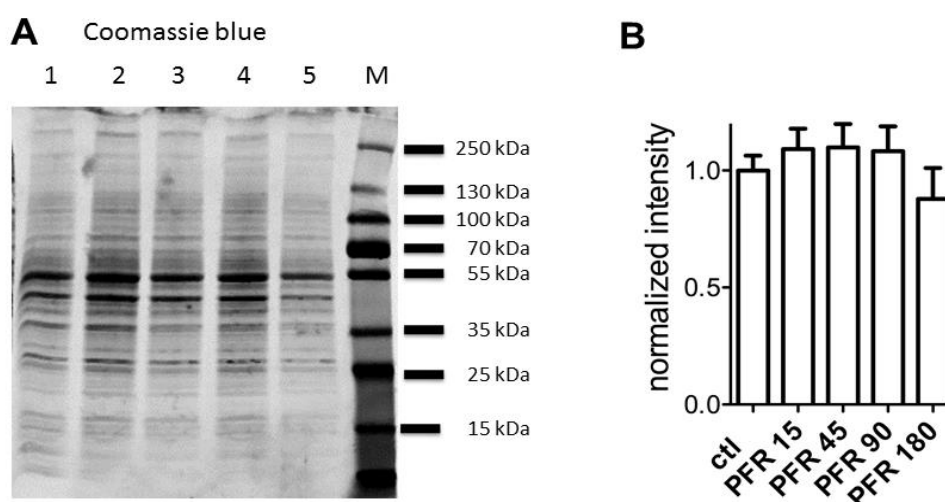


**Figure 5. Coomassie gel used for normalization of probes**

(A) Coomassie-stained SDS-PAGE gels were used to normalize their corresponding lanes of the samples from the Western blot. Lanes 1 to 5 are the probes loaded to be tested, protein marker (M).

(B) Graph representing the normalized values in duplicates from one experiment, to be used for normalization of Western blot.

#### 2.2.5.1.2 2,2,2-Trichloroethanol (TCE) normalisation

TCE was incorporated into the SDS-PAGE gels 50  $\mu$ l / gel in the separating gel. This provides fluorescent detection of proteins after ultraviolet (UV) activation for 2-3 min of the gels on 300-nm UV transilluminator. These gels were left to be blotted and then rescanned with short exposure of UV and then the image is processed by Image J, as mentioned in the

previous section of Coomassie normalization (Figure 6). This method of normalization should be more specific as blotted proteins were normalized from values from the same blot.

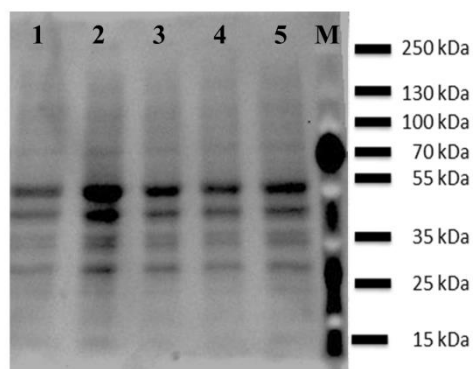


**Figure 6. TCE used for normalisation**

Samples from ECM extractions were loaded and analysed using Image J software. Values obtained from this UV scan were used for normalising the respective western blots. lanes 1 to 5 are the different probes and protein size markers (M) are given.

### **2.2.6 Acute hippocampal slice preparation**

10 weeks old Wistar rats were anesthetized with isoflurane. After decapitation, the brain was rapidly removed and immersed in an oxygenated ice-cold artificial cerebrospinal fluid (aCSF). Hippocampi were isolated in an oxygenated ice-cold aCSF and transverse hippocampal slices (350  $\mu\text{m}$ ) were prepared using a McIlwain tissue chopper (Mickle Laboratory). Slices were left to recover at room temperature for 90 min and then recovered at 32  $^{\circ}\text{C}$  for 1hr. During the whole procedure, the slices were perfused with aCSF solution which was bubbled with 95%  $\text{O}_2$  and 5%  $\text{CO}_2$ .

### **2.2.7 Enzymatic extraction of ECM with Chondroitinase ABC and induction of activity-dependent modulation**

Chemical LTP (cLTP) was induced and slices were collected in enzymatic extraction buffer (Tyrod's buffer containing chondroitinase ABC (0.1M Tris-HCL, pH 8.0 containing 0.03M Sodium acetate) for digestion of CSPGs (chondroitin sulfate proteoglycan) as described (Deepa et al., 2006). For three slices 90  $\mu\text{l}$  of the ECM extraction buffer was used. The buffer was also supplemented with Complete Protease Inhibitor Cocktail (Roche), PhosSTOP Phosphatase Inhibitor Cocktail (Roche) were triturated and centrifuged at 14000g. The supernatant was collected (ECM proteins are expected to be present there) and finally 4 x SDS Laemmli buffer was added, samples were boiled and SDS-PAGE was performed. Samples were stored at -80  $^{\circ}\text{C}$  until they were used for SDS page.

## 2.2.8 Immunostaining in hippocampal slices

Hippocampal slices were obtained as mentioned in section 2.2.5 and were used for induction of LTP as described in the previous section. After the induction of LTP, the slices were fixed with 4% PFA for overnight at 4°C. Slices were placed in 30% sucrose until they settle down. Slices were resliced at cryotome (Leica CM 3050 S ) 30 µM for ease of antibody penetration. Slices were permeabilized in 0.3% Triton X-100 in blocking solution (buffer composition described in section) and as well were blocked at room temperature. Primary antibodies diluted in blocking buffer were added to the slices and incubated for 72 hrs at 4°C. Then the slices were washed 3-4 times with 1X PBS buffer and incubated with secondary antibodies for overnight at 4°C in blocking buffer. Slices were washed 3-4 times with 1X PBS buffer and sections were washed once with MiliQ. It was mounted on a glass slide and sections were left to dry on a glass slide and Fluoromount-G™, with DAPI, was placed on sections and glass coverslip was placed on it. The images were taken using confocal laser scanning microscopy and analysed using ImageJ program.

## 2.2.9 Pharmacological treatments in acute hippocampal slices

Chemical stimulation with a combination of picrotoxin, forskolin and rolipram (PFR) in aCSF with no Mg<sup>2+</sup> was given for 15 min. After the treatment slices were collected in ECM extraction buffer as mentioned above. All the inhibitors were incubated 20-30 min prior to stimulation and were present till the end of the recovery after the chemical stimulation (Figure 7). Treatment with 2.5 mM 4-aminopyridine and 50µM bicuculline (4AP + BCC) for 10 min and subsequently 20 min recovery time was carried out under the same conditions. List of pharmacological agents and their working concentrations are mentioned in Table 3.

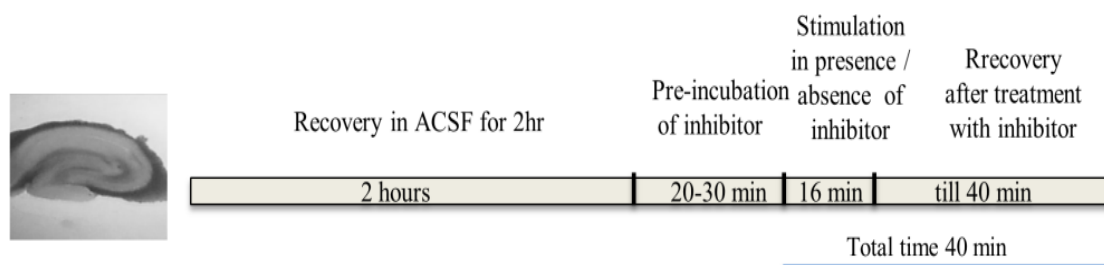


**Figure 7. Treatment paradigm for cLTP induction in the acute hippocampal slices.**

## **2.3 Microscopy and image analysis**

### **2.3.1 Confocal microscopy**

Confocal images were obtained using a Leica SP5 confocal microscope (LAS AF software, version 2.0.2; 1024x1024 pixels display resolution, 12-bit dynamic range, 63 X objectives, NA 1.40, 3 X optical zoom, pixel size app. 60 nm). Images were taken with 63 X, oil or 10 X objective as z-stacks (250 nm or 500 nm z step) based on the sample using a Leica SP5 microscope (Wetzlar, Germany) equipped with a Krypton-Argon-Ion laser (488/568/647 nm) and an acoustic-optic-tunable filter (AOTF) for selection and intensity adaptation of laser lines. Usually, 10-12 optical sections were taken with a step size of 250 nm and two-time line average at 400 Hz laser frequency. Maximum intensity projections were calculated from each fluorescence channel of the three optical frames from the image stack. Analysis was performed via using Image J (NIH, <http://rsb.info.nih.gov/ij/>).

Quantitative immunofluorescence (IF) analyses were performed using Image J and OpenView software to quantify the ECM staining around the synaptic marker (Tsuruel et al., 2006). Threshold subtraction and measurements of nuclear IF were done in a mask created according to DAPI staining using NIH ImageJ. In all experiments, synaptic puncta were defined semi-automatically by setting rectangular regions of interest (ROI) with dimensions of 0.8 X 0.8  $\mu\text{m}$  around local intensity maxima in the channel with staining for synaptic marker homer using OpenView software. Mean IF intensities were measured around synaptic ROIs in all corresponding channels using the same software and normalized to the mean IF intensities of the control group for each of the experiments.

### **2.3.2 STED microscopy**

Dual-color STED images were acquired using Leica TCS-Sp5 Ti: Sapphire dual-color STED microscope (1024x1024 pixels display resolution, 8-bit dynamic range, 100x objective, NA 1.40, 6x optical zoom, pixel size app. 25nm). Abberior STAR 580 and Atto 647N were excited using the setup pulsed diode lasers (<90 ps, 80 MHz, Pico Quant) at 531nm and 635nm and detection were done at 589-625nm and 655-685nm, respectively. Depletion was done at 730nm for the Abberior STAR 580 and at 750nm for Atto 647N. Frames were acquired at a scan speed of 700 Hz by applying 48 times line averaging. All acquired STED stacks were subsequently deconvoluted using the Huygens professional STED package (Scientific Volume Imaging, v 4.4.).



### 2.3.3 Processing of Slick V-cre slices for spine head protrusions (SHP) analysis:

Slices were re-sectioned to 50  $\mu\text{m}$  after 4% PFA overnight fixations and placing in Sucrose solution. Slices were mounted and made ready for the acquisition of images from confocal microscopy with 250 nm step size. Images were taken with 1024 x 256 pixels display resolution, 12-bit dynamic range, 63X objective, NA 1.40, 4 – 6X optical zoom, line average three times at 200 Hz. Apical secondary dendrites approximately 80  $\mu\text{m}$  far from soma were selected for dendritic protrusions analysis, images were first processed by Fiji software and stacks were set to maximum intensity. Images were applied for further processing by Process-CLAHE-keep it default and uncheck for the fast one (block size-127, histogram bins: 256, maximum slope: 3 mask: none). Images were saved as tiff file format with modification with less background, then these images were processed by neuron studio program.

## 2.4 LC-MS/MS Analysis

**Table 9. Buffer for LC-MS/MS**

Buffer	Composition
100 mM ammonium bicarbonate, pH 7.8 ~ 8.0	Ammonium bicarbonate ( $\text{NH}_4\text{HCO}_3$ ; 99%; Fluka, Steinheim, Germany); 0.39g, Deionized water; fill up to 50 mL
50 mM ammonium bicarbonate / 50% (v/v) acetonitrile	Acetonitrile (HPLC grade; JT Baker, Deventer, Holland); 25 mL, 100 mM $\text{NH}_4\text{HCO}_3$ : 25 mL
Trypsin solution	6.7 $\mu\text{g}$ / mL trypsin (sequence grade; Promega, Madison, USA) in 50 mM ammonium bicarbonate: 20 $\mu\text{g}$ trypsin dissolved in 3ml 50 mM ammonium bicarbonate
0.1% Trifluoroacetic acid / 50% acetonitrile	Acetonitrile:25 mL, Deionized water: fill up to 49.8 mL, 25% Trifluoroacetic acid (TFA; Protein sequence grade; Applied Biosystems, Warrington, UK); 0.2 mL

### 2.4.1 Fractionation of proteins by SDS-PAGE

10% SDS polyacrylamide gel was prepared and probes from cLTP treated acute hippocampal slices were run. The gels were stained with colloidal Coomassie blue.

### 2.4.2 Gel cutting

Since the aim of this analysis was to monitor the changes in ECM modulation upon activity, the gel was divided into two halves at 70 kDa. So each lane was divided into two and

processed (see Figure 8). Protein bands were excised and cut each gel pieces into small fragments using a scalpel and transferred to 1.5 ml Eppendorf tube.

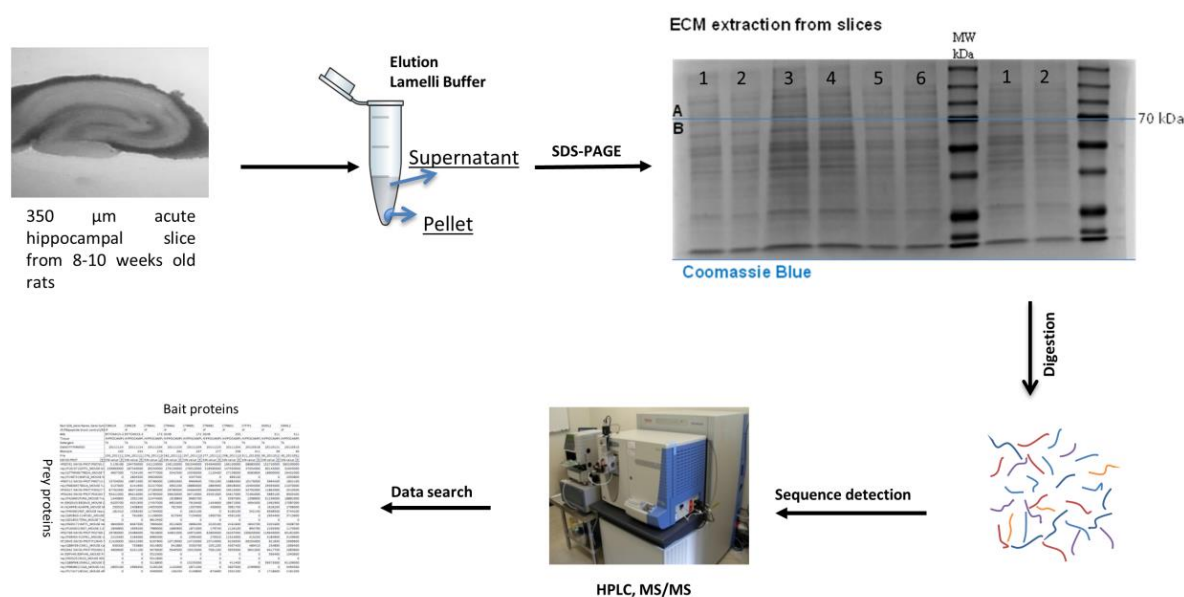


**Figure 8. Workflow of LC-MS/MS activity-dependent ECM assay**

Analysis of activity-dependent modulation of ECM protein complexes fractionated on a 10% SDS gel. Samples from 1-6 lanes were loaded followed by the marker and two more samples and the marker. The Coomassie blue stained gel from each lane was cut into two halves and as indicated by the blue line. The cut was guided by the position of the marker proteins and then each lane was cut into subsequent smaller pieces for processing as shown in the workflow.

### 2.4.3 Destaining

500 μl of 50 mM  $\text{NH}_4\text{HCO}_3$  / 50% acetonitrile was added to the gel fragments, vortexed for 20 min. The solution was discarded and 200 μl 100% acetonitrile was added and vortexed for 20 min. The gel fragments turned white and shrunk, acetonitrile was removed and discarded. 100 μL 50 mM  $\text{NH}_4\text{HCO}_3$  was added and incubated for 5 min at room temperature. 400 μl of 50 mM  $\text{NH}_4\text{HCO}_3$  / 50% acetonitrile was added and left to incubate overnight to destain the gel fragments completely, solution was removed and discarded.

### 2.4.4 Drying

200 μL 100% acetonitrile was added and vortexed for 20 min, solution was removed and the gel was dried in a SpeedVac for 30 min.

### 2.4.5 In-gel tryptic digestion

Dried gel fragments were re-swelled at 4°C for 45 min in buffer containing trypsin. Trypsin was just added enough to cover the gel fragments (50-120 μL trypsin solution/slice). 50 μL 50 mM  $\text{NH}_4\text{HCO}_3$  was added and left to digest overnight at 37°C.

#### **2.4.6 Peptide extraction and storage**

200  $\mu$ L 0.1% Trifluoroacetic acid / 50% acetonitrile was added to the gel pieces and incubated for 20 min. This step extracts the remaining peptides from the gel piece. The solution was removed and put into the same Eppendorf tube that contains the tryptic peptides diffused out of the gel piece first. This step was repeated once; solution was pooled and dried the peptide solution in SpeedVac as stated before. The samples can be stored at  $-20^{\circ}\text{C}$  for months before further analysis.

#### **2.4.7 Peptides dissolve for HPLC**

Re-dissolved the samples in 18  $\mu$ L 0.1% acetic acid, vortexed for 5 min. Transfer 16.5  $\mu$ L of the solution to a sample vial, cap the vial and put it into the loading tray at  $4^{\circ}\text{C}$ .

### **2.5 Statistical analysis**

All results of quantitative analyses are given as means  $\pm$  standard errors of the mean (SEM). Statistical analyses were performed with Prism 5 software (GraphPad Software, Inc.) using one-way ANOVA with dunnett's multiple comparison tests or Student's t-test as indicated in each figure. Statistical significance is marked as \* $p < 0.05$ , \*\* $p < 0.01$ , \*\*\* $p < 0.001$  in all plots.

### 3. Results

#### 3.1 Validation of enzymatic extraction of ECM with Chondroitinase ABC and induction of activity-dependent modulation

To assess activity-dependent modulation of ECM acute hippocampal slices were prepared and ECM was extracted. For this purpose I incubated slices with chondroitinase ABC (Ch ABC), an enzyme that digests the glycosaminoglycans (GAG) chondroitin sulfate and hyaluronic acid (HA) and thus releases ECM proteins to the supernatant (Seidenbecher et al., 2002). Immunostaining was performed to control the efficacy of enzymatic extraction of ECM on acute hippocampal slices.

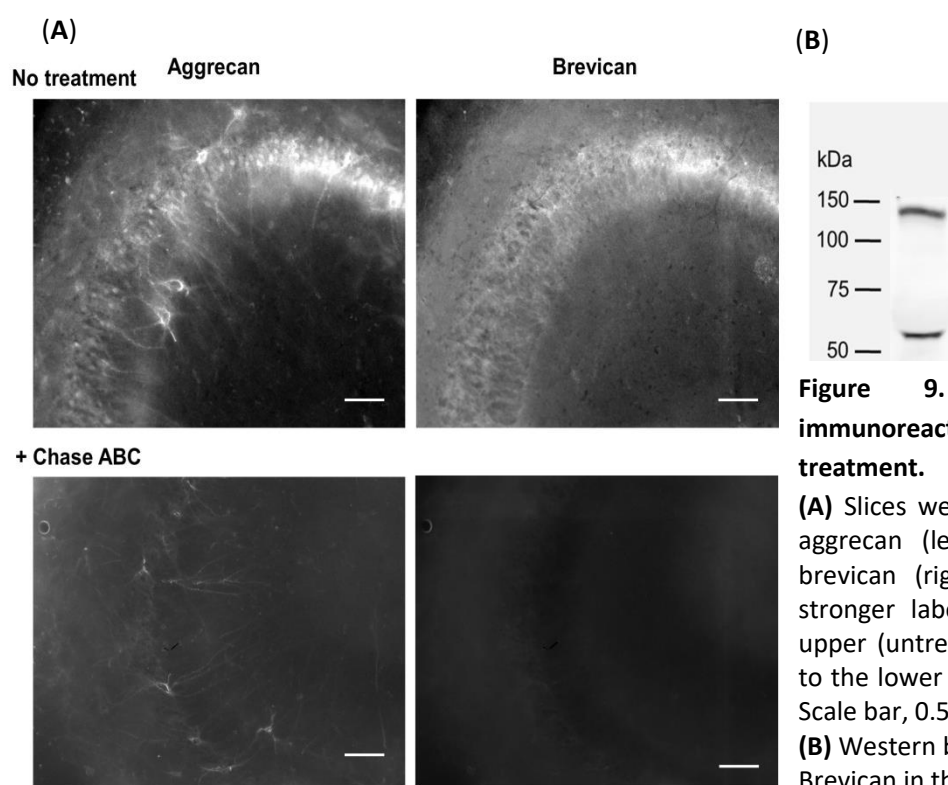


**Figure 9. Reduced ECM immunoreactivity after Ch ABC treatment.**

**(A)** Slices were stained using rb  $\alpha$  aggrecan (left panel) and gp  $\alpha$  brevican (right panel). Note the stronger labeling intensity in the upper (untreated) slices compared to the lower Ch ABC-treated slices. Scale bar, 0.5cm.

**(B)** Western blot showing extracted Brevican in the supernatant.

Slices were co-stained using antibodies against aggrecan and brevican, two well-established marker proteins for the mature ECM of the brain. As expected there was a strong reduction of staining intensity in chondroitinase ABC-treated samples as depicted in Figure 9.

The aforementioned approach suggests that proteoglycans could be extracted for biochemical analysis and for a candidate approach to search for upregulated ECM proteins upon activity-dependent modulation of ECM.

The goal of the following experiments was to investigate extracellular proteolysis during synaptic plasticity. To achieve this I have decided to use treatment with the chemical stimulants picrotoxin, forskolin and rolipram (PFR), which has been shown to induce cLTP previously (Otmakhov et al., 2004a). To validate the stimulation protocol for time of stimulation and effectivity in my system, further samples were analysed for known LTP hallmarks such as phosphorylation of extracellular signal-regulated kinases (ERK) and  $Ca^{2+}$  / calmodulin-dependent protein kinase II (CamKII). For that purpose slices were homogenized and subjected to Western Blot and increased phosphorylation of ERK was observed after stimulation with PFR for 16 min and recovery in fresh aCSF for 25 min (Figure 10A). A similar effect was observed with an alternative chemical stimulation using 4-aminopyridine and bicuculline (4AP + BCC) for 10 min and recovery for 30 min in aCSF. Phosphorylation of CamKII upon PFR stimulation was in line with ERK phosphorylation (Figure 10C). This suggests that chemical stimulants indeed elicited an LTP-like status in my model system.

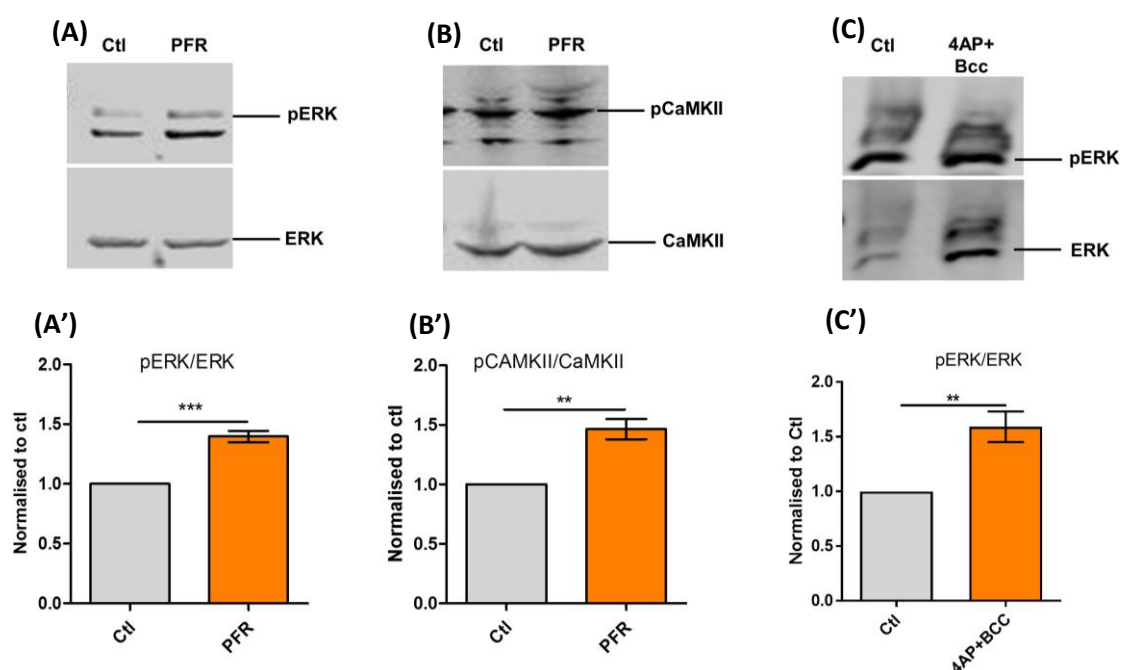


**Figure 10. Two different pharmacological stimulation paradigms led to chemical LTP in acute hippocampal slices as measured by increased phosphorylation of ERK and CamKII.**

**(A)** Quantified the Western blot of acute hippocampal slices with ms  $\alpha$  pERK and rb  $\alpha$  ERK specific antibody with above mentioned conditions. **(A')** PFR stimulation leads to phosphorylation of ERK; it has been shown here via specific antibodies. All values are normalized to control (Ctl = 1.0, n = 6, 3 slices / n; PFR =  $1.39 \pm 0.04$ , n = 6; mean  $\pm$  SEM; Unpaired t test,  $P < 0.0001$ ).

**(B)** Quantified the Western blot of acute hippocampal slices with ms  $\alpha$  CaMKII and rb  $\alpha$  pCaMKII specific antibody with above mentioned conditions. **(B')** A PFR stimulation leads to phosphorylation of CaMKII as shown here via specific antibodies. All values are normalized to control (Ctl = 1.0, n = 6, 3 slices / n; PFR =  $1.46 \pm 0.08$ , n = 6; mean  $\pm$  SEM; paired t test,  $P = 0.0028$ ).

(C) Quantified the Western blot of acute hippocampal slices with ms  $\alpha$  pERK and rb  $\alpha$  ERK specific antibody with above mentioned conditions. (C') 4AP + BCC stimulation also leads to increased phosphorylation of ERK. All values are normalized to control (Ctl = 1.0, n = 6, 3 slices / n; PFR =  $1.59 \pm 0.14$ , n = 6; mean  $\pm$  SEM; Unpaired t test, P = 0.0018).

### 3.2 Activity-induced proteolytic cleavage of brevican and ultrastructure representation of perisynaptic brevican

To monitor modulation of ECM I focused mainly on brevican as representative however in key experiments I also measured aggrecan proteolytic cleavage. Brevican was detected by both commercial pan brevican as well home-made neo-epitope antibodies which are specific to N-terminal cleavage fragment (~53kDa). The neo-epitope antibody is specific to new C-terminal emerging after proteolytic cleavage of brevican by several members of the ADAMTS family of metalloproteases. It detects exclusively the N-terminal cleavage fragment but not the recombinant protein with an additional amino-acid added to the natural C-terminus. (Figure 11). This showed the specificity of neo-epitope antibody towards the cleavage fragment.

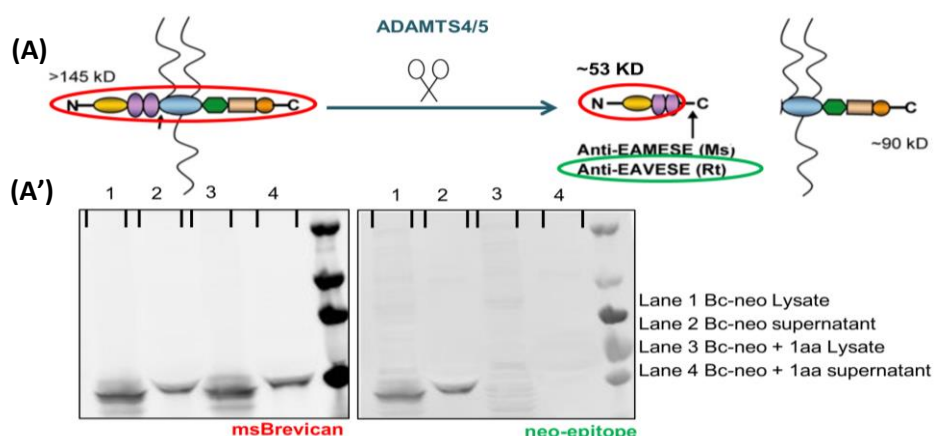


**Figure 11. Specificity of brevican cleavage detected by antibody.**

(A) Schematic representation of brevican full length protein and protease dependent cleavage site after its proteolysis. (A') Western blot of overexpressed HEK cell medium of brevican with ms  $\alpha$  Brevican antibody recognizing 53 kDa cleavage band and neo-epitope specific antibody with above mentioned conditions.

It has been suggested by (Pizzorusso et al., 2002) that ECM is mature at around 10 weeks in rodents. To test this I performed PFR stimulation on slices from young (3-4 weeks) in figure 12C and adult of 8-10 weeks (Figure 12A) and 12-13 weeks (Figure 12B). Slices were collected at regular interval 15, 45, 90, 180 min after stimulation. For the biochemical analysis commercially available mouse anti--brevican recognising full-length at 145 kDa and cleaved brevican around 53 kDa, as well as home-made neo-epitope specific antibody.

Increased cleavage of brevican was found after the stimulation by PFR, suggesting that ECM could be modified upon activity even in mature state. Results from all three data sets from different age groups suggested that 30 min after a 16 min stimulation cleavage peaked among all the investigated time points. Levels of cleaved brevican slightly decreased with ongoing recovery time and returned to control levels at 180 min (Figure 12). For further experiments 30 min after stimulation was analysed from slices of 8-10 week old rats, since effects were most robust and reproducible at this time point.

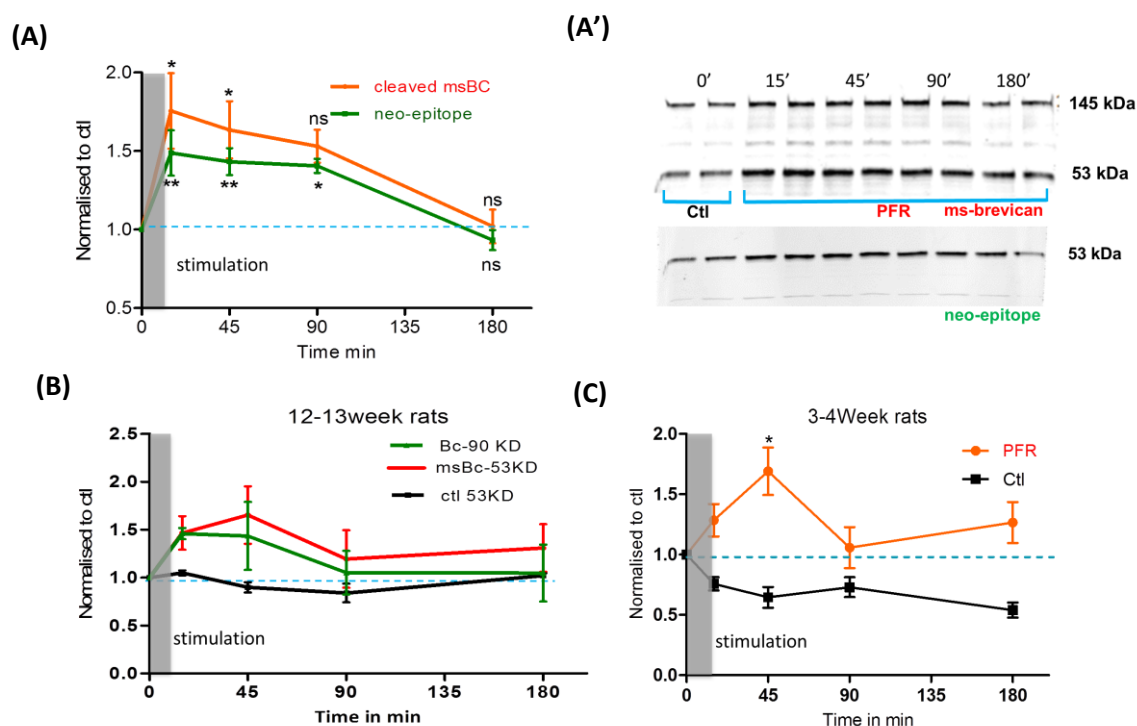


**Figure 12. Activity-Dependent Proteolytic Cleavage of brevican.**

**(A)** Quantification of cleaved fragment of brevican (53 kDa) in adult animals using ms  $\alpha$  brevican antibody (red line) and neo-epitope (green line). All values are normalized to control (**msBC** - Ctl = 1.0, n = 5, 3 slices / n; PFR 15' =  $1.64 \pm 0.21$ , n = 5; PFR 45' =  $1.55 \pm 0.16$ , n = 5; PFR 90' =  $1.45 \pm 0.10$ , n = 5; PFR 180' =  $1.02 \pm 0.10$ , n = 4; **neo-epitope** - Ctl = 1.0, n = 4, 3 slices / n; PFR 15' =  $1.48 \pm 0.14$ , n = 4; PFR 45' =  $1.43 \pm 0.08$ , n = 4; PFR 90' =  $1.40 \pm 0.04$ , n = 4; PFR 180' =  $0.93 \pm 0.06$ , n = 4; mean  $\pm$  SEM; One Way ANOVA, P = 0.0097 for cleaved msBC and for neo-epitope P = 0.0004, Dunnett's Multiple Comparison Test, \* P < 0.05, \*\* P < 0.01). **(A')** Quantified the Western blot of acute hippocampal slices with ms  $\alpha$  Brevican and neo-epitope specific antibody recognizing 53 kDa cleavage band with above mentioned conditions.

**(B)** Quantification of activity-dependent cleavage of brevican in mature (12-13 week old); it has been shown here via ms  $\alpha$  brevican (red line) and gp  $\alpha$  BC (green line) antibody. All values are normalized to control (**msBC** - Ctl = 1.0, n = 3, 3 slices / n; Ctl 15' =  $1.04 \pm 0.02$ , n = 3; Ctl 45' =  $0.89 \pm 0.05$ , n = 3; Ctl 90' =  $0.83 \pm 0.09$ , n = 3; Ctl 180' =  $1.02 \pm 0.02$ , n = 3; mean  $\pm$  SEM; One Way ANOVA, P = 0.0762, Dunnett's Multiple Comparison Test, ns; **msBC** - Ctl = 1.0, n = 3, 3 slices / n; PFR 15' =  $1.46 \pm 0.17$ , n = 3; PFR 45' =  $1.65 \pm 0.29$ , n = 3; PFR 90' =  $1.83 \pm 0.61$ , n = 3; PFR 180' =  $1.30 \pm 0.24$ , n = 3; mean  $\pm$  SEM; One Way ANOVA, P = 0.4889, Dunnett's Multiple Comparison Test, ns; **gpBC** - PFR 15' =  $1.45 \pm$

0.05, n = 3; PFR 45' = 1.43 ± 0.35, n = 3; PFR 90' = 1.05 ± 0.22, n = 3; PFR 180' = 1.04 ± 0.29, n = 3; mean ± SEM; One Way ANOVA, P = 0.4681, Dunnett's Multiple Comparison Test, non-significant).

(C) Quantification of activity-dependent cleavage of brevican in young (3-4 week old) animals acute hippocampal slices; it has been shown here via ms α brevican antibody. All values are normalized to control (msBC- Ctl = 1.0, n = 4, 3 slices / n; Ctl 15' = 0.75 ± 0.07, n = 4; Ctl 45' = 0.61 ± 0.10, n = 4; Ctl 90' = 0.66 ± 0.07, n = 4; Ctl 180' = 0.51 ± 0.07, n = 4; mean ± SEM; One Way ANOVA, P = 0.0026, Dunnett's Multiple Comparison Test, \* P < 0.05, \*\* P < 0.01, \*\*\* P < 0.001; msBC - 3 slices / n; PFR 15' = 1.28 ± 0.13, n = 6; PFR 45' = 1.69 ± 0.19, n = 6; PFR 90' = 1.05 ± 0.17, n = 6; PFR 180' = 1.26 ± 0.17, n = 6; mean ± SEM; One Way ANOVA, P = 0.0294, Dunnett's Multiple Comparison Test, \* P < 0.05).

In order to investigate whether activity-dependent proteolysis was specific for brevican or a more general mechanism, I also quantified aggrecan which is one of the key proteoglycan of the lectican family. Indeed, there was increased cleavage of aggrecan after cLTP induction with PFR compared to non-stimulated group (Figure 13A). Upon chemical stimulation with 4AP+Bcc similar results with increased cleavage of aggrecan was found as depicted in figure 13B. This suggests proteolysis is not specific for brevican but most likely affects most lecticans and therefore may generally affect the ECM structure and composition.

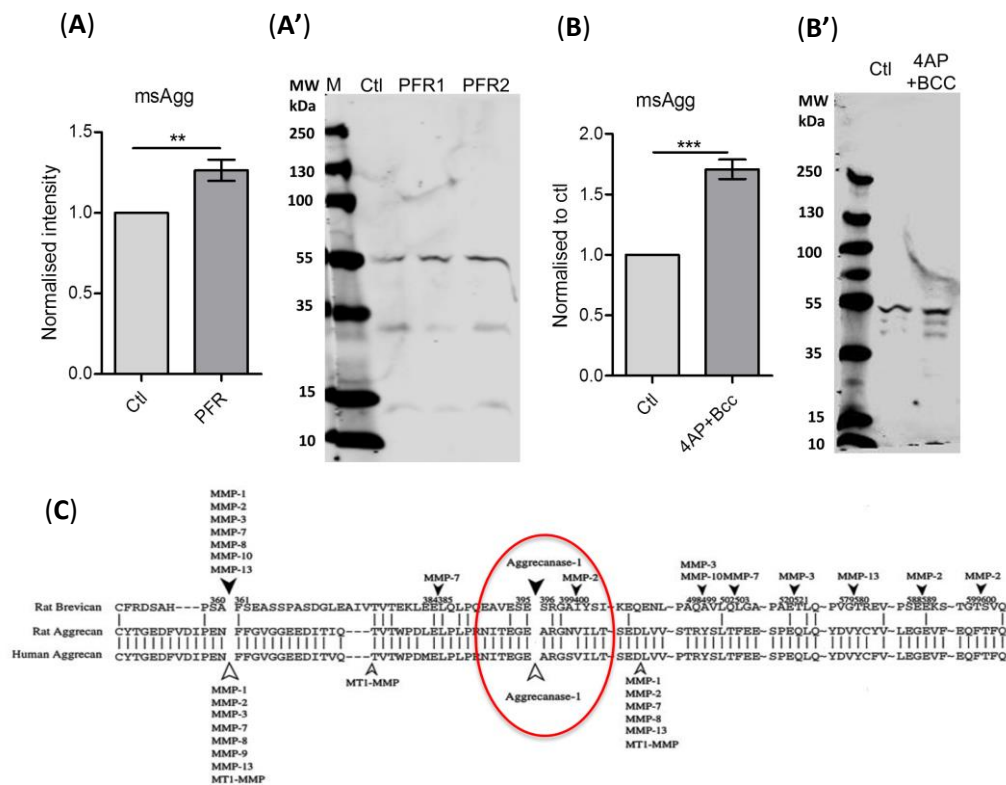


**Figure 13. Activity-dependent proteolysis of Aggrecan**

(A) Activity-dependent cleavage of aggrecan upon stimulation with PFR; it has been shown here via ms α aggrecan (Agg) antibody. All values are normalized to control (Ctl = 1.0, n = 5, 3 slices / n; PFR = 1.26 ± 0.06, n = 4; mean ± SEM; Unpaired t test, P = 0.00256, \*\* P < 0.01). (A') Quantified the Western blot of acute hippocampal slices with ms α Aggrecan antibody recognizing 53 kDa cleavage band with above mentioned conditions.

(B) Activity-dependent cleavage of aggrecan upon stimulation with 4AP+Bcc; it has been shown here via ms α aggrecan (Agg) antibody. All values are normalized to control (Ctl = 1.0, n = 3, 3 slices / n; 4AP+Bcc



=  $1.70 \pm 0.08$ ,  $n = 3$ ; mean  $\pm$  SEM; Unpaired t test,  $P = 0.0010$ , \*\*\*  $P < 0.001$ ). (B') Quantified the Western blot of acute hippocampal slices with ms  $\alpha$  Aggrecan specific antibody with above mentioned conditions. (C) Schematic representation of aggrecanase cleaving site shown in red circle for aggrecan in rat and human and rat brevican cleavage site (Nakamura et al, 2000)

Next I was interested whether I could detect brevican cleavage by immunocytochemistry after PFR stimulation in our slice system. For that purpose treated and untreated acute slices were fixed min after the treatment and further processed to slices of 30  $\mu$ m thickness (see material and method section 2.2.8 for details). Images were then taken by the confocal microscope and fluorescence intensities of the neuropil of treated hippocampal slices was quantified and compared to control slices. I observed increased immunostaining after stimulation in CA1 region of hippocampi in comparison to control slice (Figure 14). Since neuropil is rich of excitatory synaptic contacts and rarely contains cell bodies this pointed towards synaptic cleavage of brevican.

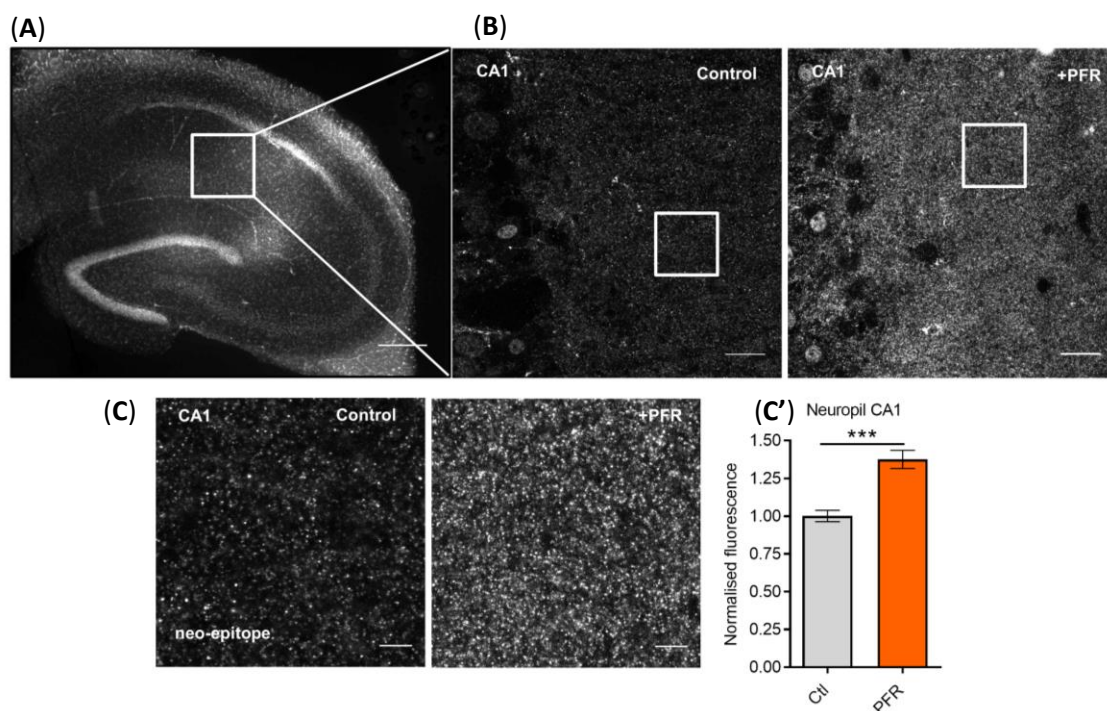


**Figure 14. Brevican cleavage is increased upon cLTP induction.**

(A) DAPI stained representative image of acute hippocampal slice showing in white box the CA1 region used for further analysis (scale bar 0.5 cm). (B) Higher magnification of the neuropil around the CA1 region stained with neo epitope antibody used for quantification (scale bar 20  $\mu$ m). (C) Activity-dependent cleavage of brevican in the neuropil of CA1 has been shown here via neo-epitope specific antibody (scale bar 5  $\mu$ m). (C') Analysis of CA1 region of acute hippocampal slices with neo-epitope antibody recognizing 53KDa cleavage fragments in the neuropil. All values are normalized to control (Ctl =  $1.0 \pm 0.037$ ,  $n = 71$  ROIs, 3 slices / n; PFR =  $1.376 \pm 0.0559$ ,  $n = 73$  ROIs; mean  $\pm$  SEM; Unpaired t test, \*\*\*  $P < 0.0001$ ).

To further test this hypothesis I co-stained the neo-epitope stained slices with antibody against the excitatory synaptic protein homer1. Next neo-epitope immunofluorescence was

quantified specifically around homer positive puncta. Indeed, it showed increased cleavage of brevican around excitatory synapses, suggesting perisynaptic cleavage of brevican (Figure 15). These findings made it interesting to look more into detail of neo-epitope localization with respect to synapse. To do so slices were scanned using dual color stimulated emission depletion (STED) microscopy, which allows resolution of 50-70 nm, superior to conventional confocal microscopy. Since only two STED channels were available I decided to image neo-epitope and gp  $\alpha$  brevican in STED channel and homer, used as synaptic marker was in confocal channel with lower resolution. In accordance with our quantitative results, neo-epitope brevican was found in close relation and segregated from full-length brevican and both cleavage and full-length protein were present perisynaptically (Figure 16).

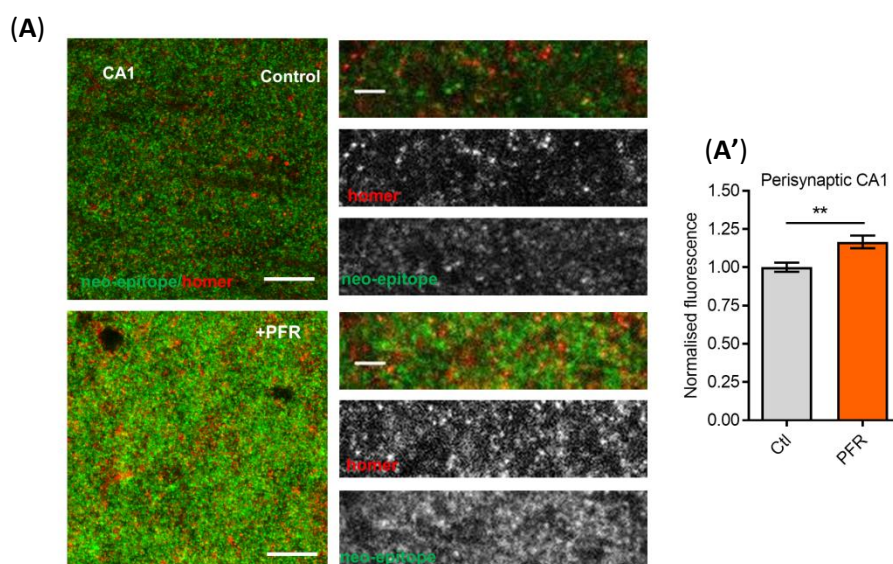


**Figure 15. Brevican is cleaved perisynaptically upon cLTP induction.**

(A) Activity-dependent cleavage of brevican upon stimulation with PFR in the neuropil in the CA1 region of the acute hippocampal slices; it has been shown here via neo-epitope specific antibody recognizing 53 kDa cleavage fragments around homer a synaptic marker in the neuropil. Overlays are shown in colors as indicated. The scale bars are 10  $\mu$ m on the overview and 3  $\mu$ m on the close-up image. (A') Analysis of CA1 region of acute hippocampal slices with neo-epitope antibody with above mentioned conditions. All values are normalized to control (Ctl =  $1.0 \pm 0.030$ , n = 17 ROIs, 3 slices / n; PFR =  $1.16 \pm 0.041$ , n = 16; mean  $\pm$  SEM; Unpaired t test, \*\* P = 0.0027)

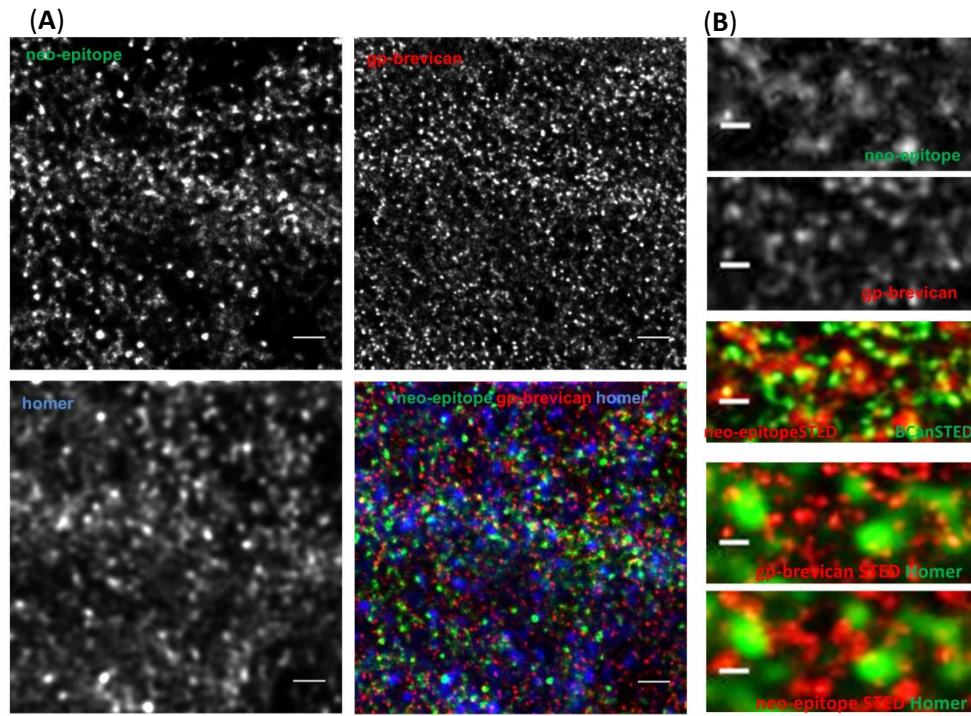


**Figure 16. Ultrastructural representation of perisynaptic brevican.**

(A) Dual-color stimulated emission depletion (STED) images of homer as a synaptic marker in the neuropil with above mentioned conditions. Homer is in confocal channel (blue), gp  $\alpha$  brevican (red) in STED channel and neo-epitope in (green) in STED channel around homer were acquired in acute hippocampal slice in the neuropil around CA1 region. (B) Detailed image of single channels are shown first, followed by overlaid images where brevican and cleaved brevican have been shown in STED channel where they are in close relation and segregated from each other present perisynaptically around homer. Overlays are shown in colors as indicated. The scale bars are 1  $\mu$ m on the overview and 0.3  $\mu$ m on the close-up images.

### 3.3 Dissection of endogenous proteases involved in degradation of brevican

It has been suggested that ECM-modulating enzymes belong to a large family of matrix metalloproteases (Ethell and Ethell 2007) and ADAMTS which have proteoglycans as their substrates (Kelwick et al., 2015). Combining our activity-dependent ECM modulation assay with pharmacological manipulation with the general inhibitor GM6001, I assessed how cleavage is affected by proteases. Slices were pre-incubated with inhibitors and were stimulated in presence of inhibitor and were left to recover in presence of inhibitor before collecting slices after stimulation. Application of broad band inhibitor GM6001 leads to complete abolishment of cleavage for all time points after stimulation with PFR (Figure 17). To dissect individual proteases involved I tested several specific protease inhibitors for ADAMTS4/5 like TIMP3 and Piceatotal along with broad spectrum protease inhibitor at specific time points as mentioned in section 2.2.9. There was a reduction in cleavage of

brevican in the presence of specific protease inhibitors (Figure 18). This trend was same with neo-epitope specific antibody suggesting involvement of ADAMTS4/5 in cleavage of brevican. I also used Timp1 which has been reported to be a protease inhibitor of MMP-9; however, there was no effect of TIMP1 on brevican cleavage. Again, to rule out unspecific effects of PFR results were replicated with stimulation by 4AP + BCC (Figure 18C).

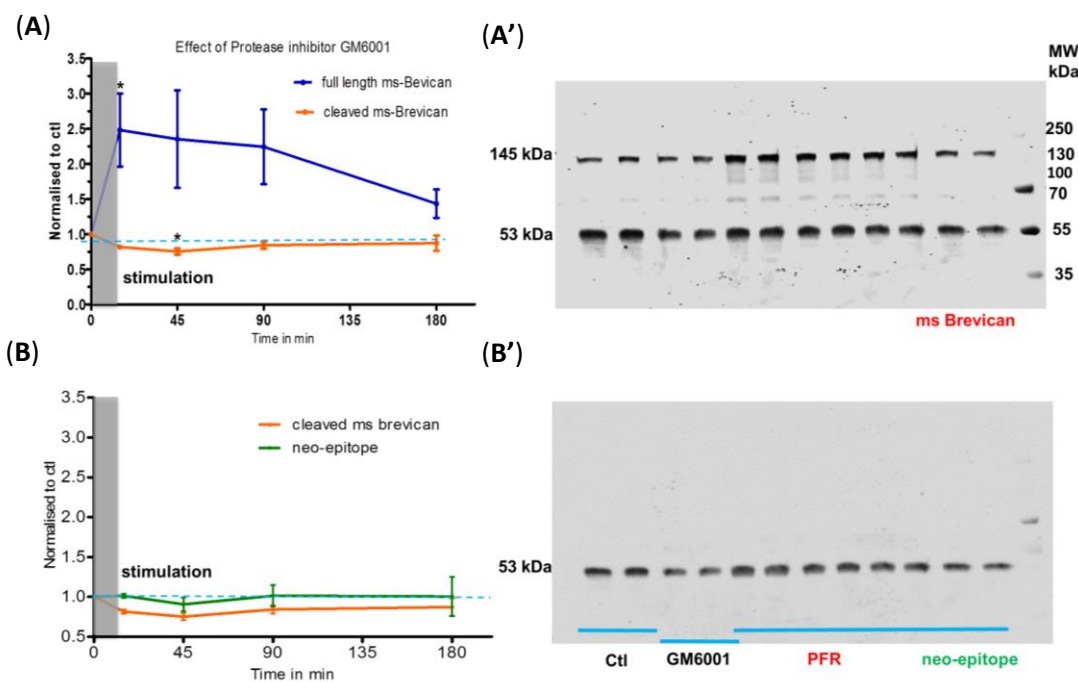


**Figure 17. Activity-Dependent Proteolytic Cleavage of brevican is abolished by broad band protease inhibitor.**

**(A)** Activity-dependent cleavage of brevican in adults (8-10 week old); it has been shown here via ms  $\alpha$  brevican antibody. All values are normalized to control (full-length **msBC**- Ctl = 1.0, n = 4, 3 slices / n; PFR 15' =  $2.0 \pm 0.26$ , n = 4; PFR 45' =  $1.60 \pm 0.24$ , n = 4; PFR 90' =  $1.74 \pm 0.24$ , n = 4; PFR 180' =  $1.25 \pm 0.11$ , n = 4; mean  $\pm$  SEM; One Way ANOVA, P = 0.0226 for full length msBC with Dunnett's Multiple Comparison Test. **msBC 53kDa**- Ctl = 1.0, n = 4, 3 slices / n; PFR 15' =  $0.81 \pm 0.02$ , n = 4; PFR 45' =  $0.75 \pm 0.04$ , n = 4; PFR 90' =  $0.84 \pm 0.05$ , n = 4; PFR 180' =  $0.87 \pm 0.10$ , n = 4; mean  $\pm$  SEM; One Way ANOVA, P = 0.0892 \* P < 0.05). **(A')** Quantified the Western blot of acute hippocampal slices with full lengthms  $\alpha$  Brevican (blue line) and cleaved ms  $\alpha$  Brevican (orange line) with above mentioned conditions.

**(B)** Activity-dependent cleavage of brevican in presence of broad band protease inhibitor detected here via ms  $\alpha$  brevican and neo-epitope antibody. All values are normalized to control (**msBC** taken from last graph to show in relations to **neo-epitope** antibody- Ctl = 1.0, n = 4, 3 slices / n; PFR 15' =  $1.013 \pm 0.02$ , n = 4; PFR 45' =  $0.90 \pm 0.08$ , n = 4; PFR 90' =  $1.014 \pm 0.13$ , n = 4; PFR 180' =  $1.004 \pm 0.24$ , n = 3; mean  $\pm$  SEM; One Way ANOVA, P = 0.9466, Dunnett's Multiple Comparison Test, ns). **(B')** Quantified the Western blot of acute hippocampal slices with neo-epitope specific antibody recognizing 53 kDa cleavage band with above mentioned conditions.

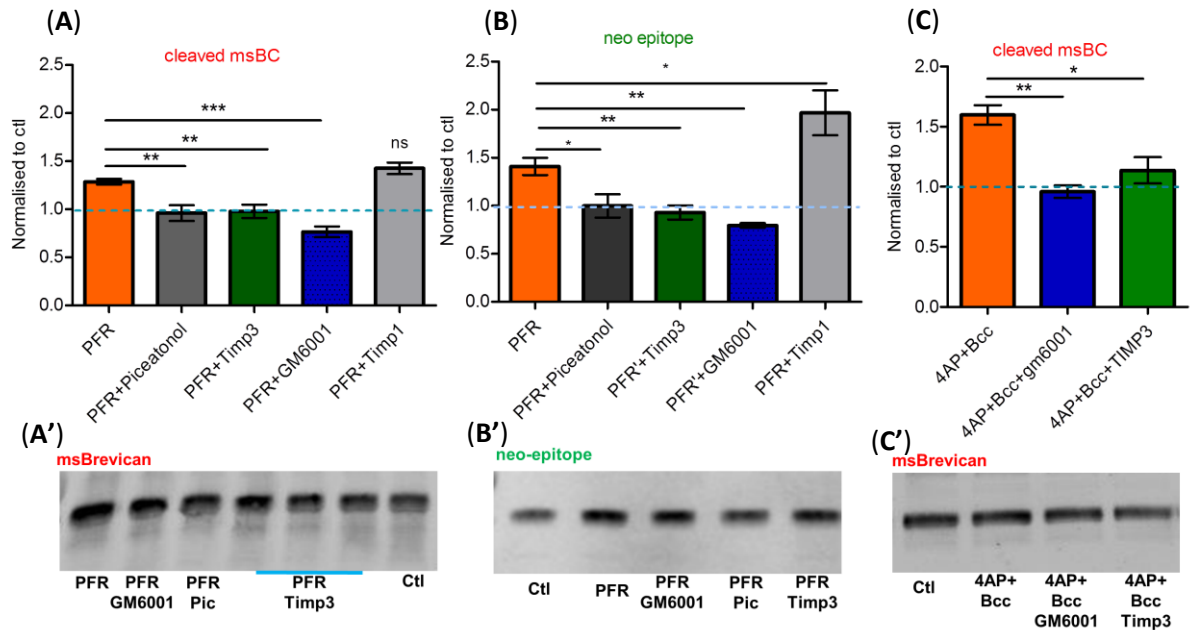


**Figure 18. ADAMTS4/5 proteases are involved in cleavage of brevican.**

(A) Activity-dependent cleavage of brevican detected with ms  $\alpha$  brevican antibody (immunoreactivity at 53 kDa). All values are normalized to control (Ctl = 1.0, n = 6, 3 slices / n; PFR =  $1.28 \pm 0.02$ , n = 6; PFR + Piceatonol =  $0.96 \pm 0.08$ , n = 5; PFR + Timp3 =  $0.97 \pm 0.07$ , n = 8; PFR + GM6001 =  $0.76 \pm 0.05$ , n = 4; PFR + Timp1 =  $1.42 \pm 0.06$ , n = 4; mean  $\pm$  SEM; One Way ANOVA,  $P < 0.0001$ , Dunnett's Multiple Comparison Test, \*\*  $P < 0.01$ , \*\*\*  $P < 0.001$ ). (A') Quantified the Western blot of acute hippocampal slices with ms  $\alpha$  Brevican antibody recognizing 53 kDa cleavage band with above mentioned conditions.

(B) Activity-dependent cleavage of brevican; it has been shown here via neo-epitope specific antibody. All values are normalized to control (Ctl = 1.0, n = 6, 3 slices / n; PFR =  $1.40 \pm 0.09$ , n = 5; PFR + Piceatonol =  $0.99 \pm 0.12$ , n = 4; PFR + Timp3 =  $0.93 \pm 0.07$ , n = 7; PFR + GM6001 =  $0.79 \pm 0.02$ , n = 4; PFR + Timp1 =  $1.96 \pm 0.23$ , n = 3; mean  $\pm$  SEM; One Way ANOVA,  $P < 0.0001$ , Dunnett's Multiple Comparison Test, \*  $P < 0.05$ , \*\*  $P < 0.01$ ). (B') Quantified the Western blot of acute hippocampal slices with neo-epitope specific antibody with above mentioned conditions.

(C) Activity-dependent cleavage of brevican upon stimulation with 4AP+Bcc detected with ms  $\alpha$  brevican antibody. All values are normalized to control (Ctl = 1.0, n = 4, 3 slices / n; 4AP + Bcc =  $1.59 \pm 0.08$ , n = 4; 4AP+Bcc+ GM6001 =  $0.95 \pm 0.05$ , n = 3; 4AP + Bcc + Timp3 =  $0.13 \pm 0.1$ , n = 3; mean  $\pm$  SEM; One Way ANOVA,  $P < 0.0024$ , Dunnett's Multiple Comparison Test, \*  $P < 0.05$ , \*\*  $P < 0.01$ ). (C') Quantified the Western blot of acute hippocampal slices with ms  $\alpha$  Brevican antibody recognizing 53KDa cleavage band with above mentioned conditions.

Our initial experiments showed that brevican and very likely other lecticans such as aggrecan are proteolytically cleaved by the ADAMTS family during cLTP induction / synaptic activity.

### 3.4 Role of proprotein convertases in cleavage of brevican

Proteases are produced as inactive zymogens and only proteolytic removal of their prodomain leads to its full enzymatic activity. This may happen intracellularly or extracellularly after secretion. In order to test whether prodomain activation plays a role during activity-dependent cleavage of brevican I treated our slices with 4-aminophenylmercuric acetate

(APMA), a compound that non-selectively cleaves prodomain and thus activates proteases. Slices were incubated with APMA alone and in the other group it was added before the stimulation with PFR. The effect of APMA treatment alone resulted in cleavage of brevican as quantified with Western blot using neo-epitope and ms anti brevican antibody. (Figure 19). But when I looked at full length protein secretion I found no effect of APMA alone suggesting it's not needed for secretion of brevican. These results points out APMA can activate the proteases to cleave without any stimulation.

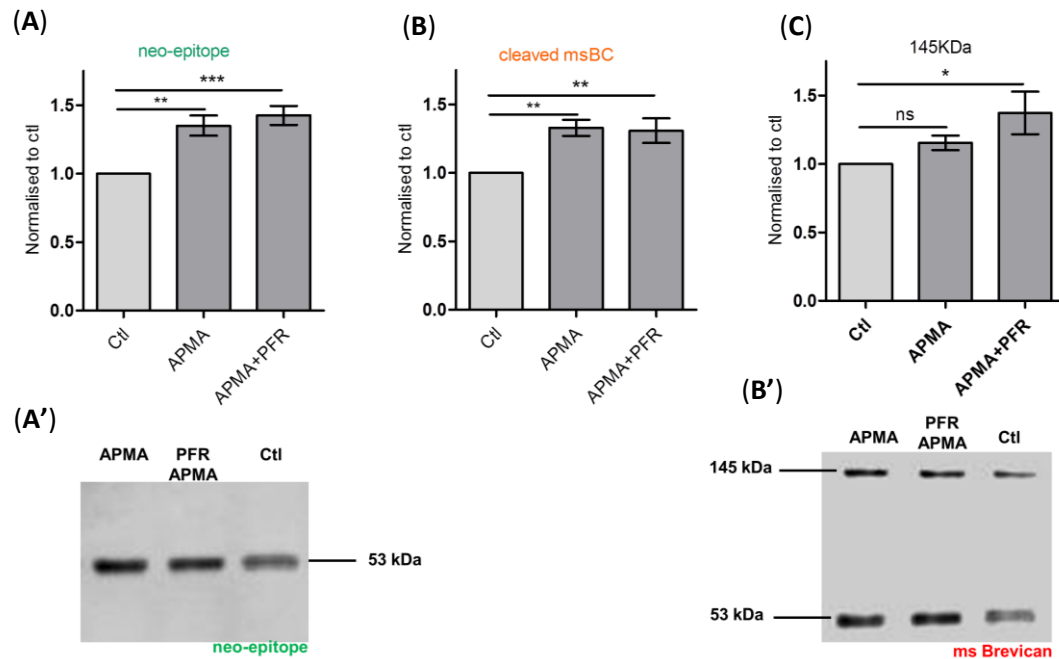


**Figure 19. APMA induces activation of proteases and cleavage of brevican.**

(A) APMA induced activation of proteases and cleavage of brevican, as shown here via neo-epitope specific antibody. All values are normalized to control (Ctl = 1.0, n = 5, 3 slices / n; APMA =  $1.35 \pm 0.07$ , n = 4; PFR + APMA =  $1.42 \pm 0.06$ , n = 3; mean  $\pm$  SEM; One Way ANOVA, P = 0.0004, Dunnett's Multiple Comparison Test, \*\* P < 0.01, \*\*\* P < 0.001). (A') Quantified the Western blot of acute hippocampal slices with neo-epitope specific antibody with above mentioned conditions.

(B) APMA induced activation of proteases and cleavage of brevican, as shown here via ms  $\alpha$  brevican antibody. All values are normalized to control (Ctl = 1.0, n = 5, 3 slices / n; APMA =  $1.32 \pm 0.05$ , n = 3; PFR + APMA =  $1.30 \pm 0.08$ , n = 3; mean  $\pm$  SEM; One Way ANOVA, P = 0.0016, Dunnett's Multiple Comparison Test, \*\* P < 0.01). (B') Quantified the Western blot of acute hippocampal slices with ms  $\alpha$  Brevican antibody recognizing 53 kDa fragment and full length band with above mentioned conditions.

(C) Role of APMA induced activation of proteases in secretion of brevican, as shown here via ms  $\alpha$  brevican antibody. All values are normalized to control (Ctl = 1.0, n = 5, 3 slices / n; APMA =  $1.15 \pm 0.05$ , n = 3; PFR + APMA =  $1.37 \pm 0.15$ , n = 4; mean  $\pm$  SEM; One Way ANOVA, P = 0.042, Dunnett's Multiple Comparison Test, \* P < 0.05).

Proprotein convertases are known to activate the inactive zymogen by removing prodomain and making them enzymatically active. To address the indispensable role of proprotein convertases (PC) in brevican cleavage, I used pharmacological broad band PC blocker as well as more specific inhibitors for the PC's PACE4 and furin. These PC's have previously been suggested to remove prodomain from ADAMTS proteases (Tortorella et al., 2005) and thus are good candidates to be involved in activity-dependent cleavage of brevican. Inhibitor for PACE4 activity abrogated most efficiently cleavage of brevican compared to stimulated group and furin, PCi (Figure 20). Suggesting that for cleavage of brevican PACE4 a proprotein convertase acts most efficiently in activating the protease.

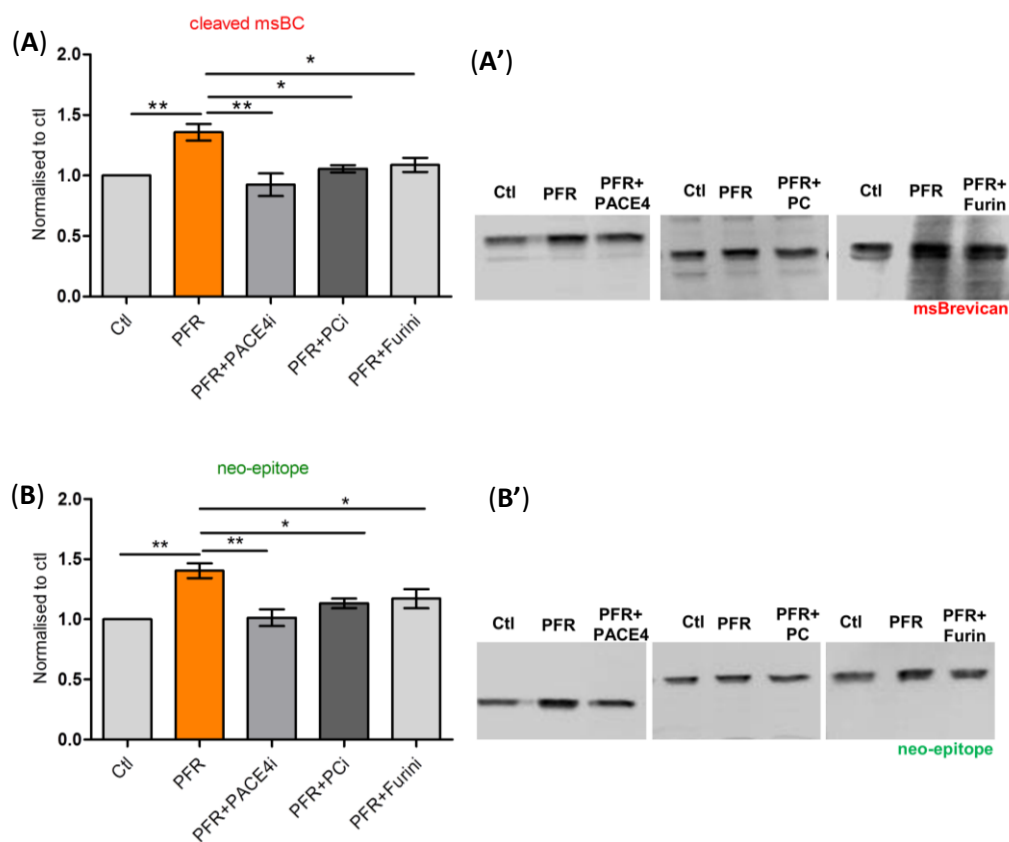


**Figure 20. Role of proprotein convertases in degradation of brevican.**

**(A)** Cleavage of brevican requires proteases to be activated by pro-protein convertases; it has been shown here via ms  $\alpha$  brevican antibody. All values are normalized to control (Ctl = 1.0, n = 18, 3 slices / n; PFR =  $1.35 \pm 0.06$ , n = 21; PFR + PACE4i =  $0.92 \pm 0.09$ , n = 4; PFR + PCi =  $1.05 \pm 0.02$ , n = 7; PFR + Furini =  $1.08 \pm 0.05$ , n = 10; mean  $\pm$  SEM; One Way ANOVA,  $P < 0.0001$ , Dunnett's Multiple Comparison Test, \*  $P < 0.05$ , \*\*  $P < 0.01$ , \*\*\*  $P < 0.001$ ). **(A')** Quantified the Western blot of acute hippocampal slices with ms  $\alpha$  Brevican antibody recognizing 53 kDa cleavage band with above mentioned conditions.

**(B)** Cleavage of brevican requires proteases to be activated by pro-protein convertases; it has been shown here via neo-epitope specific antibody. All values are normalized to control (Ctl = 1.0, n = 15, 3 slices / n; PFR =  $1.40 \pm 0.06$ , n = 14; PFR + PACE4i =  $1.01 \pm 0.06$ , n = 4; PFR + PCi =  $1.13 \pm 0.04$ , n = 7; PFR + Furini =  $1.17 \pm 0.07$ , n = 9; mean  $\pm$  SEM; One Way ANOVA,  $P < 0.0001$ , Dunnett's Multiple Comparison

Test, \*  $P < 0.05$ , \*\*  $P < 0.01$ , \*\*\*  $P < 0.001$ ). (B') Quantified the Western blot of acute hippocampal slices with neo-epitope specific antibody with above mentioned conditions.

These findings suggest that during cLTP there is activity-dependent activation of brevican-cleaving enzymes taking place, which involves PC. However, this exact identity of the protease remains elusive.

### 3.5 Cleavage of brevican requires network activity and NMDAR

Simultaneous activation of pre- and postsynaptic neurons is a prerequisite for the induction of LTP. The PFR cocktail induces LTP in an NMDA-R dependent manner by using picrotoxin which enhances neuronal network activity by reduction of GABAergic inhibition, whereas forskolin and rolipram act in combination to enhance the cAMP-mediated intercellular signalling (Otmakhov et al., 2004). I thus tested for a postsynaptic component in PFR-induced

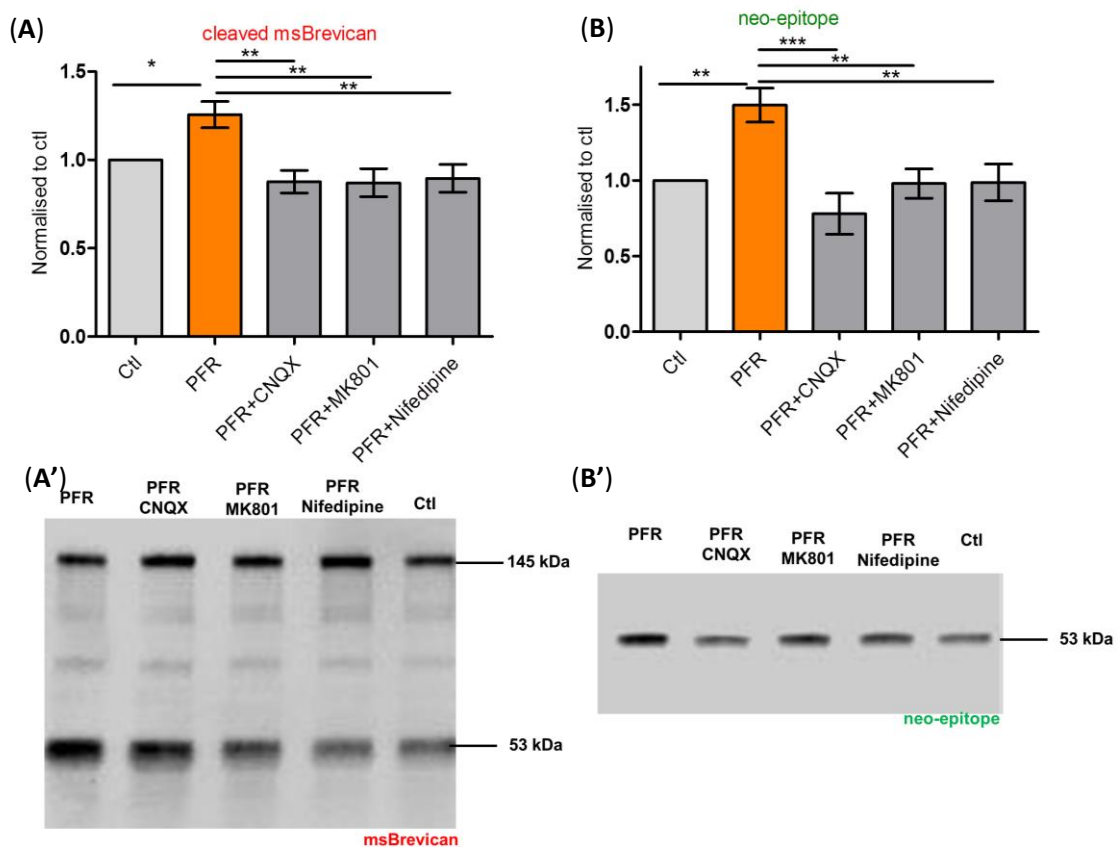


**Figure 21. Cleavage of brevican requires postsynaptic activation.**

(A) Cleavage of brevican requires postsynaptic activation as shown here via ms  $\alpha$  brevican antibody. All values are normalized to control (Ctl = 1.0, n = 5, 3 slices / n; PFR =  $1.25 \pm 0.07$ , n = 5; PFR + CNQX =  $0.87 \pm 0.06$ , n = 4; PFR + MK801 =  $0.87 \pm 0.07$ , n = 4; PFR + Nifedipine =  $0.89 \pm 0.07$ , n = 4; mean  $\pm$  SEM; One Way ANOVA,  $P = 0.0017$ , Dunnett's Multiple Comparison Test, \*  $P < 0.05$ , \*\*  $P < 0.01$ ). (A')



Quantified the Western blot of acute hippocampal slices with ms  $\alpha$  Brevican antibody recognizing 53 kDa cleavage band with above mentioned conditions.

**(B)** Cleavage of brevicin requires postsynaptic activation it has been shown here via neo-epitope antibody. All values are normalized to control (Ctl = 1.0, n = 6, 3 slices / n; PFR =  $1.49 \pm 0.11$ , n = 5; PFR + CNQX =  $0.77 \pm 0.13$ , n = 3; PFR + MK801 =  $0.97 \pm 0.09$ , n = 4; PFR + Nifedipine =  $0.98 \pm 0.12$ , n = 4; mean  $\pm$  SEM; One Way ANOVA, P = 0.0007, Dunnett's Multiple Comparison Test, \* P < 0.05, \*\* P < 0.01, \*\*\* P < 0.001). **(B')** Quantified the Western blot of acute hippocampal slices with neo-epitope specific antibody with above mentioned conditions.

ADAMTS4/5 -dependent brevicin cleavage. For this purpose I used slices which were pre-incubated 15-20 min prior to the PFR stimulation with inhibitors for each group containing CNQX, MK801 and nifedipine separately to block AMPAR, NMDAR and L-type voltage-dependent  $Ca^{2+}$  channels (VDCCs). I found that brevicin cleavage was abrogated upon blocking with AMPA, NMDAR and L-type VDCCs selective inhibitors. These results suggest that ADAMTS-driven cleavage of brevicin is dependent on postsynaptic activation (Figure 21).

In order to test whether synaptic activity was necessary I blocked action potentials with Tetrodotoxin (TTX, 2 $\mu$ M). Also under these conditions I found decreased cleavage of brevicin (Figure 22). I further confirmed the involvement of NMDAR using the NMDAR antagonist DAP5 which gave similar results as MK801. To investigate which NMDAR subunit was necessary for brevicin cleavage I pre-incubated slices with RO25698 and ifenprodil, blockers of the GluN2B subunit (Figure 22).

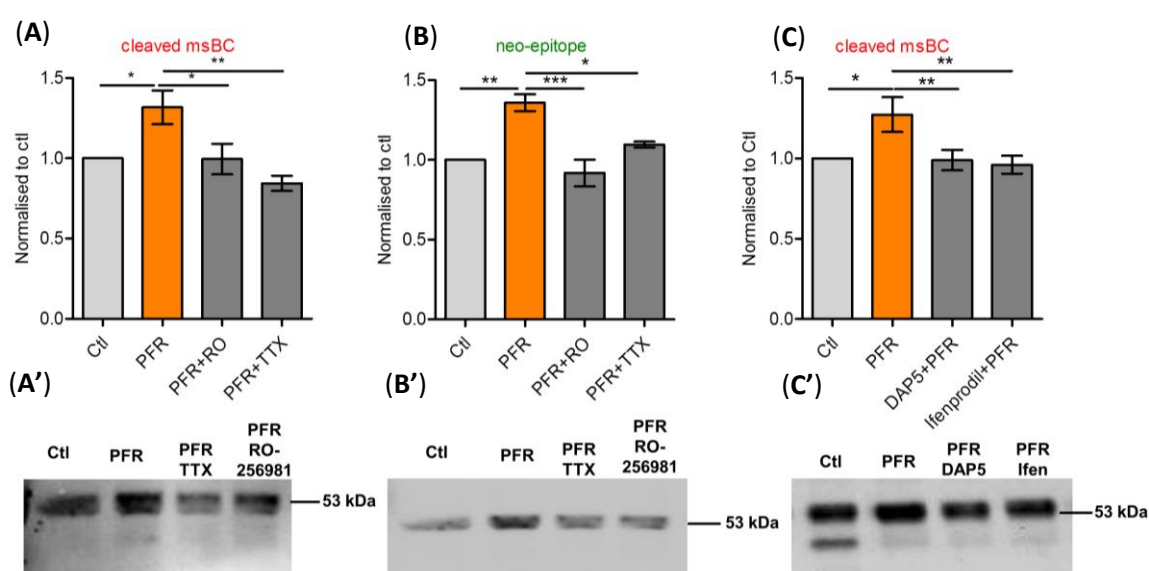


**Figure 22. Role of NR2B-NMDA receptor subunit and network activity in the activity-dependent cleavage of brevicin.**

**(A)** NR2B-NMDA receptor subunits and network activity affect cleavage of brevicin, as detected by ms  $\alpha$  brevicin antibody. All values are normalized to control (Ctl = 1.0, n = 4, 3 slices / n; PFR =  $1.31 \pm 0.10$ , n

= 4; PFR + RO =  $0.99 \pm 0.09$ , n = 4; PFR  $\pm$  TTX =  $0.84 \pm 0.04$ , n = 3; mean  $\pm$  SEM; One Way ANOVA, P = 0.0096, Dunnett's Multiple Comparison Test, \* P < 0.05, \*\* P < 0.01). **(A')** Quantified the Western blot of acute hippocampal slices with ms  $\alpha$  brevicin antibody recognizing 53 kDa cleavage band with above mentioned conditions.

**(B)** NR2B-NMDA receptor subunit and network activity affects cleavage of brevicin detected by neo-epitope specific antibody. All values are normalized to control (Ctl = 1.0, n = 4, 3 slices / n; PFR =  $1.35 \pm 0.05$ , n = 4; PFR + RO =  $0.91 \pm 0.08$ , n = 4; PFR  $\pm$  TTX =  $1.096 \pm 0.01$ , n = 3; mean  $\pm$  SEM; One Way ANOVA, P = 0.0005, Dunnett's Multiple Comparison Test, \* P < 0.05, \*\* P < 0.01, \*\*\* P < 0.001). **(B')** Quantified the Western blot of acute hippocampal slices with neo-epitope specific antibody with above mentioned conditions.

**(C)** NR2B-NMDA receptor subunit and NMDA activity affects cleavage of brevicin detected by byms  $\alpha$  brevicin antibody. All values are normalized to control (Ctl = 1.0, n = 13, 3 slices / n; PFR =  $1.27 \pm 0.10$ , n = 6; DAP5 + PFR =  $0.98 \pm 0.06$ , n = 13; Ifenprodil ( Ifen ) + PFR =  $0.96 \pm 0.05$ , n = 7; mean  $\pm$  SEM; One Way ANOVA, P = 0.0095, Dunnett's Multiple Comparison Test, \* P < 0.05, \*\* P < 0.01). **(C')** Quantified the Western blot of acute hippocampal slices with ms  $\alpha$  brevicin antibody recognizing 53 kDa cleavage band with above mentioned conditions.

Again I found that these blockers prevented brevicin cleavage after PFR treatment, suggesting GluN2B subunit of NMDA receptors to play a central role in protease activation. It implies that for the cleavage to happen network activity is needed as well, along with postsynaptic components.

### 3.6 Activity-dependent cleavage and secretion of brevicin via an NMDAR-CaMKII signalling pathway

Experiment in previous sections suggests important role of NMDA dependent mechanisms leading to modulation of ECM. To specifically test the role of NMDA alone, I used NMDA for 5 min stimulation and let the slices recover in aCSF for 25'. This brief incubation of 5 min with 50  $\mu$ M NMDA induced robust increase in secretion of brevicin and it also lead to the cleavage of brevicin (Figure 23). It implied that NMDA receptor activation is both necessary and sufficient to trigger brevicin cleavage and secretion.

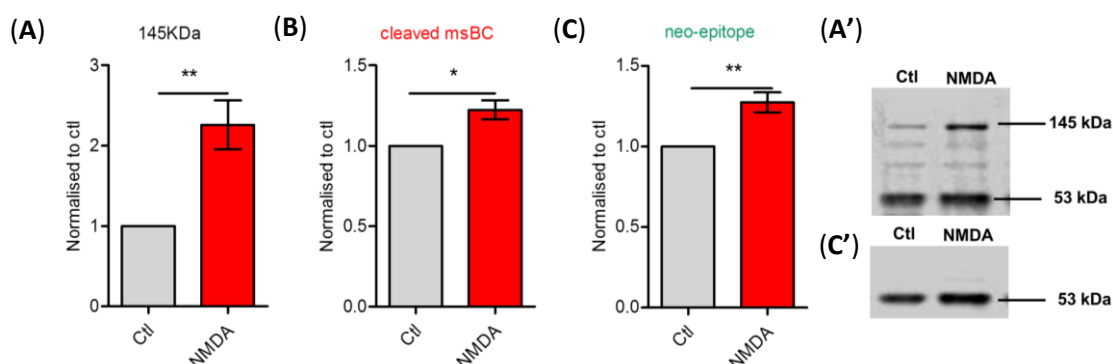


**Figure 23. NMDA can trigger secretion and activity-dependent modulation of brevicin.**

(A) NMDA stimulation alone results in secretion of brevican detected by ms  $\alpha$  brevican antibody. All values are normalized to control (Ctl = 1.0, n = 6, 3 slices / n; PFR =  $2.26 \pm 0.30$ , n = 6; mean  $\pm$  SEM; Paired t test, \*\* P = 0.0089). (A') Quantified the Western blot of acute hippocampal slices with ms  $\alpha$  Brevican antibody recognizing 53 kDa cleavage band and full length band at 145 kDa with above mentioned conditions.

(B) NMDA stimulation alone results in cleavage of brevican detected by ms  $\alpha$  Brevican antibody. All values are normalized to control (Ctl = 1.0, n = 6, 3 slices / n; PFR =  $1.224 \pm 0.05$ , n = 6; mean + SEM; Paired t test, \* P = 0.0129).

(C) NMDA stimulation alone results in cleavage of brevican detected by neo-epitope specific antibody. All values are normalized to control (Ctl = 1.0, n = 6, 3 slices / n; PFR =  $1.274 \pm 0.06$ , n = 6; mean + SEM; Paired t test, \* P = 0.0129). (C') Quantified the Western blot of acute hippocampal slices with neo-epitope specific antibody with above mentioned conditions.

One of the major signaling molecules downstream of NMDAR is CaMKII $\alpha$ . To test its involvement slices were preincubated with autocamptide-2 related inhibitor peptide (AIP) which is known to be a specific blocker of CaMKII. I found that this pre-incubation itself lead to the abrogated PFR induced cleavage and secretion of full length brevican protein (Figure 24). This indicated that activity-dependent brevican cleavage and secretion is further regulated by CaMKII signalling.

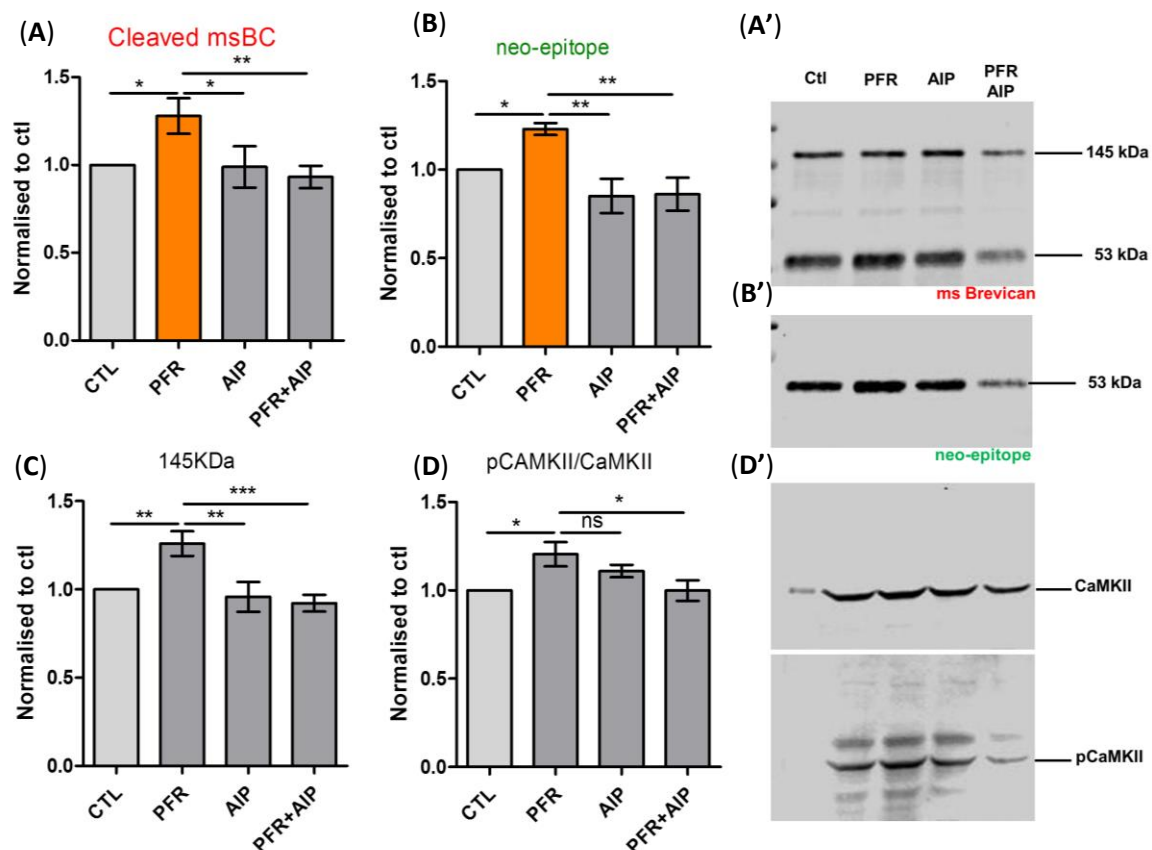


**Figure 24. Role of CaMKII signalling in the activity-dependent modulation of ECM.**

(A) cLTP dependent modulation of ECM require CaMKII signaling as shown by ms  $\alpha$  Brevicanspecific antibody . All values are normalized to control (Ctl = 1.0, n = 8, 3 slices / n; PFR =  $1.28 \pm 0.10$ , n = 6; AIP =  $0.98 \pm 0.11$ , n = 5; PFR + AIP =  $0.93 \pm 0.06$ , n = 8; mean  $\pm$  SEM; One Way ANOVA, P =

0.0140, Dunnett's Multiple Comparison Test, \*  $P < 0.05$ , \*\*  $P < 0.01$ ). (A') Quantified the Western blot of acute hippocampal slices with ms  $\alpha$  Brevicin antibody recognizing 53 kDa cleavage band and full length band at 145 kDa with above mentioned conditions.

(B) cLTP dependent modulation of ECM requires CaMKII signaling as shown by neo-epitope specific antibody. All values are normalized to control (Ctl = 1.0, n = 7, 3 slices / n; PFR = 1.23 + 0.03, n = 7; AIP = 0.85 + 0.09, n = 3; PFR + AIP = 0.86 + 0.09, n = 8; mean + SEM; One Way ANOVA,  $P = 0.0019$ , Dunnett's Multiple Comparison Test, \*  $P < 0.05$ , \*\*  $P < 0.01$ ). (B') Quantified the Western blot of acute hippocampal slices with neo-epitope specific antibody with above mentioned conditions.

(C) cLTP dependent secretion of brevicin require CaMKII signaling as shown by neo-epitope specific antibody. All values are normalized to control (Ctl = 1.0, n = 8, 3 slices / n; PFR = 1.26 + 0.06, n = 7; AIP = 0.95 + 0.08, n = 5; PFR + AIP = 0.92 + 0.04, n = 8; mean + SEM; One Way ANOVA,  $P = 0.0005$ , Dunnett's Multiple Comparison Test, \*\*  $P < 0.01$ , \*\*\*  $P < 0.001$ ).

(D) cLTP induced phosphorylation of CaMKII was reduced in presence of peptide specific blocker of CaMKII. All groups were normalized against control (Ctl = 1.00, n = 7; PFR = 1.20 + 0.06, n=7; AIP = 1.10 + 0.03, n = 6; PFR + AIP = 0.99 + 0.05, n = 7; mean + SEM; One Way ANOVA,  $P = 0.0175$ , Dunnett's Multiple Comparison Test, \*\*  $P < 0.05$ ). (D') Quantified the Western blot of acute hippocampal slices with ms  $\alpha$  CaMKII and rb  $\alpha$  pCaMKII antibodies with above mentioned conditions.

### 3.7 Role of $\beta 1$ class integrin's in the activity-dependent modulation of ECM

NMDAR function has been reported to be modulated by integrins (Bernard-Trifilo et al., 2005). Integrins are major ECM receptors and are composed of an  $\alpha$  and  $\beta$  subunit.

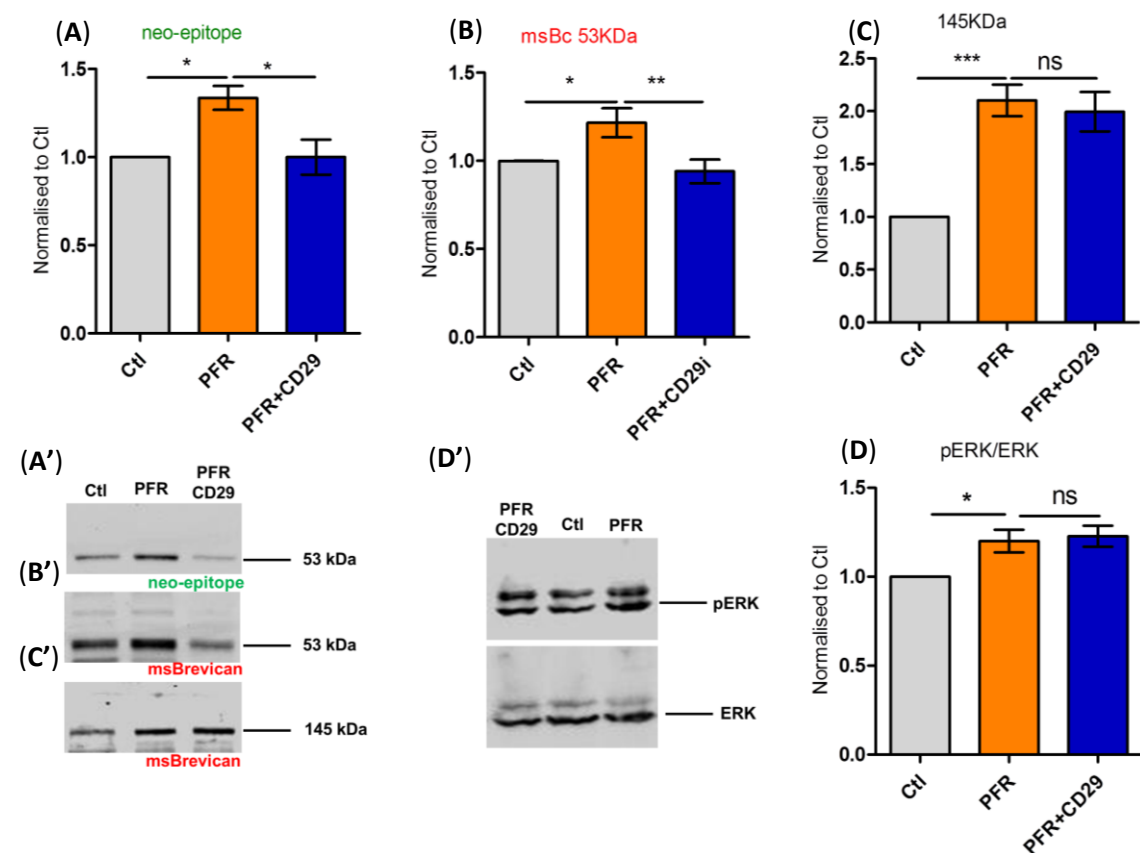


**Figure 25. Role of  $\beta 1$  class integrin's in the activity-dependent modulation of ECM.**

(A) cLTP dependent modulation of ECM require integrin dependent pathway shown by neo-epitope specific antibody. All values are normalized to control (Ctl = 1.0, n = 8, 3 slices / n; PFR = 1.33 ± 0.06, n =

5; PFR + CD29 =  $1.0 \pm 0.09$ , n = 8; mean  $\pm$  SEM; One Way ANOVA, P = 0.0101, Dunnett's Multiple Comparison Test, \* P < 0.05). **(A')** Quantified the Western blot of acute hippocampal slices with neo-epitope specific antibody with above mentioned conditions.

**(B)** cLTP dependent modulation of ECM require integrin dependent pathway shown by ms  $\alpha$  Brevican cleavage specific antibody. All groups were normalized against control (Ctl = 1.0, n = 7, 3 slices / n; PFR =  $1.21 \pm 0.08$ , n = 5; PFR + CD29 =  $0.94 \pm 0.06$ , n = 8; mean + SEM; One Way ANOVA, P = 0.0159, Dunnett's Multiple Comparison Test, \*\* P < 0.01, \* P < 0.05). **(B')** Quantified the Western blot of acute hippocampal slices with ms  $\alpha$  Brevican antibody recognizing 53 kDa cleavage band.

**(C)** cLTP dependent secretion of brevican is integrin independent pathway as shown here by ms  $\alpha$  Brevican. All groups were normalized against control (Ctl = 1.0, n = 8, 3 slices / n; PFR =  $2.1 \pm 0.14$ , n = 5; PFR + CD29 =  $1.99 \pm 0.18$ , n = 8; mean + SEM; One Way ANOVA, P < 0.0001, Dunnett's Multiple Comparison Test, \*\*\* P < 0.001). **(C')** Quantified the Western blot of acute hippocampal slices with ms  $\alpha$  Brevican antibody recognizing full length band at 145 kDa with above mentioned conditions.

**(D)** cLTP dependent phosphorylation of ERK was not abrogated by pre-incubation of CD29 functional blocker of  $\beta$ 1 class integrin's. All groups were normalized against control (Ctl = 1.0, n = 7, 3 slices / n; PFR =  $1.20 \pm 0.06$ , n = 5; PFR + CD29 =  $1.22 \pm 0.05$ , n = 6, mean  $\pm$  SEM; One Way ANOVA, P = 0.0042, Dunnett's Multiple Comparison Test, \* P < 0.05). **(D')** Quantified the Western blot of acute hippocampal slices with ms  $\alpha$  pERK and rb  $\alpha$  ERK antibodies with above mentioned conditions.

It has been reported previously that chronic treatment with anti- $\beta$ 1 function-blocking antibody alters surface diffusion of NR2B subunit (Groc et al., 2007). Therefore I used anti- $\beta$ 1 function-blocking antibody (CD29) in acute hippocampal slices to test the involvement of  $\beta$ 1- containing integrins in brevican cleavage. I pre-incubated the slices with CD29 and it was present all the time during the treatment. After processing the slices biochemically I found that there was decrease in cleavage of brevican but it had no effect on secretion of full-length protein (Figure 25). This suggests that integrin signalling is required for cleavage of brevican, but not for secretion of full length protein.

### **3.8 Screening for modulation of ECM using an unbiased LC-MS approach**

In order to investigate regulation of ECM proteins during cLTP I decided to perform an unbiased approach using liquid chromatography-mass spectrometry (LC-MS). For that purpose I stimulated the acute slices as before and collected slices after the treatments and ECM was extracted. Samples were made ready as mentioned in the method section 2.4. I not only found that indeed there was a trend towards upregulation of brevican in the extracellular space but also the other ECM molecules such as tenascin-R, neurocan and hapln1 were more abundant when I processed for the quantification of the total protein (Figure 26A). On the other hand when I separately analysed the part of fractions below 70 kDa, it was found that fraction was more abundant (Figure 26B) supporting our findings obtained biochemically. The observed trends were further investigated using Western blot, where I also included aggrecan, an important component of the PNN in the study.

Aggrecan an important proteoglycan which could not be detected by above mentioned method of extraction and analysis by LC-MS, so it was analyzed biochemically by Western blotting. It was found that there was increase in level of full length protein in comparison to control group. It suggested that upon cLTP stimulation aggrecan was also modulated (Figure 26D).

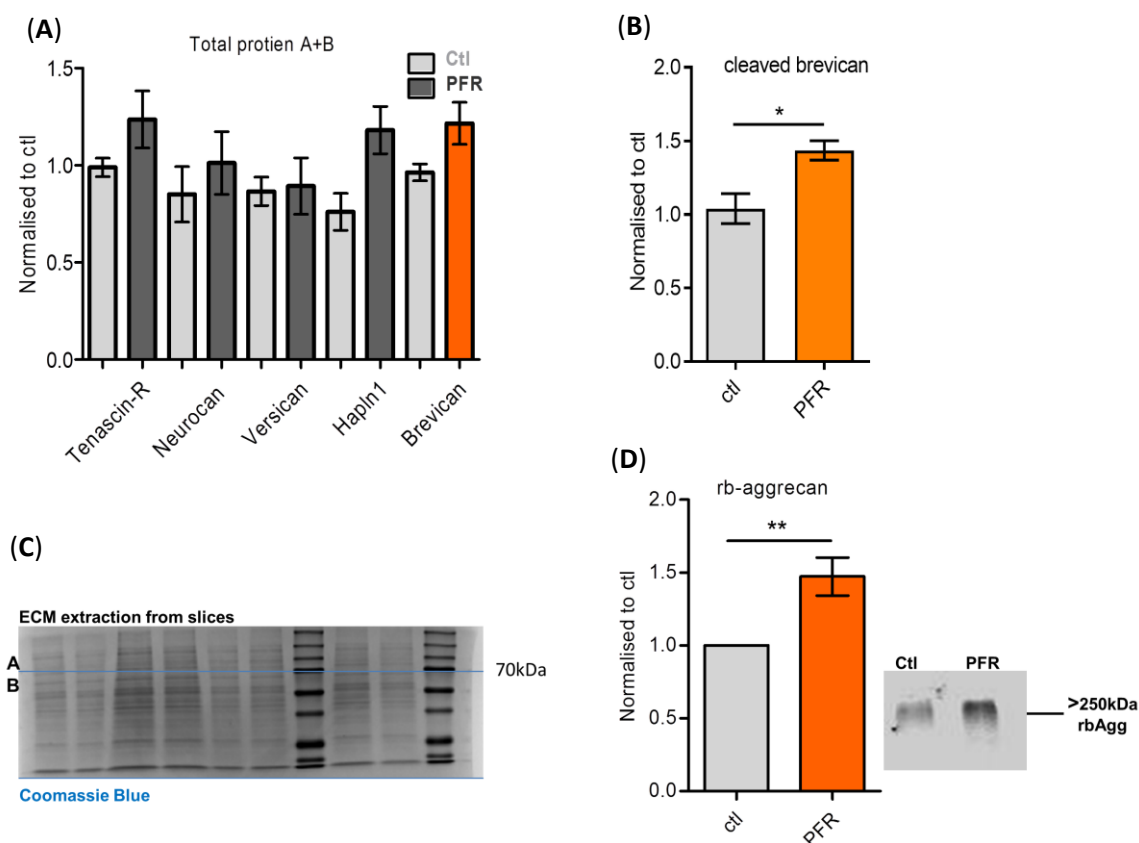


**Figure 26. Screening for modulation of ECM using an unbiased LC-MS approach.**

**(A)** Activity-dependent modulation of ECM analyzed by LC-MS approach. All values are normalized to their respective control. (**Tenascin-R**: Ctl =  $0.98 \pm 0.04$ , n = 4, 3 slices / n; PFR =  $1.23 \pm 0.14$ , n = 4; ; P = 0.1250; **Neurocan**: Ctl =  $0.85 \pm 0.14$ , n = 4; PFR =  $1.012 \pm 0.16$ , n = 4;; P = 0.62; **Versican**: Ctl =  $0.86 \pm 0.07$ , n = 4; PFR =  $0.89 \pm 0.14$ , n = 4; P = 0.90; **Hapln1**: Ctl =  $0.76 \pm 0.095$ , n = 4; PFR =  $1.18 \pm 0.12$ , n = 4; P = 0.01; **Brevican**: Ctl =  $0.96 \pm 0.04$ , n = 4; PFR =  $1.21 \pm 0.10$ , n = 4; P = 0.04; mean  $\pm$  SEM, Paired Student's t-test).

**(B)** Activity-dependent cleavage of brevican was checked for MS. All values are normalized to control (Ctl =  $1.0 \pm 0.10$ , n = 4, 3 slices / n; PFR =  $1.435 \pm 0.06$ , n = 4; mean  $\pm$  SEM; P = 0.0172, Paired Student's t-test, \* P < 0.05).

**(C)** Coomassie stained SDS-PAGE gel showing with a blue line where the gel was cut for processing two fractions separately.

**(D)** Activity-dependent modulation of aggrecan shown by WB; it has been shown here via  $\text{rb}\alpha$  aggrecan specific antibody. All values are normalized to control ((Ctl = 1.0, n = 5, 3 slices / n; PFR =  $1.472 \pm 0.1307$ , n = 4; mean  $\pm$  SEM; P = 0.0045, unpaired Student's t-test\*\* P < 0.01). **(D')** Quantified the Western blot of acute hippocampal slices with  $\text{rb}\alpha$  aggrecan specific antibody with above mentioned conditions.

### 3.9 Increased level of extracellular brevican does not result from de novo protein synthesis

Abolishment of cleavage of brevican helped us in determining that there was also more of full length brevican core-protein. Figure 27 determined whether increased abundance of ECM proteins was due to protein synthesis, it was analysed using Anisomycin (20  $\mu$ M) as protein synthesis blocker. I pre-incubated slices 20-30 min before stimulation and the blocker was present the time of experiment. There was no reduction neither in cleaved nor in full length protein in comparison to stimulation group without Anisomycin. I concluded that rather secretion than protein synthesis was responsible for increased level of extracellular brevican.

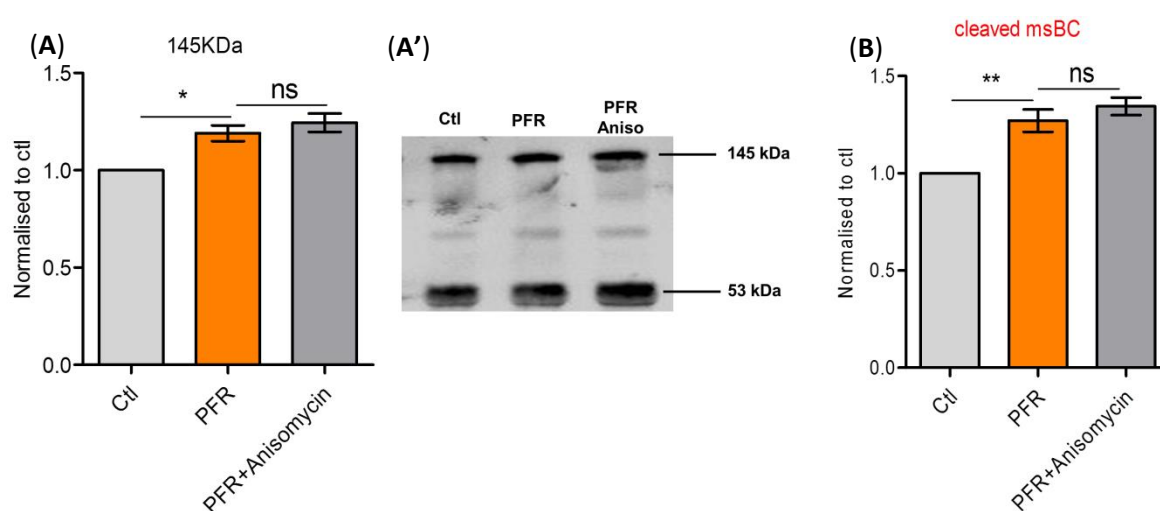


**Figure 27. Protein synthesis blocker anisomycin did not affect the activity-induced increase in brevican levels.**

(A) Activity induced increase in brevican levels results from secretion; it has been shown here via ms  $\alpha$  brevican antibody. All values are normalized to control (Ctl = 1.0, n = 3, 3 slices / n; PFR =  $1.19 \pm 0.04$ , n = 3; PFR + Anisomycin =  $1.24 \pm 0.04$ , n = 3; mean  $\pm$  SEM; One Way ANOVA, P = 0.0071, Dunnett's Multiple Comparison Test, \* P < 0.05). (A') Quantified the Western blot of acute hippocampal slices with ms  $\alpha$  Brevican antibody recognizing full length band and 53 kDa cleavage with above mentioned conditions.

(B) Effect of Anisomycin on cleavage of brevican; it has been shown here via ms  $\alpha$  brevican antibody. All values are normalized to control (Ctl = 1.0, n = 4, 3 slices / n; PFR =  $1.27 \pm 0.05$ , n = 4; PFR + Anisomycin =  $1.34 \pm 0.04$ , n = 4; mean  $\pm$  SEM; One Way ANOVA, P = 0.0007, Dunnett's Multiple Comparison Test, \*\* P < 0.01).

### 3.10 Role of glia in secretion and cleavage of brevican

It has been shown in previous studies that glia is primary source of brevican and therefore I wanted to assess the role of glia in secretion of brevican. For this purpose I used carbenoxelone (Cbxi) and endothelin (Endoi), which have previously been reported to block glia function (Blomstrand et al., 1999; Rouach et al., 2003). Cbxi blocks connexin-based

channels and inhibits voltage-gated calcium channels – on the other hand Endoi -Endogenous peptide blocker, which blocks coupling between astrocytes by dephosphorylating connexin based channels. I found that upon incubation with both mentioned blockers 20 min prior to stimulation and all the time till the end of experiment, reduced not only secretion of full length brevican but also cleavage of brevican (Figure 28). However, both compounds also abolished phosphorylation of CaMKII, indicating lack of LTP induction, which may be the reason for lack of brevican regulation.

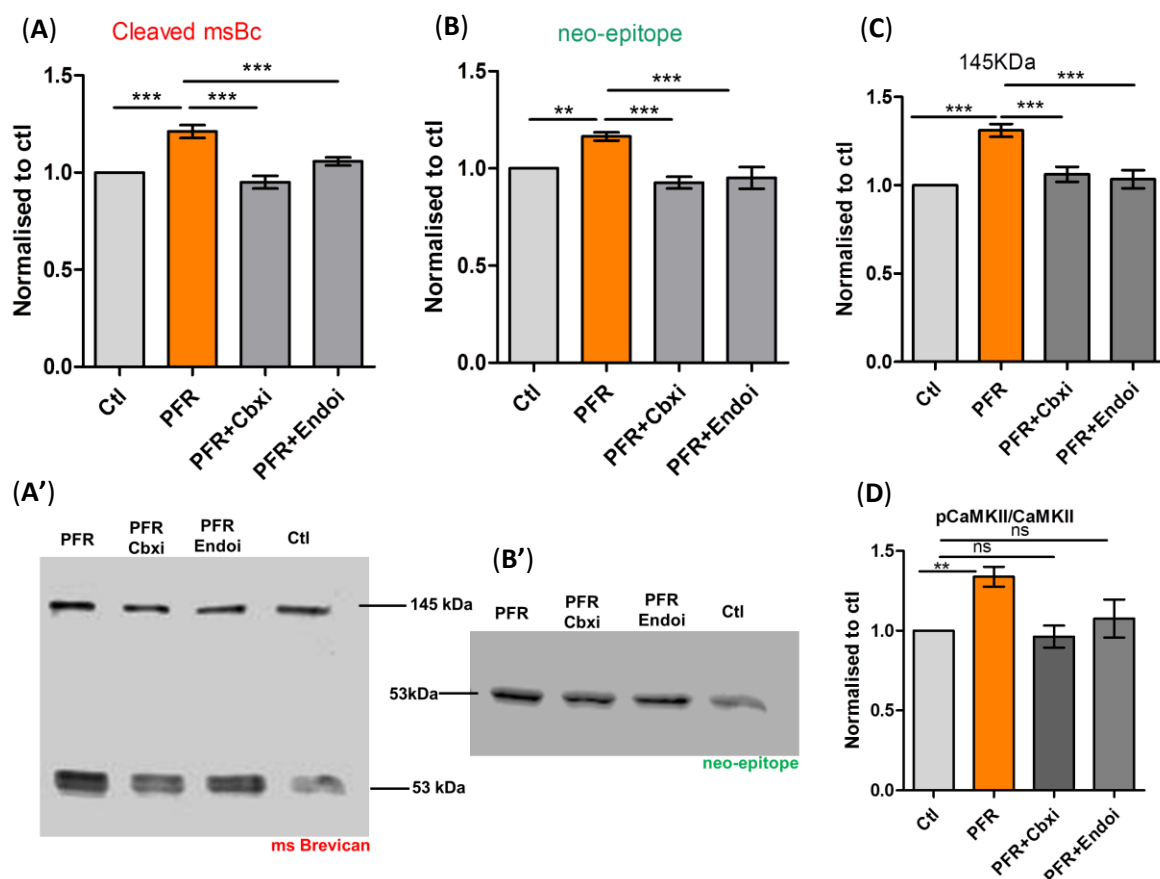


**Figure 28. Role of glia in secretion and cleavage of brevican**

(A) cLTP dependent modulation in presence of gap junction blockers for cleaved Brevican. All values are normalized to control (Ctl = 1.0, n = 8, 3 slices / n; PFR =  $1.21 \pm 0.03$ , n = 8; PFR + Cbxi =  $0.95 \pm 0.03$ , n = 6; PFR + Endoi =  $1.05 \pm 0.02$ , n = 6; mean  $\pm$  SEM; One Way ANOVA,  $P < 0.0001$ , Dunnett's Multiple Comparison Test, \*\*\*  $P < 0.001$ ). (A') Quantified the Western blot of acute hippocampal slices with ms  $\alpha$  Brevican antibody recognizing 53 kDa cleavage band and full length band at 145 kDa with above mentioned conditions.

(B) cLTP dependent modulation in presence of gap junction blockers for neo-epitope. All groups were normalized against control (Ctl = 1.0, n = 7, 3 slices / n; PFR =  $1.16 \pm 0.02$ , n = 7; PFR + Cbxi =  $0.92 \pm 0.02$ , n = 6; PFR + Endoi =  $0.95 \pm 0.05$ , n = 7; mean + SEM; One Way ANOVA,  $P = 0.0002$ , Dunnett's Multiple Comparison Test, \*\*  $P < 0.01$ , \*\*\*  $P < 0.001$ ). (B') Quantified the Western blot of acute hippocampal slices with neo-epitope specific antibody with above mentioned conditions.

(C) cLTP dependent secretion of brevican in presence of gap junction blockers. All groups were normalized against control (Ctl = 1.0, n = 8, 3 slices / n; PFR =  $1.33 \pm 0.06$ , n = 2; PFR + Cbxi =  $0.96 \pm$



0.06, n = 3; PFR + Endoi =  $1.076 \pm 0.11$ , n = 3; mean + SEM; One Way ANOVA, P = 0.016, Dunnett's Multiple Comparison Test, \*\* P < 0.01)

(D) cLTP induced phosphorylation of CaMKII was reduced in presence of gap junction blockers. All groups were normalized against control (Ctl = 1.00, n = 6; PFR =  $1.41 \pm 0.09$ , n=6; D-Ser + PFR =  $1.39 \pm 0.12$ , n=6; D-ser +PFR + CBXi =  $1.47 \pm 0.21$  n = 4; D-Ser + PFR +DAP5 =  $1.06 \pm 0.03$ , n=6 mean  $\pm$  SEM; One Way ANOVA, P = 0.0065, Dunnett's Multiple Comparison Test, \* P < 0.05). (D') Quantified the Western blot of acute hippocampal slices with ms  $\alpha$  CaMKII and rb  $\alpha$  pCaMKII antibodies with above mentioned conditions.

It has been suggested that release of D-Serine from astrocytes affects LTP induction (Henneberger et al., 2010). D-serine is co-activator of NMDA receptors and thought to be more potent agonist at glycine site on the NMDAR than glycine itself. In order to test whether glial D-serine was necessary to induce LTP and brevican cleavage, I incubated my slices with D-ser prior to the stimulation which had inhibitors were added as mentioned in section 2.2.9. Interestingly I found that D-serine alone was able to restore normal cleavage and secretion of brevican protein in presence of glia-function blocker (Figure 29).

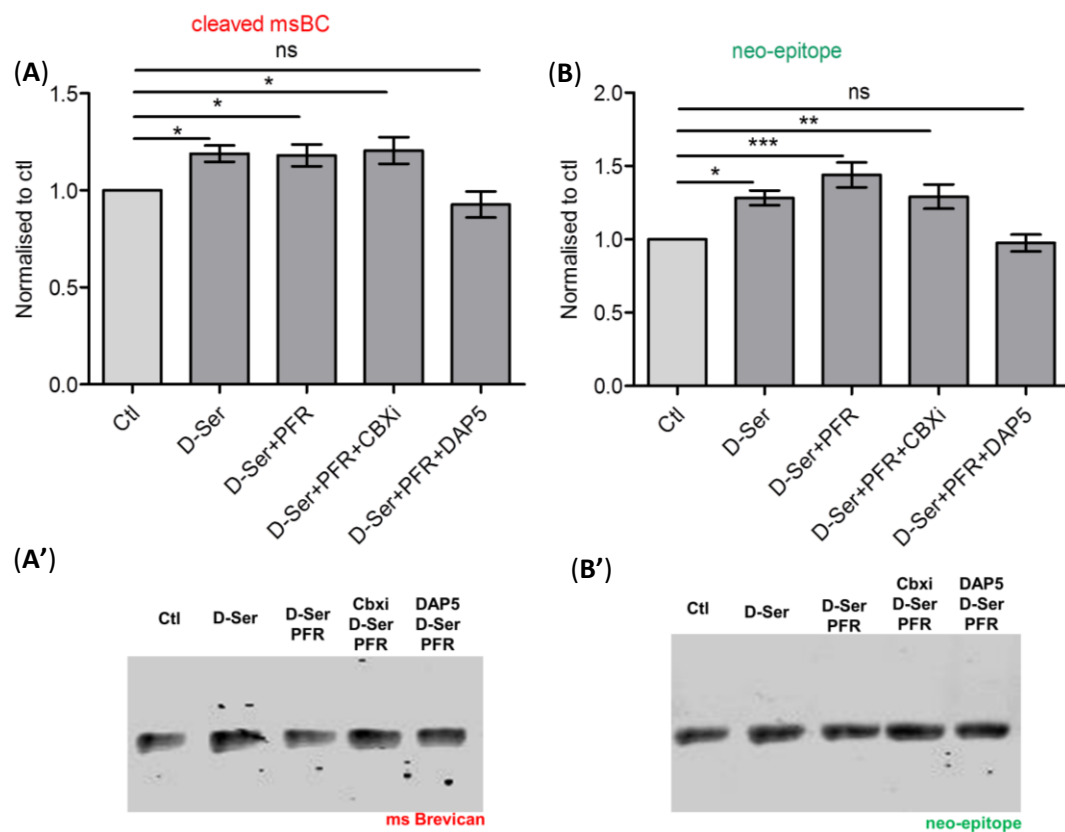


**Figure 29. Activity-dependent release of D-serine from glia is necessary for cleavage of brevican as marker of ECM.**

(A) cLTP in presence of D-Ser could rescue cleavage of brevican back, which was abolished as shown in previous fig upon CBXi pre-incubation. All values are normalized to control (Ctl = 1.0, n=11, 3 slices / n; D-Ser =  $1.18 \pm 0.04$ , n = 8; D-Ser + PFR =  $1.18 \pm 0.05$ , n = 10; D-SER + PFR + CBXi =  $1.20 \pm 0.06$ , n = 10; D-SER + PFR + DAP5 =  $0.92 \pm 0.06$ , n = 6; mean  $\pm$  SEM; One Way ANOVA, P<0.0001, Dunnett's

Multiple Comparison Test, \*  $P < 0.05$ ). (A') Quantified the Western blot of acute hippocampal slices with ms  $\alpha$  Brevican antibody recognizing 53KDa cleavage band with above mentioned conditions.

(B) cLTP in presence of D-Ser could rescue cleavage of brevican back, which was abolished as shown in previous fig upon CBXi pre-incubation, in presence of gap junction blocker. All groups were normalized against control (Ctl = 1.00, n = 10; D-Ser =  $1.28 \pm 0.05$ , n=7; D-Ser + PFR =  $1.43 \pm 0.08$ , n=9; D-ser +PFR + CBXi =  $1.29 \pm 0.08$ , n = 9; D-Ser + PFR +DAP5 =  $0.97 \pm 0.05$ , n=6; mean  $\pm$  SEM; One Way ANOVA,  $P = 0.0001$ ,Dunnett's Multiple Comparison Test, \*  $P < 0.05$ , \*\*  $P < 0.01$ , \*\*\*  $P < 0.001$ ). (B') Quantified the Western blot of acute hippocampal slices with neo-epitope specific antibody with above mentioned conditions.

In order to investigate the role of NMDAR I used DAP5 which is antagonist of NMDAR, when I looked for cleavage of brevican in the following group I observed no activity-dependent cleavage of brevican. I also checked for full length brevican protein and there was increase in its secretion upon activity induction in presence of gap junction blocker upon addition of D-Ser (Figure 30A). But again with DAP5 it was reduced. At this point it was also important to check whether it also rescues cLTP hallmark protein ERK. Interestingly on

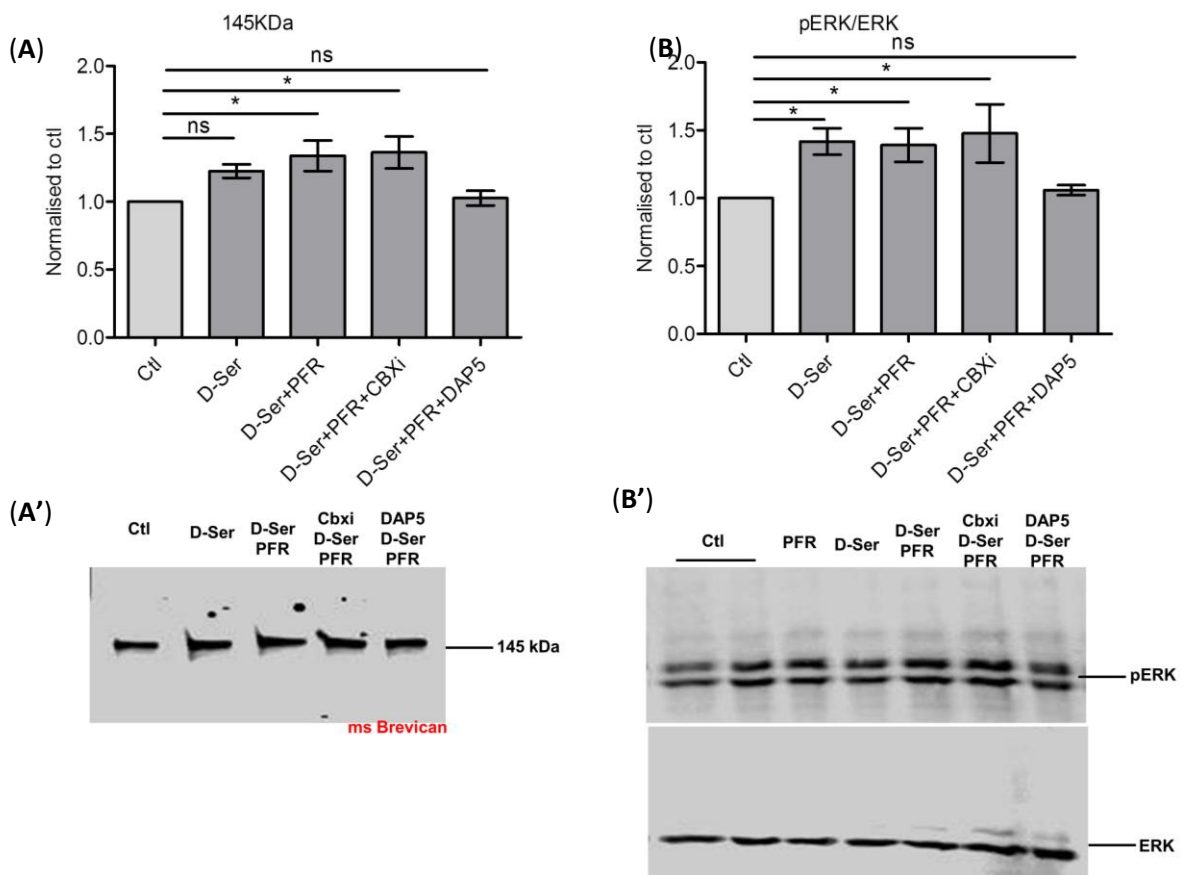


**Figure 30. Activity-dependent release of D-serine from glia is necessary for ECM modulation.**

(A) cLTP dependent increase in levels of full length brevican protein, with D-Serine alone there was trend of increase in brevican level even in presence gap junction blocker but no increase was observed in DAP5 antagonist pre-incubation group. All groups were normalized against control (Ctl =1.00, n=9, 3 slices/n; D-Ser=  $1.23 \pm 0.05$ , n = 7; D-Ser+PFR =  $1.34 \pm 0.11$  n=9; CBXi + D-Ser + PFR =  $1.36 \pm 0.11$  n=10; D-Ser + PFR + DAP5 =  $1.02 \pm 0.05$ , n=7; mean  $\pm$  SEM; One Way ANOVA,  $P < 0.0001$ ,Dunnett's Multiple

Comparison Test, \*  $P < 0.05$ ). (A') Quantified the Western blot of acute hippocampal slices with ms  $\alpha$  Brevican antibody with above mentioned condition.

(B) D-Ser induced phosphorylation of ERK was reduced by pre-incubation of DAP5, whereas D-Ser alone could lead to the phosphorylation of ERK even in presence of gap junction blocker. All groups were normalized against control (Ctl= 1.00, n = 6; D-Ser =  $1.41 \pm 0.09$ , n=6; D-Ser + PFR =  $1.39 \pm 0.12$ , n=6; D-ser +PFR + CBXi=  $1.47 \pm 0.21$  n = 4; D-Ser + PFR +DAP5 =  $1.06 \pm 0.03$ , n=6 mean  $\pm$  SEM; One Way ANOVA,  $P = 0.0065$ , Dunnett's Multiple Comparison Test, \*  $P < 0.05$ ). (B') Quantified the Western blot of acute hippocampal slices with ms  $\alpha$  pERK and rb  $\alpha$  ERK antibodies with above mentioned conditions.

induction of LTP in presence of D-Ser could bring phosphorylation of ERK, except in group with pre-incubation of NMDAR antagonist (Figure 30B). This suggests that D-Ser plays very important role of making NMDAR active and leading to secretion and cleavage of brevicin.

### 3.11 Influence of specific protease inhibitor for ADAMTS4 on induction of chemical LTP

It has been shown in previous studies that extracellular signal-regulated kinase (ERK), plays key roles in establishment of LTP and memory (Sweatt, 2001; Thomas and Huganir, 2004). I therefore investigated the ERK phosphorylation after cLTP induction (Figure 31). I found a significant increase in phosphorylation of ERK upon cLTP induction by PFR. Similar results were obtained when I used 4AP + Bcc, an alternative treatment to induce activity. I next

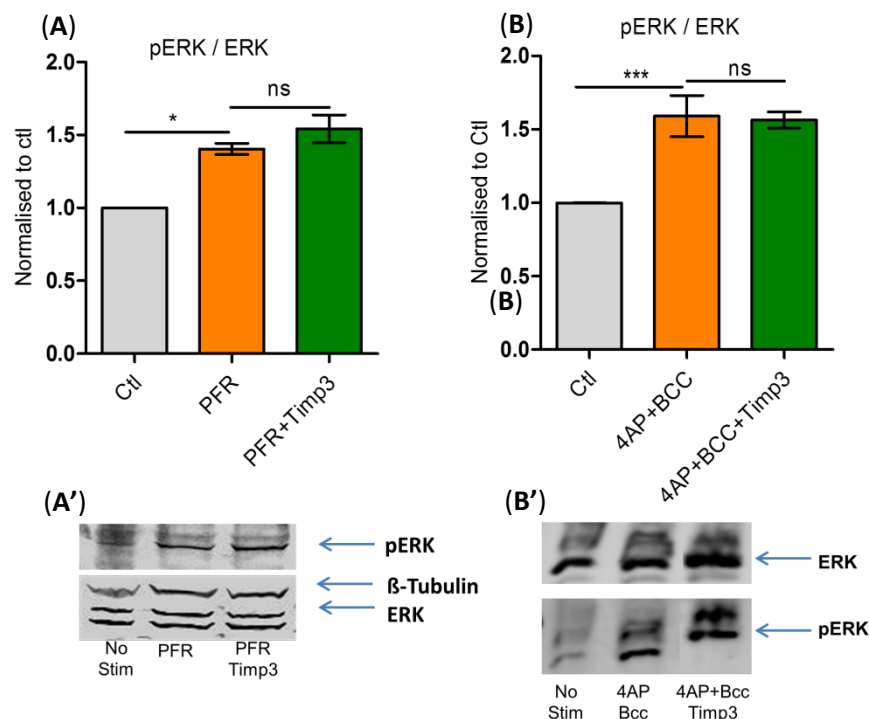


**Figure 31. Influence of an ADAMTS4-specific protease inhibitor on induction of cLTP by PFR and activity modulation by 4AP+BCC.**

(A) Application of a specific protease inhibitor of ADAMTS4, on hallmark protein upon cLTP induction by PFR. All groups were normalized against control (Ctl = 1.00, n = 3, 3 slices/n; PFR =  $1.40 \pm 0.03$ , n = 3;

PFR + Timp3 =  $1.54 \pm 0.09$ , n = 4; mean  $\pm$  SEM; One Way ANOVA, P = 0.0025, Dunnett's Multiple Comparison Test, \* P < 0.05, \*\* P < 0.01). **(A')** Quantified the Western blot of acute hippocampal slices with ms  $\alpha$  pERK and rb  $\alpha$  ERK antibodies with above mentioned conditions.

**(B)** Role of specific protease inhibitor of ADAMTS4 on hallmark protein upon synaptic activity induction by 4Ap + Bcc induction. All groups were normalized against control (Ctl = 1.00, n = 6, 3 slices/n; 4Ap + Bcc =  $1.59 \pm 0.14$ , n = 6; 4Ap + Bcc + Timp3 =  $1.56 \pm 0.05$ , n = 6; mean  $\pm$  SEM; One Way ANOVA, P<0.0001, Dunnett's Multiple Comparison Test, \*\*\* P < 0.001). **(B')** Quantified the Western blot of acute hippocampal slices with ms  $\alpha$  pERK and rb  $\alpha$  ERK antibodies with above mentioned conditions.

wondered whether PFR induced ERK phosphorylation was affected by proteolytic activity of ADAMTS4. Upon pre-incubation with specific protease inhibitor TiMP3 and broad band protease inhibitor GM6001 I found no influence on ERK phosphorylation. Similar results were obtained from experiments with 4AP+BCC, demonstrating that proteases are not directly influence establishment of LTP.

### 3.12 Activity-dependent modulation and role of proteases in modulation of dendritic protrusions

Finally I wondered whether activity-dependent modulation of ECM affects structural plasticity in acute hippocampal slices. I analyzed the number and size of dendritic spines

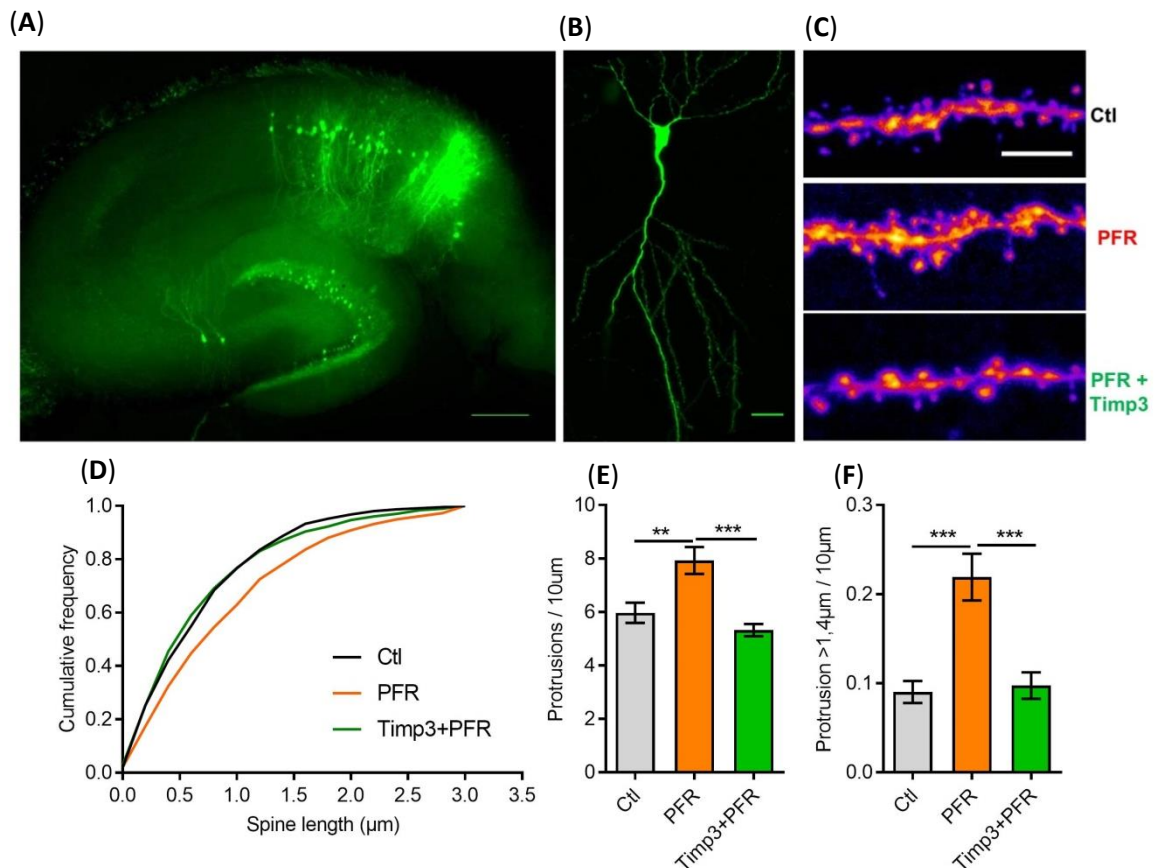


**Figure 32. Activity-dependent formation of dendritic protrusions in a proteolysis-dependent manner.**

cLTP- associated promotion of dendritic protrusions was assessed in acute hippocampal slices from 8-10 week old Thy1-YFP slick V-cre mice.

(A) Representative image of an acute hippocampal slices from Thy1-YFP slick V-cre mice with sparse neuron in CA1 region Scale bar (0.5 cm).

(B) Representative image of Thy1-YFP slick V-cre CA1 pyramidal neuron in acute hippocampal slice scale bar (20uM).

(C) Secondary apical dendrite with dendritic protrusions representing different groups (scale bar 5  $\mu$ m).

(D) Cumulative distribution of spine length revealed increase in spine length in PFR stimulated group, but this increase in length was abrogated to Control level with Timp3 pre-incubation even with PFR stimulation (n=spines/dendrites/animal; Ctl, n=462/11/6; PFR, n= 1140/18/6; Timp3+PFR, n= 677/16/6, Kolmogorov-Smirnov (KS)-test, Ctl, P=0.0354; PFR, P>0.1; Timp3+PFR, P=0.0369; PFR group alone passed the KS normality test).

(E) The bar plot shows the quantification of the increase in spine density/10 $\mu$ m (Ctl=5.97 $\pm$ 0.3759; PFR=7.929 $\pm$ 0.503; Timp3+PFR=5.321 $\pm$ 0.2302; PFR vs Ctl P<0.01, PFR vs Timp3 P<0.001 mean  $\pm$  SEM; ANOVA with Dunnett's post hoc test for comparison between groups).

(F) It shows SHP longer than 1.40uM in comparison between PFR vs Ctl, P<0.0001 and PFR-Timp3+PFR, P<0.001 (Ctl= 0.0902+0.01246; PFR = 0.2191 $\pm$ 0.02625; Timp3+PFR = 0.09742 $\pm$ 0.01489 mean  $\pm$  SEM; ANOVA with Dunnett's post hoc test for comparison between groups).

from Slick V-Cre 8-10 weeks-old mice. In the first series of experiments I investigated the activity-dependent formation of dendritic protrusion (DPs) upon cLTP induction as marker for structural changes. I analyzed secondary proximal dendrites upon stimulation and there was increase in length of SHPs longer than 1.5 $\mu$ m in comparison to control slices. To test the role of proteases, I pre-incubated the slices with the protease inhibitor Timp3. Interestingly, inhibition of proteolytic activity prevented the formation of large protrusions (Figure 32). These data suggest that that perisynaptic lectican-based ECM restricts the formation of protrusions.

### **3.13 Activity-dependent proteolytic cleavage of NG2 results in increased levels of ectodomain associated with the ECM**

In collaboration with **Dominik Sarky** and **Jacqueline Trotter** (Johannes Gutenberg University Mainz, Mainz) I wanted to investigate activity-dependent shedding of NG2 on OPC. For this purpose I subjected acute hippocampal slices to cLTP (PFR incubation) or 4AP + BCC incubation. Subsequently I extracted ECM as described in previous section and measured the level of the NG2 ectodomain of 290 KDa by Western blot. The resulting samples after chondroitinase ABC extraction contain only soluble, extracellular proteins, as membrane proteins are not extracted in the absence of detergent. These samples thus contain only shedded soluble NG2 ectodomain. Strikingly, huge increase in the NG2 levels of ectodomain was observed with PFR stimulation (Figure 33). NG2 ectodomain levels slightly

decreased with ongoing recovery time and returned to initial levels after 180 min of recovery time (Figure 33A). This brought us to identify the protease responsible for the activity-dependent ectodomain shedding, for this reason I incubated the slices in the presence of the metalloprotease inhibitor GM6001 or the ADAM10 inhibitor GI. Both compounds completely abolished the NG2 ectodomain shedding induced by PFR stimulation (Figure 33B). In the presence of the ADAM10 inhibitor GI, the ECM-associated levels of the NG2 ectodomain were reduced to below those of the control, demonstrating that basal, ADAM10-dependent cleavage of NG2 in OPC. Incubation of acute hippocampal slices with 4AP + BCC, which depolarizes neurons and affects OPC, upregulation of NG2 ectodomain levels in the ECM in a comparable fashion to stimulation with PFR (Sakry et al., 2014) (Figure 33B).

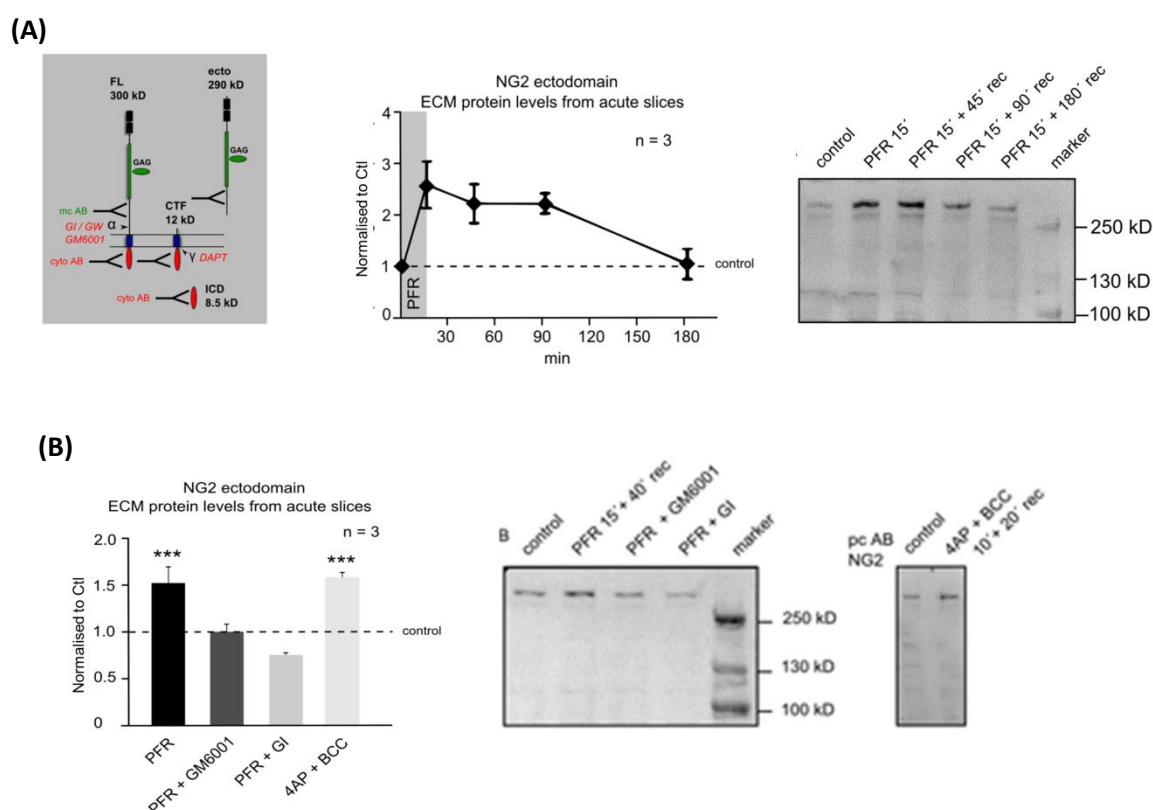


**Figure 33. Induction of cLTP leads to NG2 ectodomain shedding Activity-dependent proteolytic cleavage of NG2 results in increased levels of ectodomain associated with the ECM.**

**(A)** Schematic representation of Proteolytic Cleavage of NG2; it has been shown here by Western blot of ECM extracts of acute hippocampal slices from 8-10 weeks old rats by digestion of the glycosaminoglycan chains by chondroitinase ABC. An increase of the NG2 ectodomain was detected after chemical LTP (PFR) stimulation for 15 min. NG2 ectodomain levels within the ECM return to initial levels after 180 min of recovery time. NG2 ectodomain levels were normalized against total protein from a matching coomassie stained SDS-PAGE gel (from Sakry et al., 2014.).

**(B)** NG2 ectodomain levels increased to 1.5-fold in ECM extracts of acute hippocampal slices after 16 min stimulation with PFR. Inhibition of metalloproteases (GM6001), and ADAM10 (GI), prevented the increase of ECM-associated NG2 ectodomain. Incubation with GI reduced levels of ECM-associated NG2 ectodomain to below the control value. Treatment of the slices with 4AP + BCC for 10 min with 20 min recovery time showed the same increase in levels of ECM-associated NG2 ectodomain as seen with the PFR treatment (one way ANNOVA with Dunnett's multiple comparison test, \*\*\* P < 0.001).

## 4. Discussion

---

ECM being a net-like structure fills the gap between neurons and glia. It is secreted from neurons and glia cells and forms dense networks of proteins and glycans in the extracellular space. Structurally it enwraps neuron and chemically it is a source of diverse instructive signaling molecules that are involved in cellular growth, differentiation, activity in pathological situations and survival. Once ECM has matured, it marks the end of the critical period, as it becomes non-permissive for neuronal outgrowth and thus strongly reduces structural plasticity. However, there is still plasticity in the adult brain and it is of great interest to find the mechanism preserving structural plasticity. Here I followed the hypothesis that interplay of endogenous modifications of ECM, which includes ECM proteolysis and formation of new ECM, is a major factor in first preserving plasticity and second stabilization of modified neuronal networks. Besides ECM cleavage via proteases from the ADAMTS family, I could also identify sheddases to be involved in activity-dependent cleavage of proteoglycans and modulation of synaptic plasticity.

### 4.1 Brevican as marker of ECM and its modulation upon neuronal activity

ECM is the glue holding glia cells and synapses together, playing important role in functional and structural plasticity. ECM is a complex structure consisting of many molecules, forming a molecular meshwork around synapses of which, CSPGs lecticans are the main component. It is present perisynaptically as a marker for diffuse ECM around synapses. It is restrictive for structural plasticity and synaptogenesis and it has been shown that experimental removal of chondroitin sulfates by glycosidases leads to juvenile-like structural and functional plasticity. Among all lecticans brevican is the smallest and most abundant member of the lectican family and like the other family members also substrate of aggrecanase (Nakamura et al., 2000). In our experiments it was extracted and biochemically analysed for cleavage by specific homemade neo-epitope as well commercially available antibodies in the 8-10 week old adult rats. I found that after cLTP by PFR activity-dependent cleavage of brevican, illustrating that ECM could be modified at the adulthood and thus after it has matured past the critical periods. It was confirmed by analysing aggrecan another key member of the lectican family, where also cleavage was observed. Suggesting that mechanisms exist which allow for structural changes after closure of the critical periods.



## **4.2 Perisynaptic localization of brevican**

To gain information about localization of brevican cleavage I performed a series of immunohistochemistry of acute slices. I found increased fluorescence intensities in the stratum radiatum after cLTP induction. This pointed towards synaptic cleavage of brevican as neuropil contains mostly excitatory synaptic contacts. This became more evident when I found increased cleavage around homer positive puncta, which supported our hypothesis that brevican, was cleaved perisynaptically. After a more detailed analysis using STED microscopy, it became clearer that both cleavage and full-length protein are localized in close vicinity to the synaptic junction. I also observed that full length and the cleaved form of the protein are in close relation and segregated from each other at the perisynaptic site. The consensus in the field was such that they co-localize with each other, but above method resolved the small hot-spots of ECM labeling and provide a new insight into subcellular structures and localization of ECM components.

## **4.3 Activity-dependent modulation of ECM**

### **4.3.1 Role of proprotein convertases in cleavage of brevican**

Most proteases comprise a prodomain, which holds them in the inactive state by covering the active site. In order to activate the protease, the prodomain must be removed. This occurs by proteolytic removal of the prodomain mostly by specialized enzymes the proprotein convertases (PC). The most relevant protease for our study was ADAMTS-4, which is also produced as catalytically inactive proprotein and needs proteolytic activation (Tortorella et al., 2005). Several enzymes have been suggested to be responsible for ADAMTS4 activation of which PACE4 is a PC that especially was responsible for cleavage of the ADAMTS4/5 at RAKR<sup>212</sup> and RRRR<sup>261</sup>, respectively. However, it is unclear whether ADAMTS4 is secreted as inactive zymogen or it is activated before secretion. To clarify this I used APMA, a compound that non-selectively removes prodomain, and thus activates proteases. The fact that brevican cleavage was observed without any stimulation suggests ADAMTS4 is present in the inactive form in the extracellular space and activated by secretion of activating enzymes. It has also been suggested that PACE4 and PC5A may be secreted and thus these enzyme (Tsuji et al., 2003) may activate adamts4 extracellularly. Findings from the (Malfait et al., 2008) suggest that proteases are activated extracellularly by PACE4 from chondrocytes. Taken together these experiments suggest that effective protease activation by PACE4 leads to the modulation of CSPG ECM.

### **4.3.2 Endogenous proteases involved in degradation of brevican**

Plethoras of proteases are present in the nervous system, modulating the existing ECM around the synapses in mature as well juvenile state of the brain (Huntley, 2012). They have been broadly categorized as MMPs, ADAMs and ADAMTS based on their structure and role. It is known that lecticans can be a substrate for a number of proteases especially of proteases that were termed aggrecanase-1/-2 and later identified as ADAMTS4/5 (Nakamura et al., 2000). Degradation of brevican was diminished in presence of broad-spectrum blockers of MMPs, suggesting the involvement of proteases. This modulation of brevican as one of the lecticans was not just limited to brevican alone but also other members of the family such as aggrecan, a well-studied lectican, is degraded suggesting that brain ECM could be modified in the mature state by endogenous proteases. It has been suggested in past that aggrecan which is an important constituent in adult brain also get cleaved by ADAMTS4 (Giamanco et al., 2010) which is in line with our findings. Recent observations showed that protease activity was increased after epileptic seizures that lead to the regulation of homeostatic plasticity (Hamel et al., 2005; Valenzuela et al., 2014). In addition to this it has been found that ADAMTS4 is generated by oligodendrocytes and its mRNA peaks around the development of the cell-type generating them (Levy et al., 2015). However, its role in synaptic plasticity remains elusive. There has been a general consensus in the field that brevican is the lectican with highest expression level in the central nervous system and is degraded under pathological condition. This modulation of ECM is activity-dependent, and in line with my findings that stimulation with 4AP a potassium channels blocker and BCC, a GABA antagonist induces cleavage of brevican as well. Thus this proteolytic cleavage by endogenous protease alters the ECM at the mature state and as ECM surrounds the synapses, this may affect synaptic plasticity and synaptic functions as inhibitory constraints around them are loosened.

## **4.4 Key players involved in the modulation of perisynaptic ECM**

### **4.4.1 Cleavage of brevican requires NMDAR and network activity**

Activity-dependent modulation of ECM by PFR is dependent on the concomitant activation of the postsynaptic neuron, which is also a prerequisite for the induction of LTP (Otmakhov et al., 2004a). PFR stimulation induces LTP in an NMDAR dependent manner by enhancing neuronal network activity by reduction of GABAergic inhibition in combination with enhancing of cAMP-mediated intercellular signaling. Previous studies about the serine

protease neurotrypsin implied its role in activity-dependent cleavage of agrin at the synapses. The same study also suggests that postsynaptic NMDAR activation was mandatory for the proteolysis of agrin (Matsumoto-Miyai et al., 2009). Further NMDAR activation along with CaMKII are required for adhesion molecule neuroligin-1 proteolytic cleavage (Peixoto et al., 2012). Along that line, our study pointed towards a central role of NMDAR activation for the cleavage of brevican, as there was no activity-dependent cleavage of brevican observed in presence of NMDAR antagonist. I also noted as suggested in the literature that strong depolarization is needed to remove the  $Mg^{2+}$  block from the postsynaptic membrane (Mayer et al., 1984) and  $Mg^{2+}$  was excluded from the aCSF. Further evidence for the involvement of NMDAR in activation of proteases emerges from experiments where I applied D-serine to the slices and found that it was sufficient to restore normal cleavage of brevican in the acute slices. Antagonist applied for AMPA, L-VGCCs suggested that postsynaptic depolarization, and  $Ca^{2+}$  contributes to the activation of protease and thus cleavage of brevican. In line with this, I found that also silencing the neuron with  $Na^+$  channel blocker TTX, which prevents action potentials, reduced cleavage of brevican. This suggested that synaptic activity and activation of NMDAR, as well as VGCCs, is necessary for the modulation of ECM. This suggests  $Ca^{2+}$  to be a key second messenger in the activation of the proteolytic cascade leading to brevican cleavage.

NMDAR has CaMKII $\alpha$  as a major signaling molecule in its downstream pathway and presented results suggests it to be a key player in the modulation of ECM. It has been indicated that GluN2B-NMDAR has a high affinity for CaMKII (Strack and Colbran, 1998), CaMKII is known to be profoundly present at synapses (Peng et al., 2004) and majorly contributing to the induction of LTP (Otmakhov et al., 1997). It's also known that mutated GluN2B subunit with decreased affinity for CamKII leads to abrogated LTP (Barria and Malinow, 2005). These results are in agreement with another finding where the cytoplasmic tail of GluN2B was deleted that results in blockage of LTP (Foster et al., 2010) as binding to the cytoplasmic domain keeps CaMKII within the proximity of synaptic activity. This suggests that GluN2B subunit is also involved in targeting CaMKII to the site of  $Ca^{2+}$  influx at the PSD. Another important investigation suggests that  $Ca^{2+}$  influx during LTP is higher in LTP than LTD paradigms (Lisman, 1989). These findings altogether point towards a common consensus in the field that activated CaMKII are translocated to the synapse where they bind to GluN2B, which marks an important event for the LTP. CaMKII $\beta$  is the other isoform of CaMKII, and in the hippocampus forms the holoenzyme with CaMKII $\alpha$ . Studies have shown that alteration/deletion of CaMKII $\beta$ , disrupts targeting of CaMKII $\alpha$  to the synapse and LTP

and learning and memory gets affected in the CaMKII $\beta$ -KO mice (Borgesius et al., 2011). It also has been implicated that CaMKII $\beta$  binds to F-actin and targets the CaMKII $\alpha$  to the dendritic spines. So both isoforms of CaMKII act respectively but with a distinct function. Further, it has been described in a recent review (Nishiyama and Yasuda, 2015) that Ca<sup>2+</sup> influx triggered CaMKII to pass its signal to small GTPase and to the downstream kinases which lead to actin modulation. Thus NMDAR dependent CaMKII signaling contribute majorly to the structural changes happening during the short time window of opportunity provided with the degradation of the matrix, at the same time more matrix would be needed to incorporate these newly formed or altered synaptic structures after the plasticity has happened. This will be discussed in the next section of the thesis.

#### **4.5 Role of glia in secretion and cleavage of brevican**

Beside cleavage of brevican, I also observed an increase in the abundance of full-length brevican in ECM extracts. I found that protein synthesis blocker did not alter activity-dependent increase in brevican and thus I concluded that this increase emerges from the secretion of intracellularly stored brevican. Brevican is known to be secreted from both, neurons and glia (John et al., 2006) however; it is thought that the majority of brevican is produced by glia cells. Further, in a study in adult rat cerebellum (Yamada et al., 1997) and the hippocampal fimbria (Ogawa et al., 2001) that astroglial cells are the key source of brevican *in vivo*.

To test whether glia is the major source of activity-dependent secretion of brevican I used carbenoxolone (Cbxi). Carbenoxolone is known to block hemichannels and astrocytes mediated spontaneous activity in the cultured hippocampal cell networks (Rouach et al., 2003). The other more specific blocker used is endothelin-1 (Endoi) an endogenous peptide, which has been known to be among the most potent inhibitor of gap junction communication in astrocyte culture (Blomstrand et al., 1999). Cbxi general blocker of connexin-based channels and inhibits voltage-gated calcium channels and on the other hand Endoi - Endogenous peptide blocker, which blocks coupling between astrocytes by dephosphorylating connexin-based channels have also been implicated in total inhibition of transient hetero-synaptic depression in astrocytes of the rat hippocampal CA1 region (Andersson et al., 2007). Since its also common consensus that single hippocampal astrocyte can cover approximately 140000 synapses (Bushong et al., 2002) these intra-domain channels might be playing an important role in intersynaptic communication. One such example would be its role in transient heterosynaptic depression.

Indeed I found decreased brevicin cleavage and secretion using both Cbxi and Endoi to disturb astrocyte function, however, at the same time CaMKII phosphorylation was also reduced. This indicates that induction of cLTP failed and underlines the important role of glia in this process. Astroglia support synapses and synaptic plasticity in multiple ways and most importantly it has been shown that they secrete the NMDA receptor co-agonist D-serine. Studies in the past have pointed that D-serine is a more potent agonist for NMDA than glycine and occupies this site at functional synapses (Mothet et al., 2000). It suggested that the exogenous application of D-serine activated the glycine site of NMDAR elucidates D-serine as an endogenous ligand for the glycine site. Results from my thesis demonstrate that D-serine alone was sufficient to rescue brevicin cleavage and secretion in presence of glia functional blocker. This suggested an important role of D-serine in the activity-dependent cleavage and modification of ECM in an NMDAR dependent manner. Another finding supporting our hypothesis/findings implied  $Ca^{2+}$  dependent release of D-serine from astrocytes control NMDAR dependent plasticity (Henneberger et al., 2010). Thus, astroglia indeed plays a direct role in synaptic plasticity by providing D-serine and an indirect by NMDA receptor activation leading to secretion and cleavage of brevicin. Brevican has been shown to be produced by neurons (Seidenbecher et al., 1998) however in smaller amounts than in glia cells and is transported to the presynaptic site via axon transport (Carulli et al., 2006). This suggests that although brevicin may be mainly contributed by glia cells, activity-dependent extracellular changes of brevicin abundance and cleavage is most likely of neuronal origin.

## **4.6 Functional impact of ECM modulation**

### **4.6.1 Influence of specific protease inhibitor of ADAMTS4 on induction of chemical LTP**

Extracellular signal-regulated kinase (ERK) has been indicated as a key player in the establishment of LTP and memory (Dineley et al., 2001; Thomas and Huganir, 2004). One of three cocktails I used for cLTP was forskolin which is known to increase the levels of cAMP production, leading to the activation of ERK in hippocampal slices (Levenson et al., 2004) and ERK plays an important role in synaptic plasticity as late phase LTP requires elevated cAMP levels (Patterson et al., 2001). When I investigated cLTP induction with PFR I found phosphorylation of ERK and ERK phosphorylation was unaltered in presence of specific protease inhibitor TiMP3 and broad band protease inhibitor GM6001. These findings were also analyzed for alternative means of synaptic activity induction with 4AP + Bcc, which also

demonstrated similar findings allowing us to conclude that proteases do not directly influence the establishment of LTP. This was supported by electrophysiological assessment of LTP where protease inhibitor pre-incubation did not have a direct influence on LTP (Measured by Prof. Alexander Dityatev's group, data not shown in this thesis). These findings are in agreement with another study where it has been suggested that there were no differences in the extent of LTP between neurotrypsin-deficient and wild-type mice (Matsumoto-Miyai et al., 2009). Thus, this proposes that neither ADAMTS nor neurotrypsin has a functional effect on LTP. This is interesting since other groups of MMP's such as MMP9 or MMP3 have an impact on LTP expression. Most likely, ECM digestion because of LTP serves to allow for subsequent events, such as structural plasticity as discussed below.

#### **4.6.2 $\beta$ 1-integrin signaling affects the activity-dependent modulation of ECM**

Integrins are an important class of ECM receptors and play a role in physical and functional links between ECM and cytoskeletal signaling pathways.  $\beta$ 1-integrin-dependent signaling has been implicated in regulating the increase in NMDAR-mediated synaptic response (Bernard-Trifilo et al., 2005). They showed that RGD peptides, which activate  $\beta$ 1-integrins induce Src family kinase activity which affects the phosphorylation state of the NMDAR subunits GluN2A and GluN2B. It has also been suggested that RGD peptides can elicit elongation of existing dendritic spines and the formation of new filopodia. This effect could be blocked by function-blocking antibody against  $\beta$ 1-integrin. Thus this finding also suggested that integrins control ECM-mediated spine remodeling through NMDAR/CaMKII-dependent actin reorganization (Shi and Ethell, 2006). In my experiments, I also found that in the presence of function-blocking antibody there was a reduction of cleavage of brevican but no effect on secretion of full-length protein. Findings from the literature also suggest that chronic treatment with anti- $\beta$ 1 Integrin function-blocking antibody alters surface diffusion of GluN2B subunits (Groc et al., 2007). CSPGs have also been implicated in  $\beta$ 1-integrin signaling. This has been shown by digesting CSPGs with ChABC in live hippocampal slices, which increased spine motility and appearance of spine head protrusions (Orlando et al., 2012). This result suggests that CSPGs may be a ligand for  $\beta$ 1-integrin receptors and ECM may regulate NMDARs in an integrin-dependent manner.

Interestingly, proteases are also known to be affecting integrin signaling. Many ECM and adhesion proteins have been known to be a substrate for MMPs, including ligands for integrin such as laminin, N-cadherin, dystroglycan and proteoglycans (Lander et al., 1997).  $\beta$ 1-integrin functionality has been known to be important for synapse enlargement as well as an

increase in postsynaptic currents (Bukalo et al., 2001). Another interesting finding suggests MMP-9 affects lateral mobility in a  $\beta$ 1-integrin-dependent manner (Michaluk et al., 2009). Thus these findings suggest that  $\beta$ 1-integrin might play an important role in passing the information about ECM rearrangement, via plasticity related signaling pathways.

#### **4.6.3 Activity-dependent modulation and role of proteases in structural plasticity**

ECM has been suggested to be restrictive for structural plasticity after the critical period and thus I expected ECM cleavage to be important to allow for structural plasticity past this period. Indeed, I found no activity-dependent structural plasticity in presence of TIMP3, suggesting lectican cleavage to be crucial in this process, although LTP was normal. Studies carried out in the past suggest that ECM digestion with ChABC enzymes based on activation of  $\beta$ 1-integrins lead to increased spine dynamics (Orlando et al., 2012). Our results strongly support a parallel role of proteases in the modification of ECM, which provides a time window of opportunity to establish new synapses in the mature state. Thus, suggesting proteases are involved in the structural changes and in absence of protease activity modulation of dendritic protrusions was reduced or abolished. Another study based on protease MMP-9 depicted nicely that  $\beta$ 1-integrin activation is necessary for protease influence and that it can be functionally involved in synaptic remodeling (Michaluk et al., 2011). MMP-9 has also been implicated to be functionally involved in the formations of SHPs and the control of postsynaptic receptor distribution (Szepesi et al., 2013). They also suggested that once protease MMP-9 active cleaves ECM components and thus allowing the intracellular signaling (via  $\beta$ 1-integrin) induces the formation of SHP and modulation of ECM, this could be the model for how changes are happening perisynaptically. Another hint that spines are modulated upon activity-dependent cleavage of ECM was suggested in neurotrypsin-agrin system. Inactivation of neurotrypsin abrogated filopodia formation but did not affect LTP (Matsumoto-Miyai et al., 2009). This implicates a key role of proteases acting as a means or workforce involved mechanistically in cleavage and secretion of ECM upon activity in their niche to stabilize the new synaptic connections in the mature state.

#### **4.7 The role of Sheddases ADAM10 in NG2 cleavage in primary OPC.**

NG2 cells are OPCs expressing the transmembrane proteoglycan NG2. Besides being a precursor of oligodendrocytes this cell type has a high density of AMPAR and forms synapses with excitatory neurons (Bergles et al., 2000; Jabs et al., 2005). However, the physiological role of this neuron to OPC interaction was largely unknown. Interestingly, in

the course of a collaborative project with the group of Prof. Trotter I observed that it was possible to extract a part of NG2 ectodomain from acute hippocampal slices by using chondroitinase ABC. Thus, I found increased shedding of NG2 ectodomain, which returned to baseline level 180 min after induction of cLTP in hippocampal slices with PFR. This suggested a fast removal of ectodomain fragment after shedding, which may happen by binding to cell-surface receptors and subsequent internalization or further proteolytic processing. Stimulation with PFR in presence of ADAM10 inhibitor reduced NG2 ectodomain shedding below control levels, suggesting ADAM10 as the responsible protease involved for both the PFR-induced and constitutive cleavage in vivo. These findings were verified with another stimulation protocol using 4AP + BCC, this cocktail of chemicals is known to act by inhibiting repolarization by blocking voltage-dependent potassium channels (Tauskela et al., 2008).

To test the involvement of neurons in proteolytic cleavage of NG2 Dominik Sakry from the group of Prof. Jacky Trotter used above-mentioned stimulation protocols in isolated primary OPC (data not shown in the thesis; (Sakry et al., 2014)). PFR was unable to increase NG2 ectodomain cleavage in isolated OPC, suggesting neuronal networks and neuron to NG2 excitatory synapses to be involved in ADAM10 activation. However, treatment with 4AP + BCC leads to increased NG2 cleavage in pure OPC cultures. OPCs express voltage-dependent potassium channels (Maldonado et al., 2013) and thus 4AP + BCC lead to the depolarization of the OPCs, which was a must for activity-dependent NG2 shedding. It has been suggested that protease ADAM10 is located at excitatory post-synapse of neurons (Marcello et al., 2007), however, these findings suggest that OPC also expresses ADAM10. Past studies have confirmed that NG2 binds the PDZ domain protein GRIP in OPC, which itself binds to AMPAR forming a tripartite complex in OPC (Stegmuller et al., 2003). Increased levels of NG2 ectodomain in the ECM are present at neuron-OPC synapses because of induced activity. This shedding of NG2 ectodomain is regulated by neuronal activity. Further it had also effect on neuronal glutamate receptor current and long term synaptic plasticity in the somatosensory cortex.

## **4.8. Conclusion**

In conclusion my data suggests a mechanism for coordinated regulation of activity dependent remodeling of ECM by endogenous mechanism which is an opportunity to form newer synaptic connections at mature state. Further, I contributed to a better understanding of the



interplay between NG2 shedding from OPC's and its effect on synaptic plasticity, this has been depicted in the concluding Figure 34.

I believe that my results significantly contribute to the understanding of the mechanisms involved at mature brain ECM and role of proteases in modifying the ECM, which could be used for therapeutic purposes to cure the pathological situations of the brain.

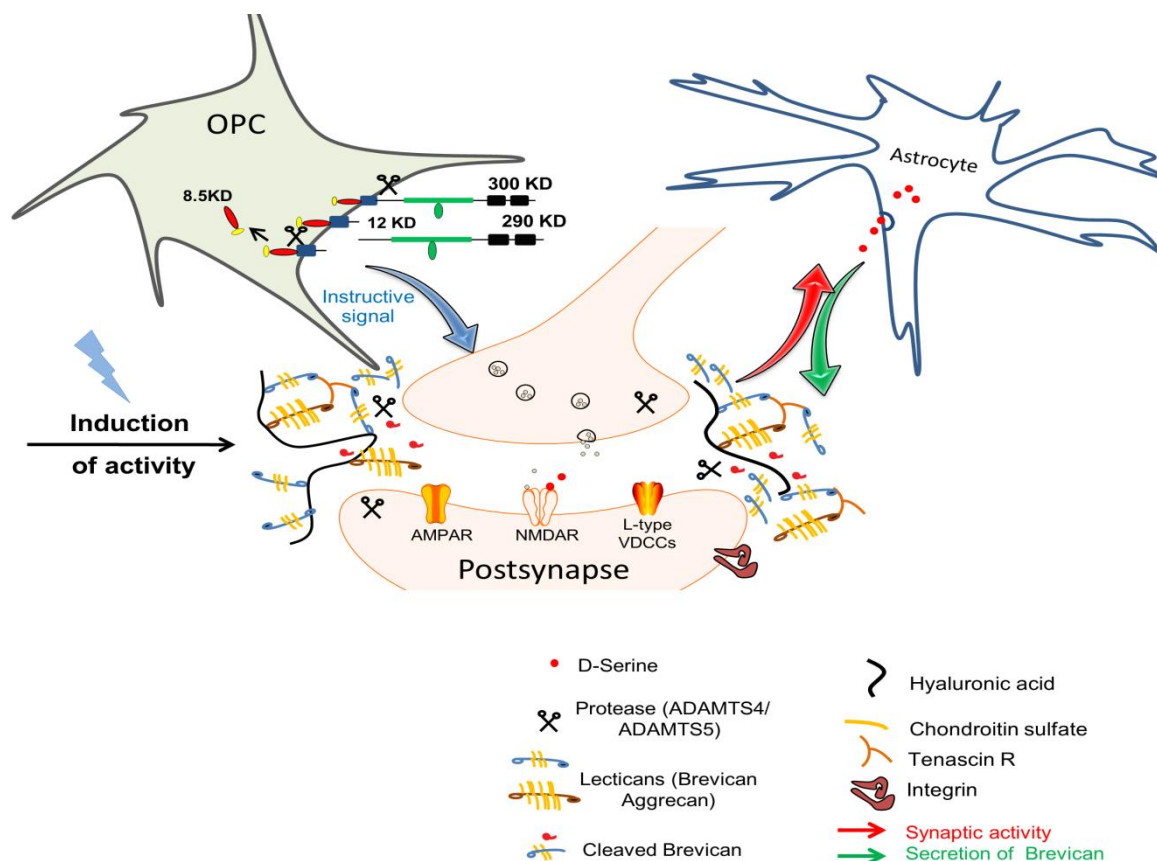


**Figure 34: Schematic presentation of putative signalling mechanisms that lead to modulation of perisynaptic ECM upon induction of synaptic activity by proteases in an NMDAR-dependent manner.**

Perisynaptic lectican-based ECM surrounds the synapses and its maturation marks the end of critical periods and has restrictive effects on structural plasticity.

In this thesis I have focussed on intrinsic mechanisms which could modulate the ECM in mature state. It was proposed that upon activity ECM could be modified by endogenous proteases such as ADAMTS4/5. Here lecticans were used as model molecules, which are processed by activated proteases upon postsynaptic activation. An important role of astrocytes was observed as they supported NMDAR activation by providing D-serine and secreting more ECM proteins. These events suggest that the ECM may regulate NMDARs in a  $\beta$ 1-integrin-dependent manner. NMDAR-dependent CaMKII signalling

contributes largely to the structural changes happening with the degradation of the matrix. ECM secretion may be needed to incorporate the newly formed synapses to stabilise them.

Furthermore, I have shown that there is bidirectional communication between neurons and oligodendrocyte precursors; neuronal activity leads to cleavage of the glial membrane NG2 protein and sheds its extracellular domain that gives instructive signals that modulates the synaptic transmission between neurons.

## 5. Bibliography

---

- Allen NJ, Barres BA (2009) Neuroscience: Glia - more than just brain glue. *Nature* 457:675-677.
- Andersson M, Blomstrand F, Hanse E (2007) Astrocytes play a critical role in transient heterosynaptic depression in the rat hippocampal CA1 region. *J Physiol* 585:843-852.
- Barria A, Malinow R (2005) NMDA receptor subunit composition controls synaptic plasticity by regulating binding to CaMKII. *Neuron* 48:289-301.
- Bassi DE, Fu J, Lopez de Cicco R, Klein-Szanto AJ (2005) Proprotein convertases: "master switches" in the regulation of tumor growth and progression. *Molecular carcinogenesis* 44:151-161.
- Bayer KU, De Koninck P, Leonard AS, Hell JW, Schulman H (2001) Interaction with the NMDA receptor locks CaMKII in an active conformation. *Nature* 411:801-805.
- Bergles DE, Roberts JD, Somogyi P, Jahr CE (2000) Glutamatergic synapses on oligodendrocyte precursor cells in the hippocampus. *Nature* 405:187-191.
- Bernard-Trifilo JA, Kramar EA, Torp R, Lin CY, Pineda EA, Lynch G, Gall CM (2005) Integrin signaling cascades are operational in adult hippocampal synapses and modulate NMDA receptor physiology. *J Neurochem* 93:834-849.
- Bliss TV, Collingridge GL (1993) A synaptic model of memory: long-term potentiation in the hippocampus. *Nature* 361:31-39.
- Blomstrand F, Giaume C, Hansson E, Ronnback L (1999) Distinct pharmacological properties of ET-1 and ET-3 on astroglial gap junctions and Ca(2+) signaling. *The American journal of physiology* 277:C616-627.
- Borgesius NZ, van Woerden GM, Buitendijk GH, Keijzer N, Jaarsma D, Hoogenraad CC, Elgersma Y (2011) betaCaMKII plays a nonenzymatic role in hippocampal synaptic plasticity and learning by targeting alphaCaMKII to synapses. *J Neurosci* 31:10141-10148.
- Bradl M, Lassmann H (2010) Oligodendrocytes: biology and pathology. *Acta neuropathologica* 119:37-53.
- Brakebusch C, Seidenbecher CI, Asztely F, Rauch U, Matthies H, Meyer H, Krug M, Bockers TM, Zhou X, Kreutz MR, Montag D, Gundelfinger ED, Fassler R (2002) Brevican-Deficient Mice Display Impaired Hippocampal CA1 Long-Term Potentiation but Show No Obvious Deficits in Learning and Memory. *Molecular and Cellular Biology* 22:7417-7427.
- Brocke L, Chiang LW, Wagner PD, Schulman H (1999) Functional implications of the subunit composition of neuronal CaM kinase II. *J Biol Chem* 274:22713-22722.
- Bukalo O, Schachner M, Dityatev A (2001) Modification of extracellular matrix by enzymatic removal of chondroitin sulfate and by lack of tenascin-R differentially affects several forms of synaptic plasticity in the hippocampus. *Neuroscience* 104:359-369.
- Bushong EA, Martone ME, Jones YZ, Ellisman MH (2002) Protoplasmic astrocytes in CA1 stratum radiatum occupy separate anatomical domains. *J Neurosci* 22:183-192.
- Carulli D, Laabs T, Geller HM, Fawcett JW (2005) Chondroitin sulfate proteoglycans in neural development and regeneration. *Curr Opin Neurobiol* 15:116-120.
- Carulli D, Rhodes KE, Brown DJ, Bonnert TP, Pollack SJ, Oliver K, Strata P, Fawcett JW (2006) Composition of perineuronal nets in the adult rat cerebellum and the cellular origin of their components. *J Comp Neurol* 494:559-577.
- Celio MR, Blumcke I (1994) Perineuronal nets--a specialized form of extracellular matrix in the adult nervous system. *Brain Res Brain Res Rev* 19:128-145.
- Creemers JW, Khatib AM (2008) Knock-out mouse models of proprotein convertases: unique functions or redundancy? *Front Biosci* 13:4960-4971.
- Cull-Candy S, Brickley S, Farrant M (2001) NMDA receptor subunits: diversity, development and disease. *Curr Opin Neurobiol* 11:327-335.
- Dalby NO, Mody I (2003) Activation of NMDA receptors in rat dentate gyrus granule cells by spontaneous and evoked transmitter release. *J Neurophysiol* 90:786-797.

- De Biase LM, Nishiyama A, Bergles DE (2010) Excitability and synaptic communication within the oligodendrocyte lineage. *J Neurosci* 30:3600-3611.
- De Bock M, Wang N, Decrock E, Bol M, Gadicherla AK, Culot M, Cecchelli R, Bultynck G, Leybaert L (2013) Endothelial calcium dynamics, connexin channels and blood-brain barrier function. *Prog Neurobiol* 108:1-20.
- de Vivo L, Landi S, Panniello M, Baroncelli L, Chierzi S, Mariotti L, Spolidoro M, Pizzorusso T, Maffei L, Ratto GM (2013) Extracellular matrix inhibits structural and functional plasticity of dendritic spines in the adult visual cortex. *Nat Commun* 4:1484.
- Deepa SS, Carulli D, Galtrey C, Rhodes K, Fukuda J, Mikami T, Sugahara K, Fawcett JW (2006) Composition of perineuronal net extracellular matrix in rat brain: a different disaccharide composition for the net-associated proteoglycans. *J Biol Chem* 281:17789-17800.
- Dineley KT, Weeber EJ, Atkins C, Adams JP, Anderson AE, Sweatt JD (2001) Leitmotifs in the biochemistry of LTP induction: amplification, integration and coordination. *J Neurochem* 77:961-971.
- Dityatev A, Seidenbecher CI, Schachner M (2010) Compartmentalization from the outside: the extracellular matrix and functional microdomains in the brain. *Trends Neurosci* 33:503-512.
- Dityatev A, Bruckner G, Dityateva G, Grosche J, Kleene R, Schachner M (2007) Activity-dependent formation and functions of chondroitin sulfate-rich extracellular matrix of perineuronal nets. *Dev Neurobiol* 67:570-588.
- Erisir A, Harris JL (2003) Decline of the critical period of visual plasticity is concurrent with the reduction of NR2B subunit of the synaptic NMDA receptor in layer 4. *J Neurosci* 23:5208-5218.
- Erondu NE, Kennedy MB (1985) Regional distribution of type II Ca<sup>2+</sup>/calmodulin-dependent protein kinase in rat brain. *J Neurosci* 5:3270-3277.
- Erreger K, Dravid SM, Banke TG, Wyllie DJ, Traynelis SF (2005) Subunit-specific gating controls rat NR1/NR2A and NR1/NR2B NMDA channel kinetics and synaptic signalling profiles. *J Physiol* 563:345-358.
- Foster KA, McLaughlin N, Edbauer D, Phillips M, Bolton A, Constantine-Paton M, Sheng M (2010) Distinct roles of NR2A and NR2B cytoplasmic tails in long-term potentiation. *J Neurosci* 30:2676-2685.
- Frischknecht R, Seidenbecher CI (2012) Brevican: a key proteoglycan in the perisynaptic extracellular matrix of the brain. *Int J Biochem Cell Biol* 44:1051-1054.
- Frischknecht R, Fejtova A, Viesti M, Stephan A, Sonderegger P (2008) Activity-induced synaptic capture and exocytosis of the neuronal serine protease neurotrypsin. *J Neurosci* 28:1568-1579.
- Frischknecht R, Heine M, Perrais D, Seidenbecher CI, Choquet D, Gundelfinger ED (2009) Brain extracellular matrix affects AMPA receptor lateral mobility and short-term synaptic plasticity. *Nat Neurosci* 12:897-904.
- Ge WP, Yang XJ, Zhang Z, Wang HK, Shen W, Deng QD, Duan S (2006) Long-term potentiation of neuron-glia synapses mediated by Ca<sup>2+</sup>-permeable AMPA receptors. *Science* 312:1533-1537.
- Giamanco KA, Morawski M, Matthews RT (2010) Perineuronal net formation and structure in aggrecan knockout mice. *Neuroscience* 170:1314-1327.
- Gibson EM, Purger D, Mount CW, Goldstein AK, Lin GL, Wood LS, Inema I, Miller SE, Bieri G, Zuchero JB, Barres BA, Woo PJ, Vogel H, Monje M (2014) Neuronal activity promotes oligodendrogenesis and adaptive myelination in the mammalian brain. *Science* 344:1252304.
- Giese KP, Fedorov NB, Filipkowski RK, Silva AJ (1998) Autophosphorylation at Thr286 of the alpha calcium-calmodulin kinase II in LTP and learning. *Science* 279:870-873.
- Gokce O, Sudhof TC (2013) Membrane-tethered monomeric neuroligin-1 domain triggers synapse formation. *J Neurosci* 33:14617-14628.

- Groc L, Choquet D, Stephenson FA, Verrier D, Manzoni OJ, Chavis P (2007) NMDA receptor surface trafficking and synaptic subunit composition are developmentally regulated by the extracellular matrix protein Reelin. *J Neurosci* 27:10165-10175.
- Hamel MG, Mayer J, Gottschall PE (2005) Altered production and proteolytic processing of brevican by transforming growth factor beta in cultured astrocytes. *J Neurochem* 93:1533-1541.
- Happel MF, Niekisch H, Castiblanco Rivera LL, Ohl FW, Deliano M, Frischknecht R (2014) Enhanced cognitive flexibility in reversal learning induced by removal of the extracellular matrix in auditory cortex. *Proc Natl Acad Sci U S A* 111:2800-2805.
- He HY, Hodos W, Quinlan EM (2006) Visual deprivation reactivates rapid ocular dominance plasticity in adult visual cortex. *J Neurosci* 26:2951-2955.
- Hedstrom KL, Xu X, Ogawa Y, Frischknecht R, Seidenbecher CI, Shrager P, Rasband MN (2007) Neurofascin assembles a specialized extracellular matrix at the axon initial segment. *J Cell Biol* 178:875-886.
- Henneberger C, Papouin T, Oliet SH, Rusakov DA (2010) Long-term potentiation depends on release of D-serine from astrocytes. *Nature* 463:232-236.
- Huntley GW (2012) Synaptic circuit remodelling by matrix metalloproteinases in health and disease. *Nat Rev Neurosci* 13:743-757.
- Hynes RO (1987) Integrins: a family of cell surface receptors. *Cell* 48:549-554.
- Hynes RO (2002) Integrins: bidirectional, allosteric signaling machines. *Cell* 110:673-687.
- Jabs R, Pivneva T, Huttmann K, Wyczynski A, Nolte C, Kettenmann H, Steinhauser C (2005) Synaptic transmission onto hippocampal glial cells with hGFAP promoter activity. *J Cell Sci* 118:3791-3803.
- John N, Krugel H, Frischknecht R, Smalla KH, Schultz C, Kreutz MR, Gundelfinger ED, Seidenbecher CI (2006) Brevican-containing perineuronal nets of extracellular matrix in dissociated hippocampal primary cultures. *Mol Cell Neurosci* 31:774-784.
- Johnson JW, Ascher P (1987) Glycine potentiates the NMDA response in cultured mouse brain neurons. *Nature* 325:529-531.
- Kelwick R, Desanlis I, Wheeler GN, Edwards DR (2015) The ADAMTS (A Disintegrin and Metalloproteinase with Thrombospondin motifs) family. *Genome biology* 16:113.
- Kennedy MB (2000) Signal-processing machines at the postsynaptic density. *Science* 290:750-754.
- Kennedy MB, McGuinness T, Greengard P (1983) A calcium/calmodulin-dependent protein kinase from mammalian brain that phosphorylates Synapsin I: Partial purification and characterization. *Journal of Neuroscience* 3:818-831.
- Kettenmann H, Kirchhoff F, Verkhratsky A (2013) Microglia: new roles for the synaptic stripper. *Neuron* 77:10-18.
- Kirson ED, Yaari Y (1996) Synaptic NMDA receptors in developing mouse hippocampal neurones: functional properties and sensitivity to ifenprodil. *J Physiol* 497 ( Pt 2):437-455.
- Lander C, Kind P, Maleski M, Hockfield S (1997) A family of activity-dependent neuronal cell-surface chondroitin sulfate proteoglycans in cat visual cortex. *J Neurosci* 17:1928-1939.
- Law AJ, Weickert CS, Webster MJ, Herman MM, Kleinman JE, Harrison PJ (2003) Expression of NMDA receptor NR1, NR2A and NR2B subunit mRNAs during development of the human hippocampal formation. *Eur J Neurosci* 18:1197-1205.
- Leduc R, Molloy SS, Thorne BA, Thomas G (1992) Activation of human furin precursor processing endoprotease occurs by an intramolecular autoproteolytic cleavage. *J Biol Chem* 267:14304-14308.
- Lee S-JR, Escobedo-Lozoya Y, Szatmari EM, Yasuda R (2009) Activation of CaMKII in single dendritic spines during long-term potentiation. *Nature* 458:299-304.
- Lemons ML, Condic ML (2008) Integrin signaling is integral to regeneration. *Exp Neurol* 209:343-352.
- Levenson JM, O'Riordan KJ, Brown KD, Trinh MA, Molfese DL, Sweatt JD (2004) Regulation of histone acetylation during memory formation in the hippocampus. *J Biol Chem* 279:40545-40559.
- Levy C, Brooks JM, Chen J, Su J, Fox MA (2015) Cell-specific and developmental expression of lectican-cleaving proteases in mouse hippocampus and neocortex. *J Comp Neurol* 523:629-648.

- Lisman J (1989) A mechanism for the Hebb and the anti-Hebb processes underlying learning and memory. *Proc Natl Acad Sci U S A* 86:9574-9578.
- Lisman J, Schulman H, Cline H (2002) The molecular basis of CaMKII function in synaptic and behavioural memory. *Nat Rev Neurosci* 3:175-190.
- Lynch MA (2004) Long-term potentiation and memory. *Physiol Rev* 84:87-136.
- Malfait AM, Arner EC, Song RH, Alston JT, Markosyan S, Staten N, Yang Z, Griggs DW, Tortorella MD (2008) Proprotein convertase activation of aggrecanases in cartilage in situ. *Arch Biochem Biophys* 478:43-51.
- Matsumoto-Miyai K, Sokolowska E, Zurlinden A, Gee CE, Luscher D, Hettwer S, Wolfel J, Ladner AP, Ster J, Gerber U, Rulicke T, Kunz B, Sonderegger P (2009) Coincident pre- and postsynaptic activation induces dendritic filopodia via neurotrypsin-dependent agrin cleavage. *Cell* 136:1161-1171.
- Matthews RT, Gary SC, Zerillo C, Pratta M, Solomon K, Arner EC, Hockfield S (2000) Brain-enriched hyaluronan binding (BEHAB)/brevican cleavage in a glioma cell line is mediated by a disintegrin and metalloproteinase with thrombospondin motifs (ADAMTS) family member. *J Biol Chem* 275:22695-22703.
- Mayer ML, Westbrook GL, Guthrie PB (1984) Voltage-dependent block by Mg<sup>2+</sup> of NMDA responses in spinal cord neurones. *Nature* 309:261-263.
- Mayer ML, MacDermott AB, Westbrook GL, Smith SJ, Barker JL (1987) Agonist- and voltage-gated calcium entry in cultured mouse spinal cord neurons under voltage clamp measured using arsenazo III. *J Neurosci* 7:3230-3244.
- Michaluk P, Mikasova L, Groc L, Frischknecht R, Choquet D, Kaczmarek L (2009) Matrix metalloproteinase-9 controls NMDA receptor surface diffusion through integrin beta1 signaling. *J Neurosci* 29:6007-6012.
- Michaluk P, Kolodziej L, Mioduszevska B, Wilczynski GM, Dzwonek J, Jaworski J, Gorecki DC, Ottersen OP, Kaczmarek L (2007) Beta-dystroglycan as a target for MMP-9, in response to enhanced neuronal activity. *J Biol Chem* 282:16036-16041.
- Michaluk P, Wawrzyniak M, Alot P, Szczot M, Wyrembek P, Mercik K, Medvedev N, Wilczek E, De Roo M, Zuschratter W, Muller D, Wilczynski GM, Mozrzymas JW, Stewart MG, Kaczmarek L, Wlodarczyk J (2011) Influence of matrix metalloproteinase MMP-9 on dendritic spine morphology. *J Cell Sci* 124:3369-3380.
- Miller SG, Kennedy MB (1986) Regulation of brain type II Ca<sup>2+</sup>/calmodulin-dependent protein kinase by autophosphorylation: a Ca<sup>2+</sup>-triggered molecular switch. *Cell* 44:861-870.
- Molinari F, Rio M, Meskenaite V, Encha-Razavi F, Auge J, Bacq D, Briault S, Vekemans M, Munnich A, Attie-Bitach T, Sonderegger P, Colleaux L (2002) Truncating neurotrypsin mutation in autosomal recessive nonsyndromic mental retardation. *Science* 298:1779-1781.
- Monyer H, Burnashev N, Laurie DJ, Sakmann B, Seeburg PH (1994) Developmental and regional expression in the rat brain and functional properties of four NMDA receptors. *Neuron* 12:529-540.
- Mothet JP, Pollegioni L, Ouanounou G, Martineau M, Fossier P, Baux G (2005) Glutamate receptor activation triggers a calcium-dependent and SNARE protein-dependent release of the gliotransmitter D-serine. *Proc Natl Acad Sci U S A* 102:5606-5611.
- Mothet JP, Parent AT, Wolosker H, Brady RO, Jr., Linden DJ, Ferris CD, Rogawski MA, Snyder SH (2000) D-serine is an endogenous ligand for the glycine site of the N-methyl-D-aspartate receptor. *Proc Natl Acad Sci U S A* 97:4926-4931.
- Nakamura H, Fujii Y, Inoki I, Sugimoto K, Tanzawa K, Matsuki H, Miura R, Yamaguchi Y, Okada Y (2000) Brevican is degraded by matrix metalloproteinases and aggrecanase-1 (ADAMTS4) at different sites. *J Biol Chem* 275:38885-38890.
- Nishiyama A, Lin XH, Stallcup WB (1995) Generation of truncated forms of the NG2 proteoglycan by cell surface proteolysis. *Mol Biol Cell* 6:1819-1832.
- Nishiyama A, Komitova M, Suzuki R, Zhu X (2009) Polydendrocytes (NG2 cells): multifunctional cells with lineage plasticity. *Nat Rev Neurosci* 10:9-22.

- Nishiyama J, Yasuda R (2015) Biochemical Computation for Spine Structural Plasticity. *Neuron* 87:63-75.
- Nour N, Mayer G, Mort JS, Salvat A, Mbikay M, Morrison CJ, Overall CM, Seidah NG (2005) The cysteine-rich domain of the secreted proprotein convertases PC5A and PACE4 functions as a cell surface anchor and interacts with tissue inhibitors of metalloproteinases. *Mol Biol Cell* 16:5215-5226.
- Ogawa T, Hagihara K, Suzuki M, Yamaguchi Y (2001) Brevican in the developing hippocampal fimbria: differential expression in myelinating oligodendrocytes and adult astrocytes suggests a dual role for brevican in central nervous system fiber tract development. *J Comp Neurol* 432:285-295.
- Orlando C, Ster J, Gerber U, Fawcett JW, Raineteau O (2012) Perisynaptic chondroitin sulfate proteoglycans restrict structural plasticity in an integrin-dependent manner. *J Neurosci* 32:18009-18017, 18017a.
- Otmakhov N, Griffith LC, Lisman JE (1997) Postsynaptic inhibitors of calcium/calmodulin-dependent protein kinase type II block induction but not maintenance of pairing-induced long-term potentiation. *J Neurosci* 17:5357-5365.
- Otmakhov N, Khibnik L, Otmakhova N, Carpenter S, Riahi S, Asrican B, Lisman J (2004a) Forskolin-induced LTP in the CA1 hippocampal region is NMDA receptor dependent. *J Neurophysiol* 91:1955-1962.
- Otmakhov N, Tao-Cheng JH, Carpenter S, Asrican B, Dosemeci A, Reese TS, Lisman J (2004b) Persistent accumulation of calcium/calmodulin-dependent protein kinase II in dendritic spines after induction of NMDA receptor-dependent chemical long-term potentiation. *J Neurosci* 24:9324-9331.
- Panatier A, Theodosis DT, Mothet JP, Touquet B, Pollegioni L, Poulain DA, Oliet SH (2006) Glia-derived D-serine controls NMDA receptor activity and synaptic memory. *Cell* 125:775-784.
- Panizzutti R, Scoriels L, Avellar M (2014) The co-agonist site of NMDA-glutamate receptors: a novel therapeutic target for age-related cognitive decline. *Current pharmaceutical design* 20:5160-5168.
- Papouin T, Ladepeche L, Ruel J, Sacchi S, Labasque M, Hanini M, Groc L, Pollegioni L, Mothet JP, Oliet SH (2012) Synaptic and extrasynaptic NMDA receptors are gated by different endogenous coagonists. *Cell* 150:633-646.
- Patterson SL, Pittenger C, Morozov A, Martin KC, Scanlin H, Drake C, Kandel ER (2001) Some forms of cAMP-mediated long-lasting potentiation are associated with release of BDNF and nuclear translocation of phospho-MAP kinase. *Neuron* 32:123-140.
- Paulissen G, Rocks N, Gueders MM, Crahay C, Quesada-Calvo F, Bekaert S, Hacha J, El Hour M, Foidart JM, Noel A, Cataldo DD (2009) Role of ADAM and ADAMTS metalloproteinases in airway diseases. *Respiratory research* 10:127.
- Peixoto RT, Kunz PA, Kwon H, Mabb AM, Sabatini BL, Philpot BD, Ehlers MD (2012) Transsynaptic signaling by activity-dependent cleavage of neuroligin-1. *Neuron* 76:396-409.
- Peng J, Kim MJ, Cheng D, Duong DM, Gygi SP, Sheng M (2004) Semiquantitative proteomic analysis of rat forebrain postsynaptic density fractions by mass spectrometry. *J Biol Chem* 279:21003-21011.
- Pierschbacher MD, Ruoslahti E (1984) Cell attachment activity of fibronectin can be duplicated by small synthetic fragments of the molecule. *Nature* 309:30-33.
- Pizzorusso T, Medini P, Berardi N, Chierzi S, Fawcett JW, Maffei L (2002) Reactivation of ocular dominance plasticity in the adult visual cortex. *Science* 298:1248-1251.
- Rauner C, Kohr G (2011) Triheteromeric NR1/NR2A/NR2B receptors constitute the major N-methyl-D-aspartate receptor population in adult hippocampal synapses. *J Biol Chem* 286:7558-7566.
- Reif R, Sales S, Dreier B, Luscher D, Wolfel J, Gisler C, Baici A, Kunz B, Sonderegger P (2008) Purification and enzymological characterization of murine neurotrypsin. *Protein expression and purification* 61:13-21.

- Reiss K, Maretzky T, Ludwig A, Tousseyn T, de Strooper B, Hartmann D, Saftig P (2005) ADAM10 cleavage of N-cadherin and regulation of cell-cell adhesion and beta-catenin nuclear signalling. *Embo j* 24:742-752.
- Rouach N, Segal M, Koulakoff A, Giaume C, Avignone E (2003) Carbenoxolone blockade of neuronal network activity in culture is not mediated by an action on gap junctions. *J Physiol* 553:729-745.
- Sakry D, Neitz A, Singh J, Frischknecht R, Marongiu D, Biname F, Perera SS, Endres K, Lutz B, Radyushkin K, Trotter J, Mittmann T (2014) Oligodendrocyte precursor cells modulate the neuronal network by activity-dependent ectodomain cleavage of glial NG2. *PLoS Biol* 12:e1001993.
- Sanhueza M, Lisman J (2013) The CaMKII/NMDAR complex as a molecular memory. *Mol Brain* 6:10.
- Schafer DP, Lehrman EK, Stevens B (2013) The "quad-partite" synapse: microglia-synapse interactions in the developing and mature CNS. *Glia* 61:24-36.
- Seidah NG (2011) What lies ahead for the proprotein convertases? *Ann N Y Acad Sci* 1220:149-161.
- Seidenbecher C, Richter K, Gundelfinger ED (1997) Brevican, a conditional proteoglycan from rat brain: characterization of secreted and GPI-anchored isoforms. In: *Neurochemistry* (Teelken AW, Korf J, eds), pp 901-904. New York: Plenum Press.
- Seidenbecher CI, Gundelfinger ED, Bockers TM, Trotter J, Kreutz MR (1998) Transcripts for secreted and GPI-anchored brevican are differentially distributed in rat brain. *Eur J Neurosci* 10:1621-1630.
- Seidenbecher CI, Smalla KH, Fischer N, Gundelfinger ED, Kreutz MR (2002) Brevican isoforms associate with neural membranes. *J Neurochem* 83:738-746.
- Seidenbecher CI, Richter K, Rauch U, Fassler R, Garner CC, Gundelfinger ED (1995) Brevican, a chondroitin sulfate proteoglycan of rat brain, occurs as secreted and cell surface glycosylphosphatidylinositol-anchored isoforms. *J Biol Chem* 270:27206-27212.
- Shen K, Meyer T (1999) Dynamic control of caMKII translocation and localization in hippocampal neurons by NMDA receptor stimulation. *Science* 284:162-166.
- Sheng M, Kim MJ (2002) Postsynaptic signaling and plasticity mechanisms. *Science* 298:776-780.
- Sheng M, Cummings J, Roldan LA, Jan YN, Jan LY (1994) Changing subunit composition of heteromeric NMDA receptors during development of rat cortex. *Nature* 368:144-147.
- Shi Y, Ethell IM (2006) Integrins control dendritic spine plasticity in hippocampal neurons through NMDA receptor and Ca<sup>2+</sup>/calmodulin-dependent protein kinase II-mediated actin reorganization. *J Neurosci* 26:1813-1822.
- Shinoe T, Goda Y (2015) Tuning synapses by proteolytic remodeling of the adhesive surface. *Curr Opin Neurobiol* 35:148-155.
- Silva AJ, Stevens CF, Tonegawa S, Wang Y (1992) Deficient Hippocampal Long-Term Potentiation in  $\beta$ -Calcium-Calmodulin Kinase II Mutant Mice. *Science* 257:201-206.
- Simon AM, Goodenough DA (1998) Diverse functions of vertebrate gap junctions. *Trends Cell Biol* 8:477-483.
- Sobczyk A, Scheuss V, Svoboda K (2005) NMDA receptor subunit-dependent [Ca<sup>2+</sup>] signaling in individual hippocampal dendritic spines. *J Neurosci* 25:6037-6046.
- Sohl G, Willecke K (2004) Gap junctions and the connexin protein family. *Cardiovascular research* 62:228-232.
- Staubli U, Vanderklish P, Lynch G (1990) An inhibitor of integrin receptors blocks long-term potentiation. *Behav Neural Biol* 53:1-5.
- Stevens ER, Esguerra M, Kim PM, Newman EA, Snyder SH, Zahs KR, Miller RF (2003) D-serine and serine racemase are present in the vertebrate retina and contribute to the physiological activation of NMDA receptors. *Proc Natl Acad Sci U S A* 100:6789-6794.
- Strack S, Colbran RJ (1998) Autophosphorylation-dependent targeting of calcium/ calmodulin-dependent protein kinase II by the NR2B subunit of the N-methyl- D-aspartate receptor. *J Biol Chem* 273:20689-20692.
- Suzuki K, Hayashi Y, Nakahara S, Kumazaki H, Prox J, Horiuchi K, Zeng M, Tanimura S, Nishiyama Y, Osawa S, Sehara-Fujisawa A, Saftig P, Yokoshima S, Fukuyama T, Matsuki N, Koyama R,



- Tomita T, Iwatsubo T (2012) Activity-dependent proteolytic cleavage of neuroligin-1. *Neuron* 76:410-422.
- Sweatt JD (2001) Protooncogenes subserve memory formation in the adult CNS. *Neuron* 31:671-674.
- Szepesi Z, Bijata M, Ruszczycki B, Kaczmarek L, Wlodarczyk J (2013) Matrix metalloproteinases regulate the formation of dendritic spine head protrusions during chemically induced long-term potentiation. *PLoS ONE* 8:e63314.
- Szklarczyk A, Lapinska J, Rylski M, McKay RD, Kaczmarek L (2002) Matrix metalloproteinase-9 undergoes expression and activation during dendritic remodeling in adult hippocampus. *J Neurosci* 22:920-930.
- Tan CL, Kwok JC, Patani R, French-Constant C, Chandran S, Fawcett JW (2011) Integrin activation promotes axon growth on inhibitory chondroitin sulfate proteoglycans by enhancing integrin signaling. *J Neurosci* 31:6289-6295.
- Taniguchi T, Kuroda R, Sakurai K, Nagahama M, Wada I, Tsuji A, Matsuda Y (2002) A Critical Role for the Carboxy Terminal Region of the Proprotein Convertase, PACE4A, in the Regulation of Its Autocatalytic Activation Coupled with Secretion. *Biochemical and Biophysical Research Communications* 290:878-884.
- Thomas GM, Huganir RL (2004) MAPK cascade signalling and synaptic plasticity. *Nat Rev Neurosci* 5:173-183.
- Tortorella MD, Arner EC, Hills R, Gormley J, Fok K, Pegg L, Munie G, Malfait AM (2005) ADAMTS-4 (aggrecanase-1): N-terminal activation mechanisms. *Arch Biochem Biophys* 444:34-44.
- Townsend M, Yoshii A, Mishina M, Constantine-Paton M (2003) Developmental loss of miniature N-methyl-D-aspartate receptor currents in NR2A knockout mice. *Proc Natl Acad Sci U S A* 100:1340-1345.
- Trotter J, Karram K, Nishiyama A (2010) NG2 cells: Properties, progeny and origin. *Brain Res Rev* 63:72-82.
- Tsuji A, Sakurai K, Kiyokage E, Yamazaki T, Koide S, Toida K, Ishimura K, Matsuda Y (2003) Secretory proprotein convertases PACE4 and PC6A are heparin-binding proteins which are localized in the extracellular matrix. Potential role of PACE4 in the activation of proproteins in the extracellular matrix. *Biochim Biophys Acta* 1645:95-104.
- Valenzuela JC, Heise C, Franken G, Singh J, Schweitzer B, Seidenbecher CI, Frischknecht R (2014) Hyaluronan-based extracellular matrix under conditions of homeostatic plasticity. *Philos Trans R Soc Lond B Biol Sci* 369:20130606.
- VanSaun M, Herrera AA, Werle MJ (2003) Structural alterations at the neuromuscular junctions of matrix metalloproteinase 3 null mutant mice. *J Neurocytol* 32:1129-1142.
- Volterra A, Meldolesi J (2005) Astrocytes, from brain glue to communication elements: the revolution continues. *Nat Rev Neurosci* 6:626-640.
- Worsdorfer P, Maxeiner S, Markopoulos C, Kirfel G, Wulf V, Auth T, Urschel S, von Maltzahn J, Willecke K (2008) Connexin expression and functional analysis of gap junctional communication in mouse embryonic stem cells. *Stem cells (Dayton, Ohio)* 26:431-439.
- Wu GY, Cline HT (1998) Stabilization of dendritic arbor structure in vivo by CaMKII. *Science* 279:222-226.
- Yamada H, Watanabe K, Shimonaka M, Yamaguchi Y (1994) Molecular cloning of brevican, a novel brain proteoglycan of the aggrecan/versican family. *J Biol Chem* 269:10119-10126.
- Yamada H, Fredette B, Shitara K, Hagihara K, Miura R, Ranscht B, Stallcup WB, Yamaguchi Y (1997) The brain chondroitin sulfate proteoglycan brevican associates with astrocytes ensheathing cerebellar glomeruli and inhibits neurite outgrowth from granule neurons. *J Neurosci* 17:7784-7795.
- Yamaguchi Y (2000) Lecticans: organizers of the brain extracellular matrix. *Cell Mol Life Sci* 57:276-289.
- Zhang H, Kelly G, Zerillo C, Jaworski DM, Hockfield S (1998) Expression of a cleaved brain-specific extracellular matrix protein mediates glioma cell invasion In vivo. *J Neurosci* 18:2370-2376.
- Zimmermann DR, Dours-Zimmermann MT (2008) Extracellular matrix of the central nervous system: from neglect to challenge. *Histochemistry and cell biology* 130:635-653.

## 6. Abbreviations

---

ADAM	A disintegrin and metalloproteinase
ADAMTS	A disintegrin and metalloproteinase with thrombospondin motifs
AMPA	$\alpha$ -amino-3-hydroxy-5-methyl-4-isoxazolepropionic acid
APMA	4-aminophenylmercuric acetate
AP-2	Clathrin adapter protein 2
APC	Adenomatous polyposis coli
APV	(2R)-amino-5-phosphonovaleric acid
BSA	Bovine serum albumin
$\alpha$ 7-nAChR	$\alpha$ 7 subunit of the nicotinic acetylcholine receptor
CaMKII	Ca <sup>2+</sup> /Calmodulin-dependent protein kinase II
CD29	Function blocking $\beta$ 1-integrin antibody
ChABC	Chondroitinase ABC
cLTP	chemically induced Long-Term Potentiation
CNQX	6-cyano-7-nitroquinoxaline-2,3-dione
CNS	Central nervous system
CRD	Cysteine-rich domain
CREB	cAMP response element-binding protein
CSPG	Chondroitin sulfate proteoglycan
Ctl	Control
DIV	Days in vitro
ECM	Extracellular matrix
ERK1/2	Extracellular signal-regulated protein kinases 1/2
GluN2B	NMDA receptor subunit 2B
GJ	Gap junction

HAPLN	Hyaluronan and proteoglycan link protein
HEK293-T	Human Embryonic Kidney Cells
Hyase	Hyaluronidase
IB	Immunoblots
IF	Immunofluorescence
Ifen	Ifenprodil
KO	Knock out
LamG	Laminin-G domain
LTD	long-term depression
LTP	Long-term potentiation
MMP	Matrix metalloproteinase
NMDAR	N-methyl D-aspartate receptor
PC	Proprotein convertase
PFA	Paraformaldehyde
PFR	Picrotoxin, Forskolin, Rolipram
RT	Room temperature
SDS-PAGE	sodium dodecyl sulfate polyacrylamide gel electrophoresis
SEM	standard error of the mean
SFK	Src family kinase
TCE	2,2,2-Trichloroethanol
TIMP	Tissue inhibitor of metalloproteinases
WT	Wild type

## 7. Figures

---

Figure 1.	ECM and it's components in detail; mature and degraded ECM.	8
Figure 2.	Conserved site found over the different members of the lectican family.	9
Figure 3.	Structure of MMP, ADAM and ADAMTS	11
Figure 4.	Schematic representation of proprotein convertase.	12
Figure 5.	Coomassie gel used for normalization of probes	26
Figure 6.	TCE used for normalisation	27
Figure 7.	Treatment paradigm for cLTP induction in the acute hippocampal slices.	28
Figure 8.	Workflow of LC-MS/MS activity-dependent ECM assay	31
Figure 9.	Reduced ECM immunoreactivity after Ch ABC treatment	33
Figure 10.	Two different pharmacological stimulation paradigms led to chemical LTP in acute hippocampal slices as measured by increased phosphorylation of ERK and CamKII.	34
Figure 11.	Specificity of brevican cleavage detected by antibody	35
Figure 12.	Activity-Dependent Proteolytic Cleavage of brevican.	36
Figure 13.	Activity-dependent proteolysis of Aggrecan	37
Figure 14.	Brevican cleavage is increased upon cLTP induction.	38
Figure 15.	Brevican is cleaved perisynaptically upon cLTP induction.	39
Figure 16.	Ultrastructural representation of perisynaptic brevican.	40
Figure 17.	Activity-Dependent Proteolytic Cleavage of brevican is abolished upon broad band protease application.	41
Figure 18.	Specific protease involved in degradation of brevican.	42
Figure 19.	APMA induces activation of proteases and cleavage of brevican.	43
Figure 20.	Role of proprotein convertases in degradation of brevican.	44
Figure 21.	Cleavage of brevican requires postsynaptic activation.	45
Figure 22.	Role of NR2B-NMDA receptor subunit and network activity in the activity-dependent modulation of ECM	46
Figure 23.	NMDA can trigger secretion and activity-dependent modulation of brevican	47
Figure 24.	Role of CaMKII signalling in the activity-dependent modulation of ECM	48

Figure 25.	Role of $\beta 1$ class integrin's in the activity-dependent modulation of ECM	49
Figure 26.	Screening for modulation of ECM using an unbiased LC-MS approach	51
Figure 27.	Protein synthesis blocker anisomycin didn't change activity induced increase in brevican levels.	52
Figure 28.	Role of glia in secretion and cleavage of brevican	53
Figure 29.	Activity-dependent release of D-serine from glia is necessary for cleavage of brevican as marker of ECM.	54
Figure 30.	Activity-dependent release of D-serine from glia is necessary for ECM modulation.	55
Figure 31.	Influence of an ADAMTS4-specific protease inhibitor on induction of cLTP by PFR and activity modulation by 4AP+BCC.	56
Figure 32.	Activity-dependent formation of dendritic protrusions in a proteolysis-dependent manner.	57
Figure 33.	Induction of cLTP leads to NG2 ectodomain shedding Activity-dependent proteolytic cleavage of NG2 results in increased levels of ectodomain associated with the ECM.	59
Figure 34	Schematic presentation of putative signalling mechanisms that lead to modulation of perisynaptic ECM upon induction of synaptic activity by proteases in an NMDAR-dependent manner.	70

## 8. Scientific publications

---

- Sharma KP, **Singh JB**, Sharma SK. Mechanisms of cAMP-induced sustained activation of extracellular signal-regulated kinase in the hippocampus. *Neuroreport*;25(7):470-4,2014 May 7.
- Valenzuela JC, Heise C, Franken G, **Singh J**, Schweitzer B, Seidenbecher CI, Frischknecht R. Hyaluronan-based extracellular matrix under conditions of homeostatic plasticity. *Phil. Trans. R. Soc. B* 369:20130606 (2014).
- Sakry D, Neitz A, **Singh J**, Frischknecht R, Marongiu D, Biname F, Perera SS, Endres K, Lutz B, Radyushkin K, Trotter J, Mittmann T. Oligodendrocyte Precursor Cells Modulate the Neuronal Network by Activity-Dependent Ectodomain Cleavage of Glial NG2. *PLoS Biol* 12(11):e1001993 (2014).
- **Accession number** of clones at EMBL Nucleotide Sequence Database Accession No (s): Accession#: FN556348- FN556374 have been submitted (2009).

## 9. Curriculum vitae

---

Name: Jeet Bahadur

Family name: Singh

Date of birth: 31<sup>st</sup> december 1989

Place of birth: Lucknow, India

Nationality: Indian

Parents: Mr. Vijay kumar singh  
Mrs. Heera singh

### **Education**

2001/2002: High School Central Board of Secondary Education (CBSE board)

2002-2004: Intermediate CBSE Board

2004-2009: Integrated M.Sc. (Microbiology), Allahabad Agriculture Institute-  
Deemed University, Allahabad, India

2010-2011: Worked as Project Assistant at National Brain Research Centre, Delhi,  
India on Learning and Memory Project

2011-2017: Doctoral Thesis. Otto von Guericke Universität  
-Leibniz Institute for Neurobiology, Magdeburg, Germany

## 10. Erklärung

---

Hiermit erkläre ich, dass ich die von mir eingereichte Dissertation zum dem Thema  
**“Role of the Perisynaptic Extracellular Matrix in Synaptic Plasticity”**  
selbständig verfasst, nicht schon als Dissertation verwendet habe und die benutzten  
Hilfsmittel und Quellen vollständig angegeben wurden.

Weiterhin erkläre ich, dass ich weder diese noch eine andere Arbeit zur Erlangung des  
akademischen Grades doctor rerum naturalium (Dr. rer. nat.) an anderen Einrichtungen  
eingereicht habe.

Magdeburg, .....

---

(Jeet Bahadur Singh)